# The Origin of phonolites and trachytes from the Col de Guéry area

## Le Mont-Dore, Massif Central, France

*By*
Ulla Bernth, Robert Brousse,
Robert Frei and Henning Sørensen

1742

Matematisk-fysiske Meddelelser **50**

Det Kongelige Danske Videnskabernes Selskab
*The Royal Danish Academy of Sciences and Letters*

Commission Agent: C. A. Reitzels Forlag
Copenhagen 2002

# Abstract

The volcanic rocks of the Col de Guéry area in the Mont-Dore massif (Massif Central, France) comprise silica-undersaturated as well as silica-saturated rocks: basanites, trachybasalts, trachyandesites, trachytes and phonolites. They were emplaced from 2.5 to 0.7 Ma ago, a group of phonolites and trachytes forming a separate event at around 2.0 Ma.

Based on major- and trace-element data as well as on $^{87}Sr/^{86}Sr$ and $^{143}Nd/^{144}Nd$ initial ratios, the sequence from basanite to some of the trachytes may be comagmatically formed by fractionation of an essentially unmodified mantle-derived basanitic magma. The transition from silica-undersaturated to silica saturated rocks may be explained by fractionation of amphibole.

The group of trachytes and phonolites formed 2.0 Ma ago are mineralogically as well as geochemically related. They are enriched in Na, K, Rb, Cs, Zr and Th and depleted in Mg, Fe, Ca, Sc, Ni, Nb, Ta, Ba, Sr, Ti, P and the REE, especially the MREE. They differ from most other phonolites and trachytes in having low contents of Nb, Ta, REE and Ba and in displaying no or very weak Eu anomalies. The missing Eu anomalies in these feldspar-rich rocks are interpreted to be a result of high oxygen fugacities in the magmas. This may also explain the low contents of Nb and Ta, which are interpreted to be results of fractionation of hematite-ilmenite solid solutions.

The trachytes and phonolites contain enclaves of tephritic composition which may be segregations of minerals from the magma chambers in which the trachytic and phonolitic melts developed by crystal fractionation processes. This implies that the enclaves are comagmatic with their host rocks. Alternatively, they may represent disintegrated modified globules of basic magma injected into the magma chambers. The enclaves as well as their host rocks contain xenocrysts of forsteritic olivine, bytownite and Ti-Al-rich diopside-hedenbergite. This may indicate magma mixing as a possible mechanism in the petrogenesis of these trachytes and phonolites. The 2.0 Ma trachytes and phonolites may then have been formed by separate pulses of magma that mixed in deep magma reservoirs and subsequently underwent fractional crystallization. Interdiffusion of trace elements between coexisting melts has resulted in a decoupling of isotopic and chemical systems. According to the $^{87}Sr/^{86}Sr$ and the $^{143}Nd/^{144}Nd$ initial ratios, mixing of melts formed by partial melting in a slightly depleted mantle source of oceanic island type with melts of HIMU type and melts formed in an enriched mantle have been involved in the genesis of the 2.0 Ma trachytes and phonolites combined with some crustal assimilation and subsequent hydrothermal alteration of some of the rocks.

Ulla Bernth[1], Robert Brousse[2], Robert Frei[3] and Henning Sørensen[3]
1 Ådalsvej 26, DK-4340, Tølløse; Denmark
2 38 Rue Langlois, F-92160, Antony, France
3 Geological Institute, University of Copenhagen, Øster Voldgade 10, DK-1350 Copenhagen K, Denmark
Corresponding author: Henning Sørensen, e-mail hennings@geo.geol.ku.dk

Printed in Denmark by Special-Trykkeriet Viborg a-s
ISSN 0023-3323. ISBN 87-7876-302-9

# 1. Introduction

The Mont-Dore massif (Auvergne, Massif Central, France) is an intraplate volcanic complex located between the Chaînes des Puys to the north and Cézalier and Cantal to the south (Fig. 1). It is made up of a variety of volcanic rocks, including trachytes and phonolites which form the subject of the present paper. A number of occurrences of these rocks are found in the Col de Guéry area (Fig. 1). This area therefore represents an ideal target area for the study of the origin of trachytic and phonolitic melts and for the examination of the source and evolution of these melts including evaluation of the relative importance of fractional crystallization, magma mixing, crustal contamination and differences in chemical composition of the source regions of the melts. All occurrences of trachytes and phonolites in the area were sampled in order to describe the entire compositional variation.

Recent studies of the phonolites from the Mont-Dore massif (Briot *et al.*, 1991) and from the Cantal massif (Wilson *et al.*, 1995) indicate that they may have been formed by fractionation of alkali basaltic–basanitic magmas in deep magma chambers subsequent to exhaustion of contamination of the melts with continental crustal material. According to Cantagrel & Baubron (1983) the phonolites were formed from pulses of magma which were not directly related to the volcanic rocks exposed at the present surface.

Phonolites are generally enriched in elements such as Rb, Ba, Zr, Th, REE, Nb and Ta. The phonolites studied by us differ from the general trace element situation by a depletion in Nb, Ta, the REE, especially the MREE, and also Ba in spite of high contents of K. A petrological study of the Col de Guéry area was presented by Bernth (1996) and some preliminary results of the project have been published by Sørensen et al. (1999).

# Geological relationships

## Age relationships

The Mont-Dore massif has an elliptical shape, measuring 35 km from east to west

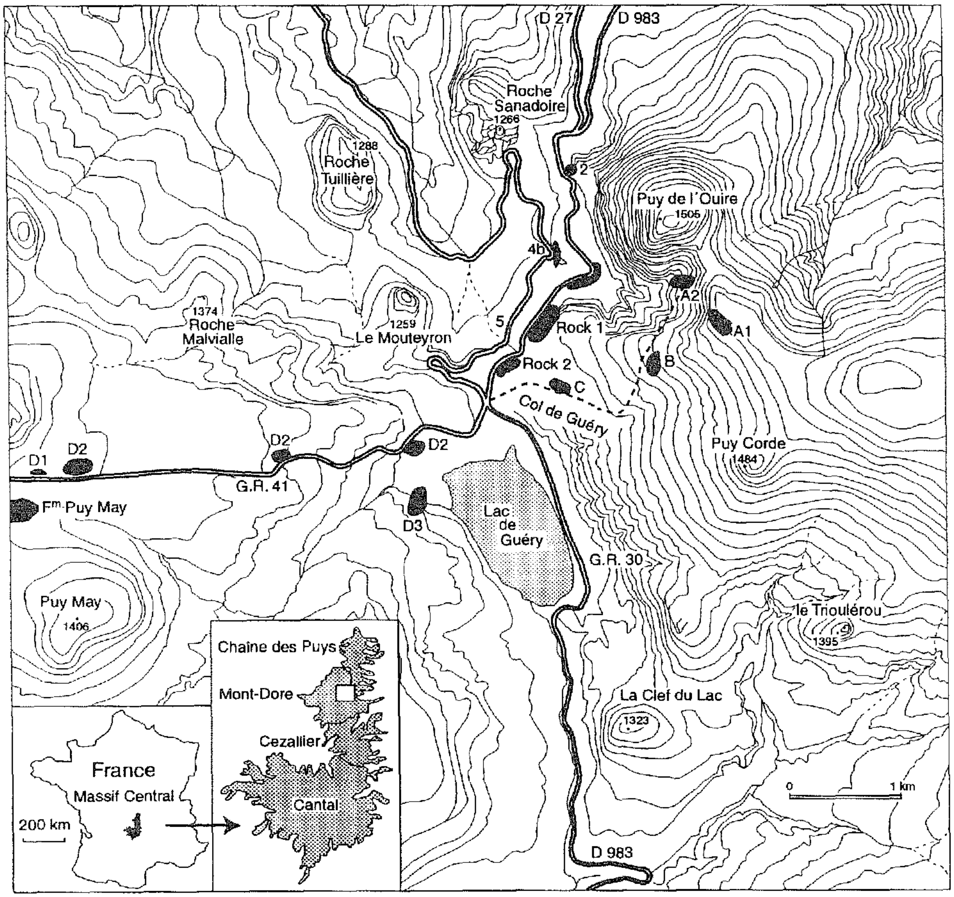

Fig 1. Sketch map of the Col de Guéry area showing location of samples.

and 16 km from north to south (Brousse & Lefèvre, 1990). It is located at the intersection of two major volcano-tectonic lines directed north-south and northwest-southeast. The central part is made up of a caldera (Brousse & Julien, 1987) which is concealed beneath younger volcanic products, its outlines being known mainly from geophysical data. The Col de Guéry area is located close to the NE margin of the caldera.

A tectonic event about 4 Ma ago is considered to have caused the injection of differentiated, silica-saturated and silica-undersaturated magmas (Cantagrel & Baubron, 1983; Brousse & Julien, 1987), and to have initiated the building of the Mont-Dore massif on a Hercynian basement which had already been covered by volcanics during Miocene and early Pliocene times.

Based on more than 100 K-Ar dates, Cantagrel & Baubron (1983) have established the chronology of the magmatic activity. Already Glangeaud *et al.* (1965) distinguished three magmatic cycles (see also Brousse & Lefèvre, 1990). This leads to the following scheme of events:

- “pre-Mont-Dore” volcanism: > 6 Ma
- “ante-caldera” volcanism, (*the Lower Series*): > 3 Ma
- “syn-caldera” volcanism: 3 Ma
- “post-caldera” volcanism, (*the Middle Series*): 3.0 – 1.6 Ma
- Puy de Sancy volcanism, (*the Upper Series*): 1.0 – 0.25 Ma

The rocks of the three magmatic series follow silica-saturated and silica-undersaturated trends.

The Lower Series is poorly represented and is only found in the outer parts of the massif or along the faults of the Haute-Dordogne depression. The series is discontinuous from basanite to *qz* normative trachyte and comendite. There are no intermediate rocks (Brousse *et al.*, 1979, Brousse & Lefevre, 1990).

The syn-caldera volcanism is marked by vast eruptions of rhyolitic pumice, the Nappe de Ponce, which covers more than 350 km$^2$ and represents the partial tapping of a reservoir of differentiated magma.

The trachytes and phonolites studied in the present paper belong to the Middle Series which comprises the most voluminous rocks inside the caldera. The silica-undersaturated trend evolves from ankaramite over basanite/tephrite, hawaiite, ordanchite (hauyne tephrite/trachyandesite), trachyte to phonolite. The silica-saturated trend is represented by sancyite (variety of trachyandesite), doréite (mugearite, basaltic trachyandesite), trachyte and rhyolite. Trachyandesitic rocks predominate and were erupted during two periods: 2.5 – 2.1 Ma and 1.9 – 1.6 Ma ago. The Puy de l’Ouire trachyandesite (Fig. 1) is dated to 2.2 ± 0.15 Ma (Morel *et al.*, 1992). The trachytes and phonolites were formed at about 2.0 Ma during a separate event (Cantagrel & Baubron, 1983).

The Upper Series is made up of a silica-undersaturated series from basalt to phonolite, and a silica-saturated one from mugearite to trachyte.

## The Col de Guéry area

The general geology in the Col de Guéry area is covered by the geological map sheet Bourg-Lastic (Brousse *et al.*, 1989). The rocks in this area (Fig. 1) were examined along road D.983 from east of Roche Sanadoire to Col de Guéry (localities

2, 4b and 5) and along the small road G.R.41 to $F^{me}$ de Puy May. A number of volcanic necks were also examined. These include Roche Malvialle, Mouteyron, Roche Tuilière, Roche Sanadoire, Puy Cordé and Trioulérou. Some samples were collected at the localities marked A, B and C ( Fig. 1).

Exposures are generally poor, which means that contact relations between the investigated rocks could only rarely be determined. The trachytes and phonolites appear to form separate necks intruding deposits of pyroclastic rocks and lacustrine sediments. No intersecting relationships between trachytes, phonolites, basanites, trachyandesites, etc. have been observed. The determination of age relationships therefore rests entirely upon the K/Ar datings (cf. compilations by Cantagrel & Baubron, 1983, and Brousse *et al.*, 1989).

Trachytic and phonolitic rocks were found at Trioulérou (2.01 ± 0.06 Ma), $F^{me}$ de Puy May (no age data), Puy Cordé (2.03 ± 0.11 Ma), Roche Sanadoire (1.83 ± 0.10 Ma), Roche Tuilière (2.10 ± 0.10 Ma), Roche Mouteyron (1.92 ± 0.10 Ma), and along the road D. 983 (no age data available). New K-Ar ages of 2.33 ± 0.03 Ma and 2.17 ± 0.03 Ma have been determined by P.Y. Gillot, Université de Paris Sud, for le Trioulérou and Puy Cordé phonolites, respectively (personal information). These new data are different from those of Cantagrel & Baubron (1983) and indicate that a revision of the K/Ar dating of the Mont-Dore volcanic rocks is needed in the light of the improvement of the methods since the ages determined by Cantagrell & Baubron were published. For the sake of consistency we use the dates of Cantagrel & Baubron (1983) in the present paper.

Trachyandesitic to trachybasaltic rocks (ordanchites) were examined at Roche Malvialle, localities 2, 5, $A_1$ and C; potassic trachyandesite at Puy de l'Ouire; hawaiitic rocks at locality $D_2$; and basanite at locality $D_3$ (Fig. 1).

Many of the rocks of the area have been described under local names, such as doréite, ordanchite and sancyite. We have classified the rocks on the basis of the TAS diagram (Fig. 2) proposed by IUGS (Le Maitre, 1989).

## Petrography

### Trachytes and phonolites

The Col de Guéry trachytes and phonolites are fine-grained to aphanitic grey rocks, often fissile, sometimes vesicular, and generally porphyritic. They are composed of the same minerals, but in varying proportions and appear to show a continuum in chemical (Fig. 2) and modal composition. There are macrocrysts of feldspar, olivine, amphibole, pyroxene, Fe-Ti oxides and in cases biotite, sodalite, hauyne-nosean, zircon and titanite.

Macrocrysts of alkali feldspar occur as single crystals and in clusters. In some

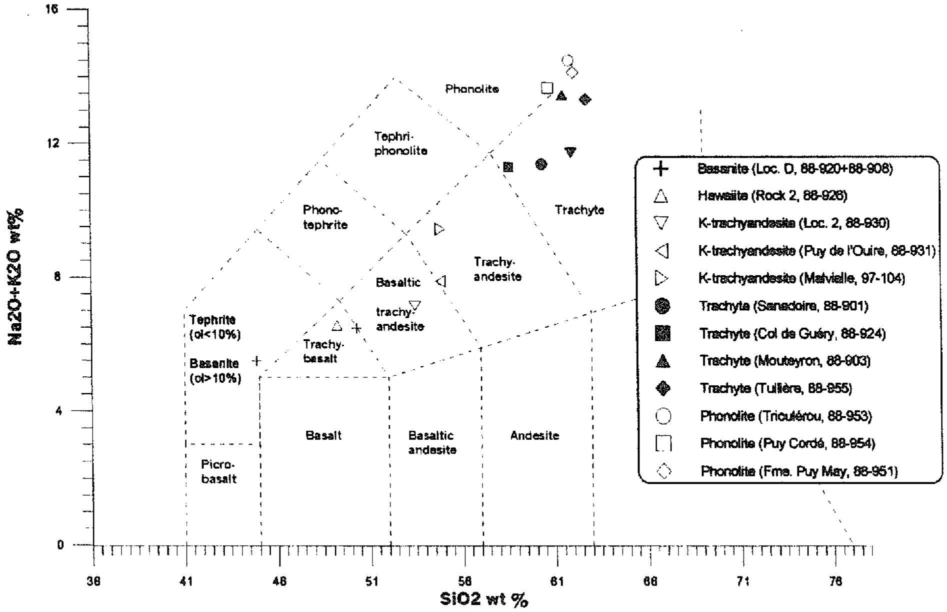

Fig. 2. The total alkali-silica (TAS) diagram (Le Maitre 1989) with plots of the analyzed samples.

rocks the clusters also contain grains of plagioclase, clinopyroxene and Fe-Ti oxides. The alkali feldspar grains show zoning, in cases discontinuous zoning with partially resorbed cores of alkali feldspar or plagioclase. The plagioclase grains often have corroded outlines and may be overgrown by alkali feldspar. The feldspar grains have melt inclusions in their marginal zones.

The feldspathoids belong to the sodalite-haüyne-nosean group, often blue in hand specimens, but generally brownish to black in thin section. They are partly to entirely substituted by pigmentary material. Nepheline has been observed in the Trioulérou phonolite as clusters of stout crystals.

Clinopyroxene macrocrysts are prismatic grains of green diopside-hedenbergite and stout crystals of brown diopside-hedenbergite. The clinopyroxenes show continuous and discontinuous zoning. The Trioulérou phonolite also contains grains of aegirine augite.

Prismatic amphibole macrocrysts are pleochroic in brown and green colours and have kaersutitic to pargasitic compositions. They often display zonation and generally have destabilization rims of clinopyroxene and/or Fe-Ti oxides. Some amphibole macrocrysts have hollow cores and swallow-tails and some show embayments along their margins.

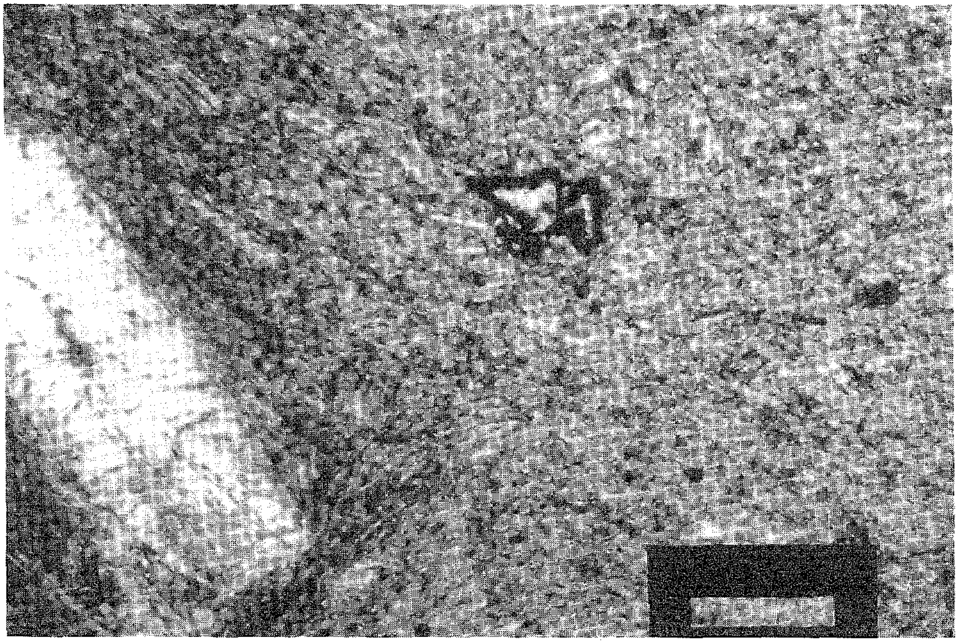

Fig. 3. Small olivine crystals with black rims and alkali feldspar phenocryst in phonolite, Puy Cordé (88-954,3), plane polarized light, scale = 0.6 mm).

The Trioulérou and Puy Cordé phonolites and the Sanadoire trachyte have small grains of olivine, which may form clusters (Fig. 3). They often have corroded shapes and have brownish to black reaction rims.

The trachytes and the Puy Cordé phonolite additionally contain phenocrysts of biotite, generally with black destabilization rims.

Crystals and irregularly shaped grains of titanite are generally present. Zircon occurs in the Trioulérou phonolite as brownish grains of irregular shape with black rims and as prismatic crystals in the Sanadoire trachyte.

The matrix of these rocks has a trachytic texture and is dominated by laths of alkali feldspar with interstitial plagioclase, feldspathoids, clinopyroxene, amphibole, titanite, apatite and Fe-Ti oxides. At Mouteyron and Roche Tuilière, the acicular pyroxenes of the matrix are clustered together in clouds, a feature characteristic for agpaitic phonolites according to Azambre & Girod (1966).

The Trioulérou and Puy Cordé phonolites have an agpaitic index of 1.01-1.05 but contain minerals such as plagioclase, diopside, kaersutite, titanite and Fe-Ti oxides, which are typical for miaskitic phonolites and nepheline syenites. The Trioulérou and F$^{me.}$ de Puy May phonolites have minute grains of unidentified Zr-Ti-rich minerals, which occur interstitially in the matrix. This may indicate an evolution toward an agpaitic mineralogy in the final stages of crystallization.

### Trachyandesite and trachybasalt

These rock types are dark grey, porphyritic, often vesicular. There are phenocrysts of clinopyroxene, amphibole and biotite, the two last-named with destabilization rims, olivine with black rims, alkali feldspar (with inclusions of pyroxene, apatite and Fe-Ti oxides and sometimes feldspathoids), plagioclase, titanite, Fe-Ti oxides and in some rocks also feldspathoids. The feldspar grains often have corroded outlines.

Rims around amphibole phenocrysts have an inner zone of pyroxene, feldspathoids and Fe-Ti oxides, and an outer zone of Fe-Ti oxides. As in the phonolites, some amphibole phenocrysts have hollow cores.

The matrix consists of feldspar laths, pyroxene, Fe-Ti oxides and rare foids.

### Basanite and hawaiite

The basanite forms columnar structures and has phenocrysts of olivine, clinopyroxene and Fe-Ti oxides in a matrix of plagioclase, olivine, clinopyroxene and Fe-Ti oxides. The hawaiitic trachybasalt is vesicular and has phenocrysts of clinopyroxene and plagioclase in a matrix of plagioclase, alkali feldspar, pyroxene and Fe-Ti-oxides.

### Enclaves

In the Col de Guéry area enclaves are found in basaltic trachyandesites, trachytes and phonolites, but in rather limited number. We have examined two types of enclaves from trachytes and phonolites. The first type forms rounded or angular masses measuring up to a few cm across and is composed of aggregates of mm-sized grains of amphibole, clinopyroxene, plagioclase, biotite, apatite, etc. (Figs. 4, 5). The second type forms ball-like or lenticular bodies, up to 10 cm or more across, of porphyritic and vesicular rocks having mm-sized phenocrysts in a fine-grained to aphanitic matrix (Figs. 6, 7). They are grey to black. The contacts are generally sharp and wavy (Fig. 8), but without chilling and crenulation. There are cases of gradual disintegration of the enclaves into the host rock (Fig. 9). The contact zones of the enclaves may be disrupted into smaller fragments and even single crystals floating in the surrounding rocks. The feldspar laths of the trachytes and phonolites wrap the enclaves (Fig. 8), but the trachytic texture of the adjacent host rocks may be disturbed, the latter being broken up into nodular bodies in which the feldspar laths are arranged concentrically and parallel to the surface of the balls (Fig. 10). The surface of these nodular bodies may be covered by rusty pigmentation, which gives the hand specimens a speckled appearance. The lenticular enclaves appear to

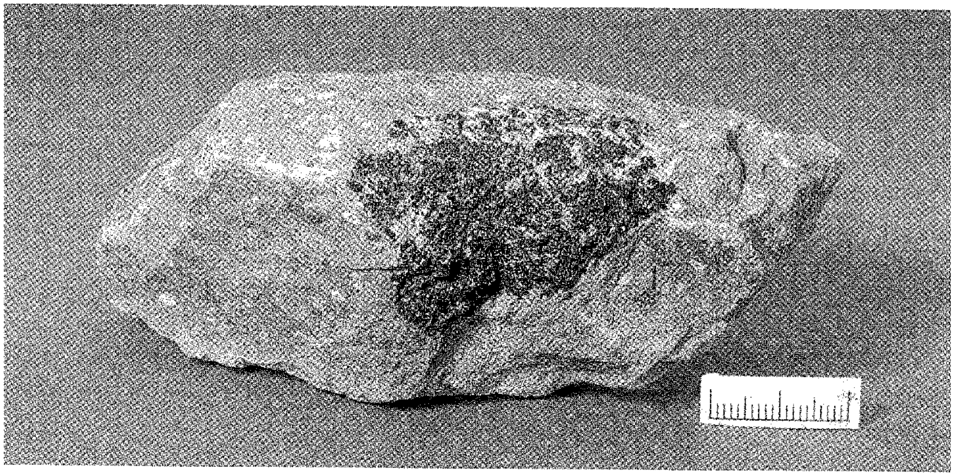

Fig. 4. Hand specimen of cumulitic enclave enclosed in trachyte, Roche Sanadoire (88-901). Scale = 2 cm.

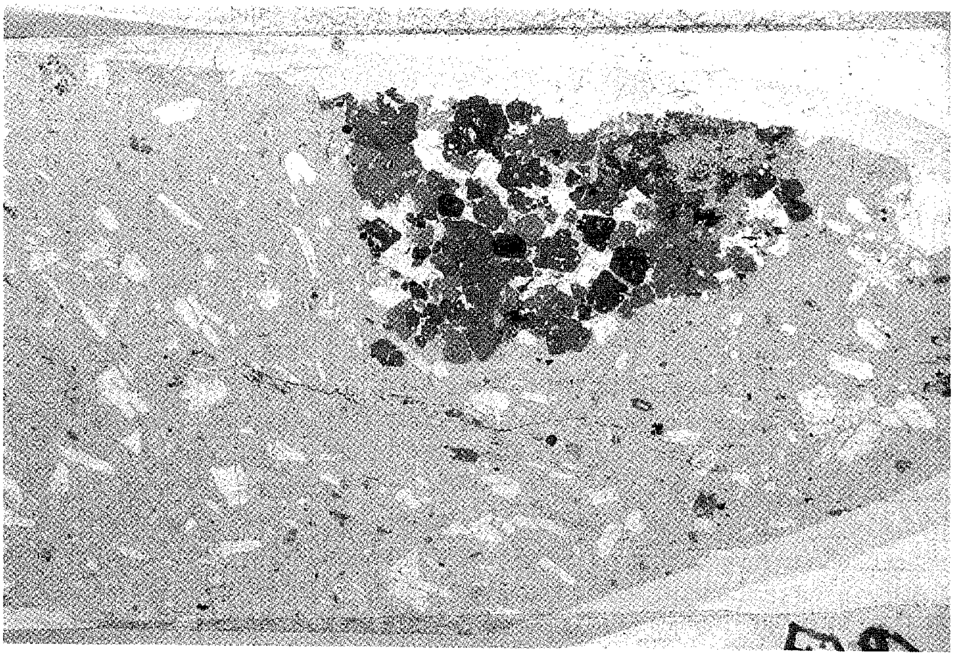

Fig. 5. Whole thin section of cumulitic enclave enclosed in trachyte. The enclave is dominated by large crystals of kaersutite (brown) associated with clinopyroxene (green), biotite, apatite, Fe-Ti oxides (black) and plagioclase (white) (Roche Sanadoire (88-901,1), plane polarized light, field of view is 3 cm wide).

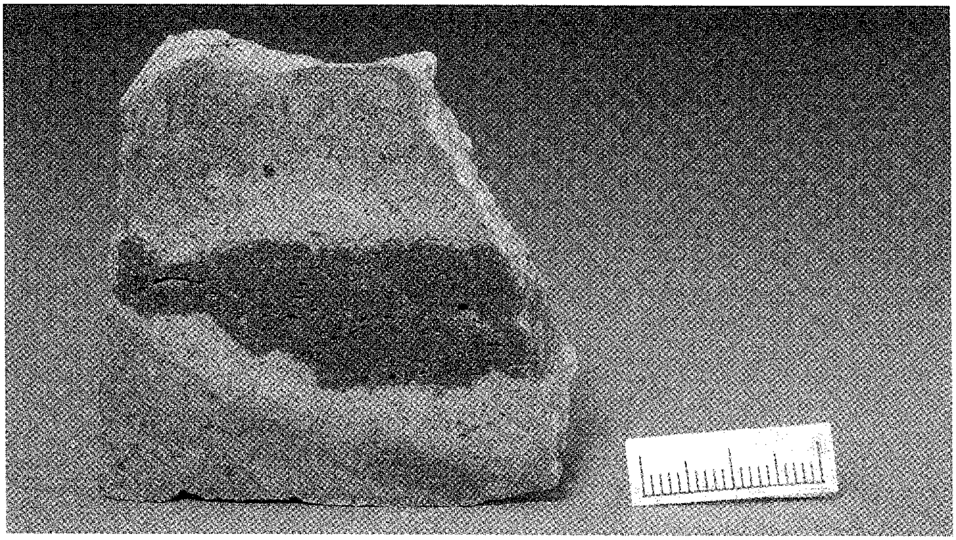

Fig. 6. Hand specimen of slightly vesicular, flattened tephritic enclave with sharp contacts against phonolite, Puy Cordé (97-108a), scale = 2 cm). Note that the phonolite is bleached in contact with the enclave.

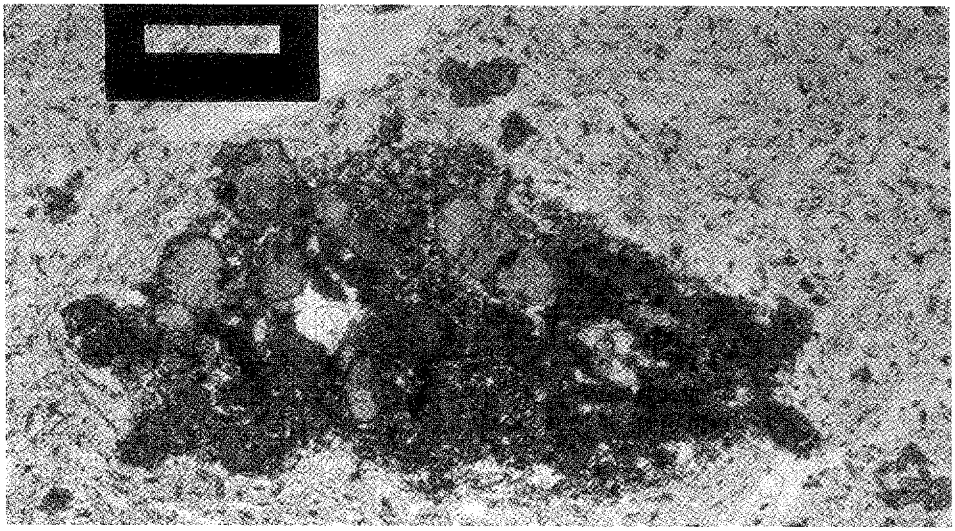

Fig. 7. Tephritic mini-enclave, Puy Cordé (97-108b). It is conformably wrapped by the alkali feldspar of the phonolite and slightly disintegrated into the latter. The tephrite has phenocrysts of amphibole (brown) with black destabilization rims in a dense matrix. Centre left: vesicle with crystal of albite. The enclosing phonolite contains clusters of tiny crystals of green clinopyroxene and brown amphibole (plane polarized light, scale 0.6 mm).

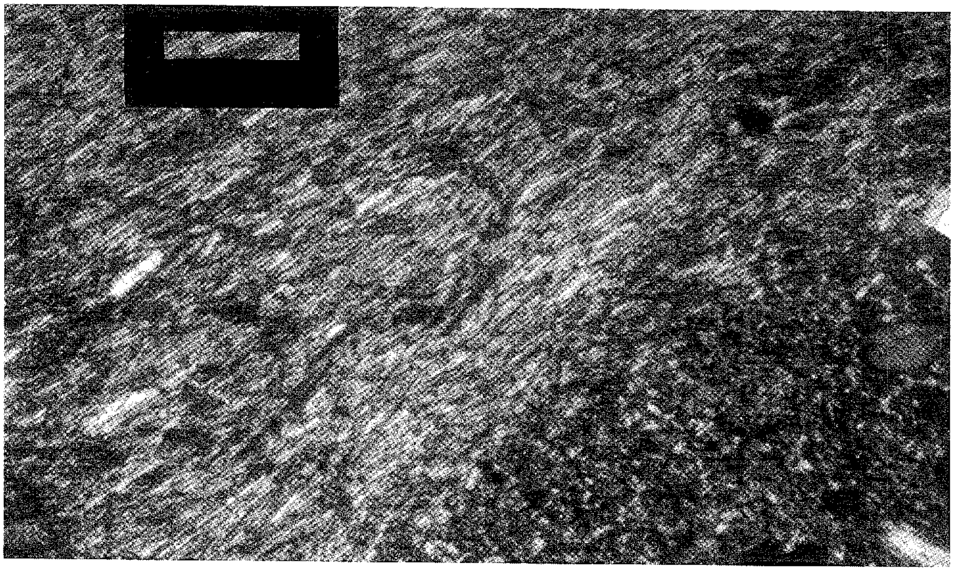

Fig. 8. Sharp contact between tephritic enclave and phonolite, Trioulérou (II). The feldspar laths of the phonolite are conformable with the contact. The enclave has phenocrysts of plagioclase, amphibole and clinopyroxene in a fine-grained matrix (crossed polarizers, scale 0.6 mm).

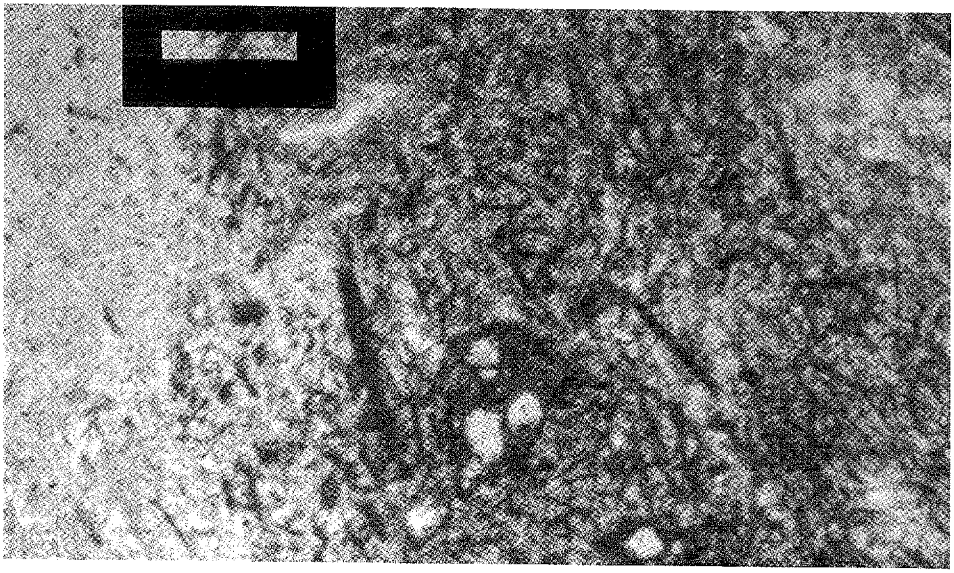

Fig. 9. Diffuse contact between enclave and phonolite, Trioulérou (I). The enclave shows a cluster of olivine grains and acicular grains of kaersutite in a fine-grained matrix (plane polarized light, scale 0.6 mm).

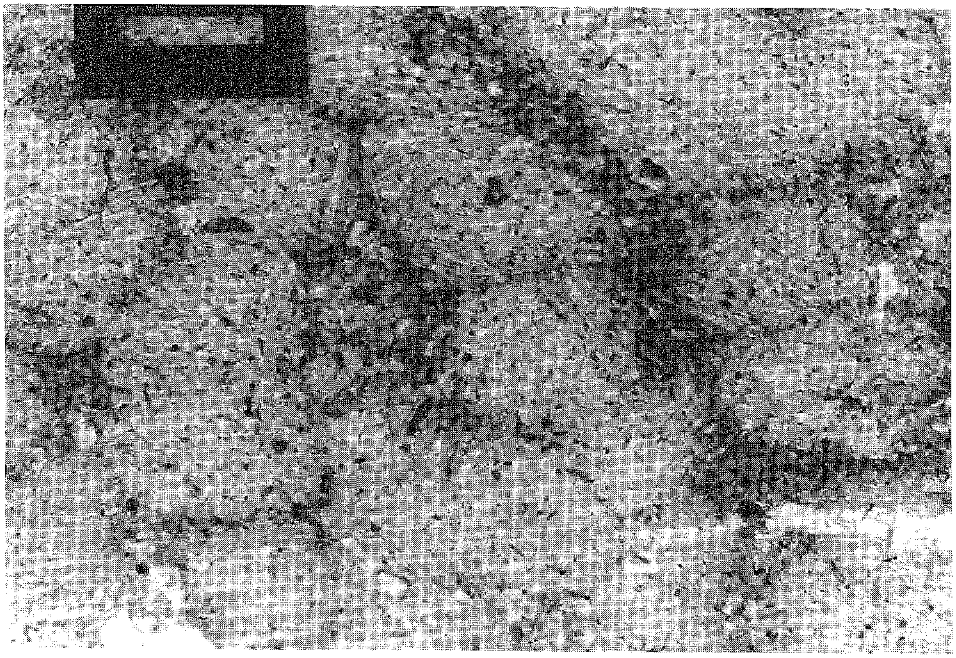

Fig. 10. Nodular structure in phonolite adjacent to enclave, Puy Cordé (97-108c). The phonolite is broken up into nodular bodies made up of concentrically arranged feldspar laths, the surfaces of some nodules are covered by brown pigmentation (plane polarized light, scale 0.6 mm).

have been flattened and drawn out in connection with the eruption of the host rocks.

The second type of enclaves contains macrocrysts of brown kaersutitic to pargasitic amphibole, brownish and greenish diopside-hedenbergite and green aegirine augitic clinopyroxene, forsterite-rich olivine, biotite, plagioclase, alkali feldspar, sodalite, hauyne/nosean and in cases nepheline. Accessories are titanite, Fe-Ti oxides and apatite. Amphibole may constitute up to 80 vol. % of the phenocrysts.

The macrocrysts of the individual minerals often form clusters. The olivine grains are generally fresh, but with corroded outlines and often overgrown by brown amphibole and/or iron oxides(Figs. 9, 11). In some enclaves olivine is more or less completely substituted by iddingsite and iron oxides (Fig 9). The amphibole forms slender prismatic grains which are generally non-deformed. They show colour zonation, are sometimes hollow with swallow-tails (Fig. 12), and may have thin black destabilization rims, especially in the marginal parts of the enclaves. The green diopside-hedenbergite and the aegirine augite both occur as short prismatic grains, the brownish clinopyroxene as stout crystals, which are often bent or broken

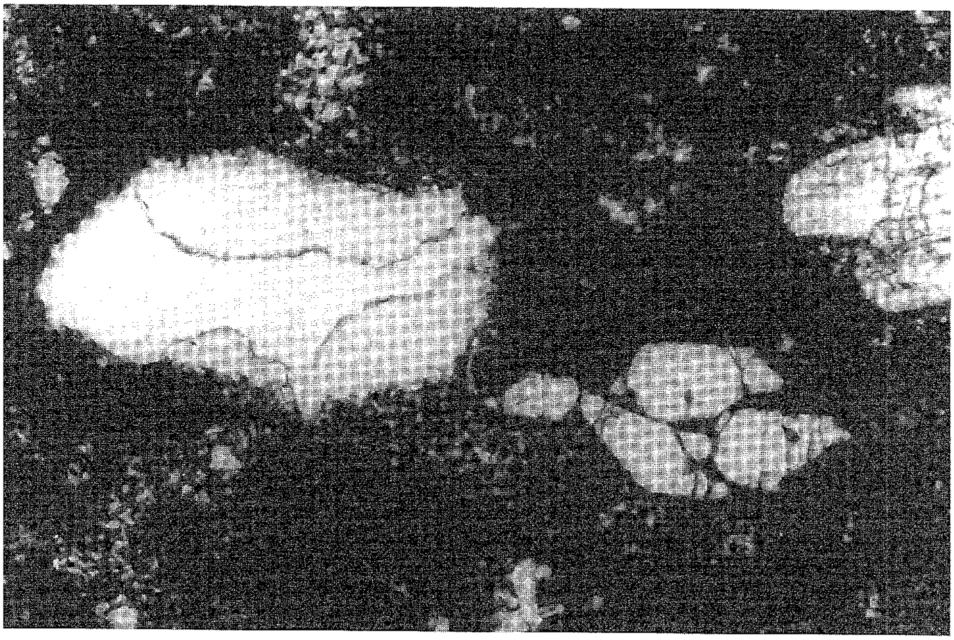

Fig. 11. Enclave in Puy Cordé phonolite (97-108c). Aggregate of slightly corroded crystals of olivine, vesicle with crystals of analcime. Upper right: aggregate of plagioclase crystals (plane polarized light, the olivine cluster is 1 mm long).

(Fig. 13). The feldspars and pyroxenes have inclusions of Fe-Ti oxides and apatite and show zonation. The titanite macrocrysts may be bent or broken and often show corroded outlines.

The matrix of some enclaves is dominated by acicular grains of brown amphibole, often arranged in a criss-cross felted fashion, with smaller amounts of acicular green clinopyroxene. In other enclaves the matrix is dominated by acicular green clinopyroxene with smaller amounts of brown amphibole. Fe-Ti oxides and apatite are always present. Feldspars and feldspathoids occupy the interstices between the above-mentioned minerals. The feldspathoids are isotropic and according to microprobe analyses of sodalitic composition.

Vesicles often have one or more of the minerals analcime, albite and nosean covering the walls (Fig. 7, 11), and they may be partly filled by calcite.

The trachyte along road D. 983 (Fig. 1) contains enclaves made up of aggregates of olivine crystals, the Sanadoire trachyte xenoliths of granites, and the Mouteyron and Sanadoire trachytes xenoliths of mylonitized quartzite.

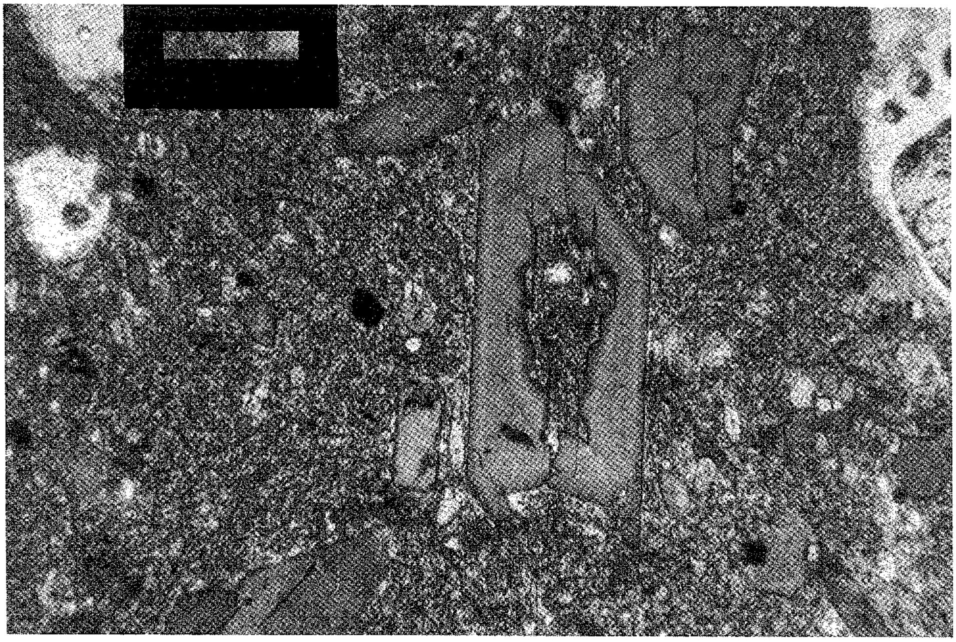

Fig. 12. Enclave, Trioulérou (97-107a). The phenocrysts are zoned crystals of kaersutite (brown), the largest crystal is hollow and is terminated by a mini-swallow-tail (plane polarized light, scale 0.6 mm).

## Analytical methods

Analyses of major and trace elements of silicate minerals were performed on a Camebax electron microprobe at Laboratoire de Pétrographie–Volcanologie, Université de Paris-Sud. Standard analytical conditions on this facility were 12 kv acceleration voltage, a 12 nA beam current, and counting times of 12-15 seconds. Some measurements were made on a Jeol JXCA 733 four channel electron microprobe at the Geological Institute, University of Copenhagen. The standard analytical conditions on this machine were 15 kv acceleration voltage, 15 nA beam current and counting times of 20 seconds. The data are ZAF corrected using the Tracor-Northern Correction Routine.

The detection of Zr-bearing minerals in the phonolites from F$^{me.}$ de Puy May and Trioulérou, was carried out at Laboratoire de Pétrographie–Volcanologie by means of Energy Dispersive Spectrometry, 15 kv acceleration voltage and counting time of 60 seconds.

Rock samples were analyzed by X-ray fluorescence methods. Major elements

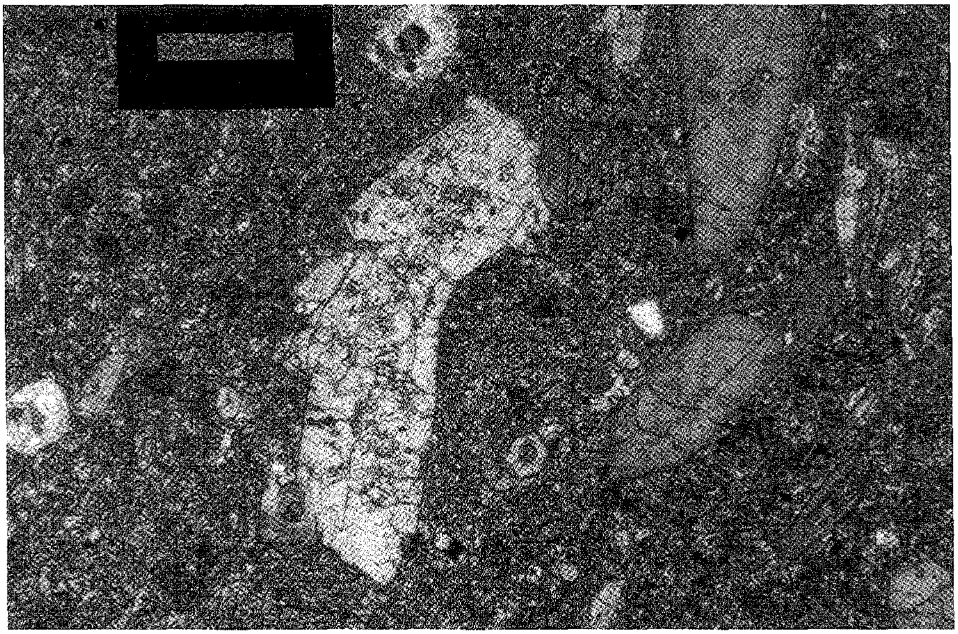

Fig. 13. Enclave, Trioulérou (97-107a). Bent zoned crystal of Al-Ti-rich clinopyroxene (white) together with zoned crystals of kaersutite (brown) in fine-grained matrix (plane polarized light, scale 0.6 mm).

were measured in glass discs at the Geological Survey of Greenland (now the Geological Survey of Denmark and Greenland), Copenhagen, and minor and trace elements in pressed powder pellets at the Geological Institute, University of Copenhagen. Na and Mg were determined by atomic absorption spectrometry and the volatile elements as loss on ignition. The REE, Th, Ta and Hf were determined by instrumental neutron activation analyses and U by the delayed neutron method at the National Research Laboratory Risø, Roskilde.

Chemical separation of Sr and REEs from whole rocks was carried out on conventional cation exchange columns, followed by a separation using HDEHP-coated beads (BIO-RAD) charged in 6 mm quartz glass columns. Purification of the Sr fraction was achieved by pass-over micro-columns containing SrSpec resin. Lead was separated conventionally in 0.5 mm glass columns charged with anion exchange resin, followed by a clean-up on 200 µl Teflon® columns. A standard HBr-HCl-$HNO_3$ elution recipe was applied for both column steps. Total Pb procedural blanks remained <125 pg, which relative to the amount of Pb in the analyzed samples is negligible. Isotope analyses were carried out on a VG Sector 54-IT instrument. Nd ratios were normalized to$^{146}$Nd/$^{144}$Nd = 0.7219. The main value for our internal JM Nd standard (referenced against La Jolla) during the period of measurement was 0.51115 for $^{143}Nd/^{144}Nd$, with a $2\sigma$ external reproducibility of ± 0.000011 (five measurements). The mean value of the NBS 987 Sr standard was 0.710248 for $^{87}Sr/^{86}Sr$, with a $2\sigma$ external reproducibilty of ± 0.000011 (four measurements). Fractionation for Pb was controlled by repetitive analysis of the NBS 981 standard (values of Todt *et al.*, 1993) and amounted to 0.103 ± 0.007 %/amu ($2\sigma$, n = 5).

## Mineral chemistry

*Feldspars*: Representative chemical analyses of feldspars are presented in Table 1. Sanidine is most widespread as phenocrysts and matrix mineral in trachytes and phonolites and covers a wide compositional field: $Ab_{30-53}Or_{44-67}An_{1-7}$ (wt. %). Anorthoclase is also present: $Ab_{42-87}Or_{12-37}An_{1-8}$, partly as ternary feldspar: $Ab_{47-64}Or_{27-37}An_{9-17}$.

The basaltic and trachybasaltic rocks have plagioclase $An_{50-60}$; the trachyandesitic rocks $An_{30-50}$; trachytes $An_{20-60}$; and phonolites $An_{19-31}$, but $An_{55-75}$ in their enclaves.

Sanidine microlites are predominant matrix minerals, except in the basaltic rocks. Most feldspar grains show normal zonation. In some rocks, the zoned feldspar grains have bytownite or andesine cores overgrown by sanidine.

*Feldspathoids*: The feldspathoids are sodalite, which occurs as colourless grains in thin section, and hauyne/nosean occurring as dark-coloured grains, often with black rims and black intersecting lines (cf. Brousse *et al.*, 1969). Representative chemical analyses of sodalite are presented in Table 1. The nepheline from Trioulérou has not been analyzed.

*Olivine*: Olivine occurs as crystals in basanite and as corroded grains in the trachytes and phonolites and some of their enclaves. In the trachytes and phonolites it has rims of clinopyroxene, amphibole and Fe-Ti oxides. In some rocks it is altered into iddingsite and iron oxides. All analyzed olivine grains have the composition $Fo_{79-82}$ (Table 2).

*Pyroxenes*: Pyroxene occurs as macrocrysts and as matrix microlites in all the rock types described, including the enclaves. They plot in the QUAD field (Morimoto, 1988) and belong to the diopside – hedenbergite series (Fig. 14). Two types of QUAD pyroxene can be distinguished. The green clinopyroxene is predominant in trachytes, phonolites and their enclaves. It is poor in Ti and Al, having very low contents of $^{vi}Al$ and less than 50 % wo. The brownish type contains up to 3.40 %

Table 1. Representative microprobe analyses of feldspars and feldspathoids from volcanic rocks of the Col de Guéry area. The feldspar formulae calculated on the basis of 8 oxygens. The feldspathoid formulae calculated on the basis of 21 oxygens.

Feldspars

| **Rock no.** | **88-948** | **88-948** | **88-948** | **88-924** | **88-924** | **88-924** | **88-951** | **88-951** | **88-951** | **88-953** | **88-953** | **88-953** | **88-953** | **88-953** |
|---|---|---|---|---|---|---|---|---|---|---|---|---|---|---|
| **RockType** | **Hawaiite** | **Hawaiite** | **Hawaiite** | **Trachyte** | **Trachyte** | **Trachyte** | **Phonolite** | **Phonolite** | **Phonolite** | **Phonolite** | **Phonolite** | **Phonolite** | **Phonolite** | **Phonolite** |
| $SiO_2$ | 56.58 | 48.25 | 63.55 | 64.66 | 62.91 | 57.41 | 65.72 | 65.55 | 66.64 | 63.51 | 66.04 | 65.49 | 65.70 | 65.64 |
| $TiO_2$ | – | – | – | – | – | – | 0.01 | 0.01 | 0.01 | 0.01 | 0.18 | 0.01 | 0.01 | 0.01 |
| $Al_2O_3$ | 27.21 | 31.97 | 21.02 | 19.96 | 21.69 | 27.27 | 19.47 | 19.77 | 18.76 | 22.96 | 18.76 | 19.71 | 19.19 | 20.30 |
| $Fe_2O_3$ | 0.81 | 0.64 | 0.23 | 0.44 | 0.54 | 0.48 | 0.22 | 0.01 | 0.49 | 0.46 | 0.58 | 0.01 | 0.46 | 0.01 |
| MgO | – | – | – | – | – | – | 0.01 | 0.01 | 0.01 | 0.16 | 0.01 | 0.01 | 0.01 | 0.01 |
| CaO | 9.65 | 15.36 | 2.46 | 0.86 | 2.68 | 8.78 | 0.59 | 0.63 | 0.23 | 4.05 | 0.34 | 0.63 | 0.31 | 0.77 |
| $Na_2O$ | 6.08 | 2.63 | 6.75 | 5.98 | 8.33 | 6.03 | 6.66 | 7.39 | 6.69 | 8.68 | 5.52 | 6.97 | 6.45 | 7.14 |
| $K_2O$ | 0.44 | 0.18 | 5.11 | 7.73 | 2.21 | 0.36 | 7.88 | 7.47 | 8.44 | 1.73 | 8.61 | 7.23 | 8.11 | 6.75 |
| TOTAL | 100.77 | 99.03 | 99.12 | 99.63 | 98.36 | 100.33 | 100.56 | 100.84 | 101.27 | 101.56 | 100.04 | 100.06 | 100.24 | 100.63 |
| Si | 2.54 | 2.24 | 2.87 | 2.93 | 2.84 | 2.57 | 2.95 | 2.93 | 2.98 | 2.79 | 2.98 | 2.94 | 2.96 | 2.93 |
| Al | 1.44 | 1.75 | 1.12 | 1.07 | 1.16 | 1.44 | 1.03 | 1.04 | 0.99 | 1.19 | 1.00 | 1.04 | 1.02 | 1.07 |
| Ti | 0.00 | 0.00 | 0.00 | 0.00 | 0.00 | 0.00 | 0.00 | 0.00 | 0.00 | 0.00 | 0.01 | 0.00 | 0.00 | 0.00 |
| $Fe^{3+}$ | 0.03 | 0.02 | 0.01 | 0.02 | 0.02 | 0.02 | 0.01 | 0.00 | 0.02 | 0.02 | 0.02 | 0.00 | 0.02 | 0.00 |
| Mg | 0.00 | 0.00 | 0.00 | 0.00 | 0.00 | 0.00 | 0.00 | 0.00 | 0.00 | 0.01 | 0.00 | 0.00 | 0.00 | 0.00 |
| Ca | 0.46 | 0.76 | 0.12 | 0.04 | 0.13 | 0.42 | 0.03 | 0.03 | 0.01 | 0.19 | 0.02 | 0.03 | 0.01 | 0.04 |
| Na | 0.53 | 0.24 | 0.59 | 0.53 | 0.73 | 0.52 | 0.58 | 0.64 | 0.58 | 0.74 | 0.48 | 0.61 | 0.56 | 0.62 |
| K | 0.03 | 0.01 | 0.29 | 0.45 | 0.13 | 0.02 | 0.45 | 0.43 | 0.48 | 0.10 | 0.50 | 0.41 | 0.47 | 0.38 |
| Oxygen | 8.00 | 8.00 | 8.00 | 8.00 | 8.00 | 8.00 | 8.00 | 8.00 | 8.00 | 8.00 | 8.00 | 8.00 | 8.00 | 8.00 |
| Cattot | 5.02 | 5.02 | 5.01 | 5.02 | 5.01 | 4.99 | 5.05 | 5.08 | 5.06 | 5.03 | 5.00 | 5.04 | 5.04 | 5.04 |
| $Or_t$ | 2.47 | 1.05 | 29.31 | 44.07 | 12.91 | 2.13 | 42.60 | 38.84 | 44.89 | 9.44 | 49.81 | 39.39 | 44.62 | 36.99 |
| $Ab_1$ | 51.96 | 23.41 | 58.84 | 51.81 | 73.95 | 54.23 | 54.72 | 58.41 | 54.08 | 72.00 | 48.54 | 57.72 | 53.94 | 59.47 |
| $An_1$ | 45.57 | 75.54 | 11.85 | 4.12 | 13.15 | 43.64 | 2.68 | 2.75 | 1.03 | 18.56 | 1.65 | 2.88 | 1.43 | 3.54 |
| Or wt.% | 2.72 | 0.99 | 35.68 | 53.05 | 16.72 | 2.37 | 52.08 | 48.22 | 54.95 | 11.96 | 59.50 | 48.75 | 54.54 | 46.04 |
| Ab wt.% | 37.60 | 14.47 | 47.14 | 41.04 | 63.01 | 39.75 | 44.02 | 47.71 | 43.55 | 60.03 | 38.15 | 47.00 | 43.38 | 48.70 |
| An wt.% | 59.68 | 84.53 | 17.18 | 5.90 | 20.27 | 57.88 | 3.90 | 4.07 | 1.50 | 28.01 | 2.35 | 4.25 | 2.08 | 5.25 |

$Or_1$ = orthoclase (K/(K+Na+Ca)x100, $Ab_1$ = albite (Na/(K+Na+Ca)x100, $An_1$ = anorthite (Ca/(K+Na+Ca)x100
Or wt.% = ($K_2O/K_2O+Na_2O+CaO$)x100, Ab wt.% = ($Na_2O/K_2O+Na_2O+CaO$)x100, An wt.% = ($CaO/K_2O+Na_2O+CaO$)x100

Feldspathoids

| **Rock no.** | **88-924** | **88-924** |
|---|---|---|
| **RockType** | **Trachyte** | **Trachyte** |
| $SiO_2$ | 35.10 | 35.13 |
| $TiO_2$ | 0.00 | 0.00 |
| $Al_2O_3$ | 28.54 | 29.57 |
| FeO | 0.22 | 0.49 |
| MgO | 0.00 | 0.00 |
| CaO | 6.45 | 6.00 |
| Na2O | 16.77 | 17.63 |
| $K_2O$ | 2.83 | 1.53 |
| TOTAL | 89.91 | 90.35 |
| Si | 6.109 | 6.021 |
| Al | 5.854 | 5.972 |
| Ti | 0.000 | 0.000 |
| $Fe^2$ | 0.032 | 0.070 |
| Mg | 0.000 | 0.000 |
| Ca | 1.203 | 1.102 |
| Na | 5.659 | 5.858 |
| K | 0.628 | 0.335 |
| oxy | 21 | 21 |

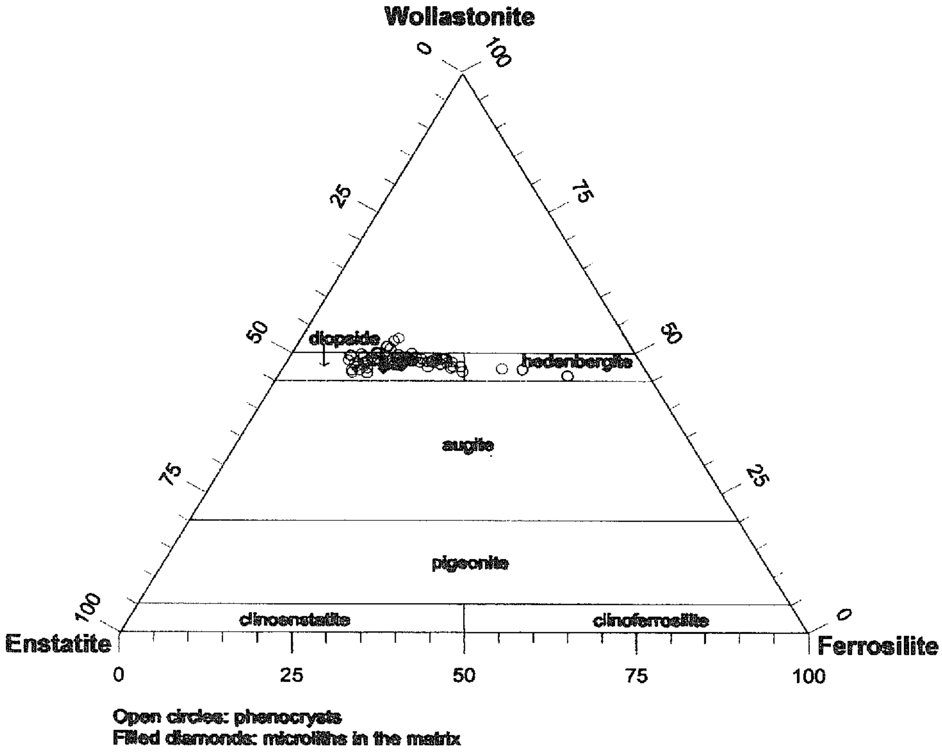

Fig. 14. The wo-en-fs diagram showing plots of analysed clinopyroxenes.

$TiO_2$ and 9.50 % $Al_2O_3$ having up to 0.050 $^{vi}Al$ per formula unit and about 50 % wo (Table 2). Stout prismatic crystals of this pyroxene occur in the trachyte along road D. 983, in the Sanadoire trachyte, as scarce small crystals in the Puy Cordé and Trioulérou phonolites, and as corroded grains in some enclaves in trachytes and phonolite. It is similar to the clinopyroxenes of the trachyandesites. The Trioulérou phonolite and some of the enclaves have prismatic grains of aegirine augite.

*Amphiboles*: The amphibole occurs as macrocrysts and as matrix microlites. The macrocrysts have developed black destabilization rims in the trachytes and phonolites, less so in the enclaves in these rocks. Amphibole inclusions in clinopyroxene and plagioclase in rocks and enclaves indicate an early crystallization.

According to Leake *et al.* (1997), the amphiboles are pargasite and kaersutite (Table 3, Fig. 15). The two amphiboles coexist; in one sample from Trioulérou an amphibole phenocryst has a core of pargasite and a rim of kaersutite. Amphibole

Table 2. Representative chemical analyses of olivines and clinopyroxenes from volcanic rocks of the Col de Guéry area. The olivine formulae calculated on the basis of 4 oxygens. The clinopyroxene calculated on the basis of 6 oxygens.

Olivines

| Rock no. | 88-953 | 88-953 |
|---|---|---|
| RockType | Phonolite | Phonolite |
| $SiO_2$ | 38.98 | 39.92 |
| $Al_2O_3$ | 0.01 | 0.01 |
| $TiO_2$ | 0.01 | 0.14 |
| $Cr_2O_3$ | 0.01 | 0.01 |
| FeO | 17.69 | 16.84 |
| MnO | 0.31 | 0.24 |
| NiO | 0.06 | 0.15 |
| MgO | 42.54 | 43.18 |
| CaO | 0.43 | 0.26 |
| $Na_2O$ | 0.01 | 0.01 |
| $K_2O$ | 0.01 | 0.01 |
| TOTAL | 100.07 | 100.77 |
| | | |
| Si | 0.991 | 1.066 |
| Al | 0.000 | 0.000 |
| Ti | 0.000 | 0.003 |
| Cr | 0.000 | 0.000 |
| $Fe^{2+}$ | 0.376 | 0.355 |
| Mn | 0.007 | 0.005 |
| Ni | 0.001 | 0.003 |
| Mg | 1.613 | 1.622 |
| Ca | 0.012 | 0.007 |
| Na | 0.000 | 0.000 |
| K | 0.000 | 0.000 |
| Mg# | 0.81 | 0.82 |
| Fa - % | 19 | 18 |
| Fo - % | 81 | 82 |

Clinopyroxenes

| Rock no. | 88-948 | 88-948 | 88-948 | 88-924 | 88-924 | 88-924 | 88-941 | Sanad.[1] | 88-951 | 88-951 | 88-951 | 88-953 | 88-953 | 88-953 | 88-953 | 97-107 | 97-107 |
|---|---|---|---|---|---|---|---|---|---|---|---|---|---|---|---|---|---|
| RockType | Hawaiite | Hawaiite | Hawaiite | Trachyte | Trachyte | Trachyte | Trachyte | Trachyte | Phonolite | Phonolite | Phonolite | Phonolite | Phonolite | Phonolite | Phonolite | Enclave | Enclave |
| $SiO_2$ | 49.21 | 43.91 | 41.06 | 49.49 | 49.09 | 48.32 | 47.17 | 42.15 | 50.91 | 48.25 | 49.49 | 49.54 | 46.84 | 45.78 | 43.53 | 48.97 | 46.82 |
| $TiO_2$ | 1.81 | 3.86 | 6.57 | 1.36 | 1.48 | 1.57 | 2.55 | 2.30 | 0.72 | 1.18 | 1.64 | 1.03 | 1.63 | 2.45 | 3.40 | 1.41 | 2.97 |
| $Al_2O_3$ | 4.34 | 8.27 | 10.33 | 3.81 | 4.16 | 6.04 | 5.09 | 12.30 | 2.48 | 4.23 | 2.95 | 2.67 | 1.96 | 7.74 | 8.50 | 5.40 | 3.89 |
| $Cr_2O_3$ | 0.84 | 0.00 | 0.00 | 0.69 | 1.19 | 1.09 | 1.06 | 0.00 | 0.13 | 0.01 | 0.01 | 0.01 | 0.01 | 0.01 | 0.20 | 0.01 | 0.17 |
| FeO | 6.74 | 7.79 | 8.01 | 7.86 | 8.23 | 5.52 | 10.00 | 13.60 | 10.72 | 13.24 | 12.12 | 11.78 | 20.50 | 7.54 | 8.11 | 10.83 | 11.41 |
| MnO | 0.09 | 0.16 | 0.00 | 0.55 | 0.39 | 0.16 | 0.43 | 0.00 | 1.09 | 1.12 | 1.40 | 1.39 | 2.56 | 0.01 | 0.15 | 1.09 | 1.38 |
| MgO | 14.54 | 11.43 | 10.93 | 13.18 | 12.49 | 14.29 | 11.42 | 12.70 | 10.83 | 9.01 | 9.48 | 9.42 | 3.23 | 12.41 | 11.28 | 9.02 | 8.68 |
| CaO | 23.05 | 22.99 | 23.30 | 23.28 | 22.85 | 23.70 | 21.48 | 15.20 | 22.42 | 21.81 | 20.99 | 20.82 | 17.37 | 22.87 | 22.59 | 18.97 | 20.03 |
| $Na_2O_2$ | 0.49 | 0.47 | 0.76 | 0.81 | 0.79 | 0.61 | 1.01 | 1.70 | 1.46 | 1.86 | 1.88 | 2.06 | 3.43 | 0.53 | 0.66 | 3.35 | 2.19 |
| TOTAL | 101.11 | 99.55 | 100.98 | 101.01 | 100.67 | 101.30 | 100.20 | 100.95 | 100.98 | 100.97 | 100.17 | 98.89 | 97.73 | 99.44 | 99.54 | 99.39 | 97.78 |
| | | | | | | | | | | | | | | | | | |
| $Fe_2O_3^{I}$ | 4.54 | 4.43 | 6.59 | 5.66 | 4.22 | 5.73 | 4.78 | 15.11 | 6.37 | 9.91 | 6.68 | 7.27 | 11.25 | 5.24 | 6.20 | 9.98 | 6.82 |
| $FeO^{I}$ | 2.66 | 3.80 | 2.08 | 2.77 | 4.43 | 0.36 | 5.70 | 0.00 | 4.99 | 4.32 | 6.11 | 5.24 | 10.38 | 2.83 | 2.53 | 1.85 | 5.28 |
| Sum | 101.56 | 99.99 | 101.64 | 101.58 | 101.09 | 101.87 | 100.68 | 102.46 | 101.62 | 101.96 | 100.84 | 99.62 | 98.86 | 99.96 | 100.16 | 100.39 | 98.46 |
| | | | | | | | | | | | | | | | | | |
| Si | 1.799 | 1.660 | 1.526 | 1.820 | 1.820 | 1.755 | 1.769 | 1.539 | 1.892 | 1.806 | 1.866 | 1.886 | 1.873 | 1.708 | 1.631 | 1.830 | 1.811 |
| $Al^{IV}$ | 0.187 | 0.340 | 0.452 | 0.165 | 0.182 | 0.245 | 0.225 | 0.461 | 0.108 | 0.187 | 0.131 | 0.114 | 0.092 | 0.292 | 0.369 | 0.170 | 0.177 |
| $Al^{VI}$ | 0.000 | 0.029 | 0.000 | 0.000 | 0.002 | 0.014 | 0.000 | 0.068 | 0.001 | 0.000 | 0.000 | 0.006 | 0.000 | 0.049 | 0.050 | 0.067 | 0.000 |
| Ti | 0.050 | 0.110 | 0.184 | 0.038 | 0.041 | 0.043 | 0.072 | 0.063 | 0.020 | 0.033 | 0.047 | 0.029 | 0.049 | 0.069 | 0.096 | 0.040 | 0.086 |
| Cr | 0.024 | 0.000 | 0.000 | 0.020 | 0.035 | 0.031 | 0.031 | 0.000 | 0.004 | 0.000 | 0.000 | 0.000 | 0.000 | 0.000 | 0.006 | 0.000 | 0.005 |
| $Fe^{2+}$ | 0.081 | 0.120 | 0.065 | 0.085 | 0.137 | 0.011 | 0.179 | 0.000 | 0.155 | 0.135 | 0.193 | 0.167 | 0.347 | 0.088 | 0.079 | 0.058 | 0.171 |
| $Fe^{3+}$ | 0.125 | 0.126 | 0.184 | 0.157 | 0.118 | 0.157 | 0.135 | 0.415 | 0.178 | 0.279 | 0.190 | 0.208 | 0.339 | 0.147 | 0.175 | 0.281 | 0.198 |
| Mn | 0.003 | 0.005 | 0.000 | 0.017 | 0.012 | 0.005 | 0.014 | 0.000 | 0.034 | 0.036 | 0.045 | 0.045 | 0.087 | 0.000 | 0.005 | 0.034 | 0.045 |
| Mg | 0.793 | 0.644 | 0.606 | 0.723 | 0.690 | 0.774 | 0.639 | 0.691 | 0.600 | 0.503 | 0.533 | 0.535 | 0.193 | 0.690 | 0.630 | 0.502 | 0.501 |
| Ca | 0.903 | 0.931 | 0.928 | 0.917 | 0.908 | 0.922 | 0.863 | 0.595 | 0.893 | 0.875 | 0.848 | 0.849 | 0.744 | 0.914 | 0.907 | 0.759 | 0.830 |
| Na | 0.035 | 0.034 | 0.055 | 0.058 | 0.057 | 0.043 | 0.073 | 0.120 | 0.105 | 0.135 | 0.137 | 0.152 | 0.266 | 0.038 | 0.048 | 0.243 | 0.164 |
| | | | | | | | | | | | | | | | | | |
| En | 41.67 | 35.36 | 33.97 | 38.40 | 37.25 | 41.51 | 35.17 | 40.63 | 32.86 | 28.06 | 30.22 | 30.39 | 11.87 | 37.52 | 35.18 | 31.39 | 29.44 |
| Fs | 10.84 | 13.52 | 13.97 | 12.85 | 13.77 | 9.00 | 17.28 | 24.41 | 18.25 | 23.13 | 21.68 | 21.32 | 42.26 | 12.79 | 14.19 | 21.15 | 21.72 |
| Wo | 47.49 | 51.12 | 52.06 | 48.75 | 48.98 | 49.49 | 47.55 | 34.95 | 48.89 | 48.81 | 48.10 | 48.28 | 45.87 | 49.70 | 50.64 | 47.46 | 48.84 |
| Mg (%) | 86.95 | 80.20 | 83.47 | 81.88 | 77.01 | 92.92 | 70.61 | 85.20 | 67.11 | 62.18 | 58.70 | 59.51 | 21.61 | 84.56 | 82.68 | 59.98 | 56.87 |
| $Fe^{2+}$+ Mn(%) | 9.21 | 15.57 | 8.95 | 11.55 | 16.63 | 1.92 | 21.33 | 0.00 | 21.14 | 21.14 | 26.21 | 23.58 | 48.60 | 10.78 | 11.02 | 10.99 | 24.52 |
| Na (%) | 3.84 | 4.23 | 7.58 | 6.57 | 6.36 | 5.16 | 8.07 | 14.80 | 11.74 | 16.69 | 15.09 | 16.91 | 29.79 | 4.66 | 6.30 | 29.03 | 18.62 |

Sum = (TOTAL + $Fe_2O_3$ + $FeO^{I}$) - FeO  $FeO^{I}$: Corrected FeO  $Fe_2O_3^{I}$: Corrected $Fe_2O_3$  $Al^{VI} = Al_{tot} - Al^{IV}$  $Al^{IV}$ = 2.00 - Si  [1] Brousse, 1961

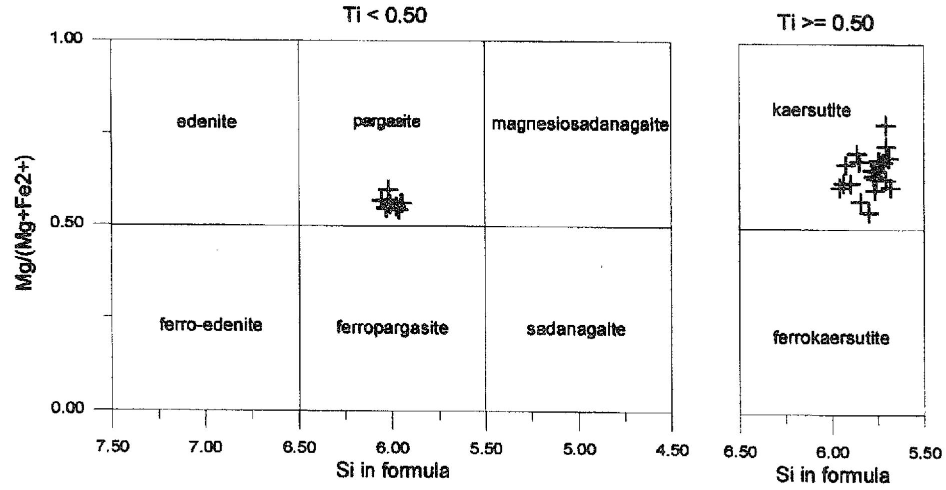

Fig. 15. Plots of the amphiboles according to Leake *et al.*(1997).

phenocrysts from the F$^{me.}$ de Puy May phonolite have kaersutite cores and marginal zones of pargasite.

*Mica*: Brown mica is found in trachytes, phonolites and most enclaves. It occurs as phenocrysts generally with inclusions of pyroxene, feldspar, apatite and Fe-Ti oxides. The micas from the trachytes along road D. 983 and at Roche Sanadoire, are biotite (Table 3), those from the Puy Cordé phonolite are phlogopite (Julien, 1988).

*Fe-Ti oxides*: Fe-Ti oxides occur both as euhedral phenocrysts, as microlites in the matrix, and as rims around other minerals, primarily the amphibole phenocrysts. Generally, the oxides are associated with pyroxene, amphibole and titanite crystals. In reflected light the Fe-Ti grains appear homogeneous, exsolution lamellae or other exsolution textures could not be observed.

The Fe-Ti oxides have $FeO_{tot.}$ contents between 60 and 82 wt.% and $TiO_2$ between 8 and 22 wt.%. With the exception of grains from hawaiite, all other analysed grains belong to the ilmenite – hematite solid solution series (Table 4, Fig. 16) and have high contents of Mn (0.54 to 4.62 wt.% MnO).

*Titanite*: Titanite is a common accessory mineral in the phonolites, trachytes, trachyandesites and trachybasalts. It is often associated with pyroxene, amphibole, feldspars, feldspathoids, Fe-Ti oxides and apatite and generally contains inclusions of Fe-Ti oxides and apatite.

Table 3. Representative chemical analyses of amphiboles and micas from volcanic rock, Col de Guéry area. Amphibole formulae calculated on the basis of 23 oxygens. The micas calculated on the basis of 22 oxygens.

Amphiboles

| **Rock no.** | **88-924** | **88-924** | **88-951** | **88-951** | **88-951** | **88-953** | **88-953** | **88-953** | **88-953** |
|---|---|---|---|---|---|---|---|---|---|
| **RockType** | **Trachyte** | **Trachyte** | **Phonolite** | **Phonolite** | **Phonolite** | **Phonolite** | **Phonolite** | **Phonolite** | **Phonolite** |
| $SiO_2$ | 39.03 | 40.35 | 38.94 | 38.13 | 39.00 | 38.26 | 39.51 | 38.13 | 39.04 |
| $Al_2O_3$ | 13.58 | 12.12 | 11.63 | 13.52 | 12.00 | 13.43 | 12.08 | 13.83 | 13.19 |
| $TiO_2$ | 5.61 | 5.64 | 4.25 | 4.82 | 3.89 | 5.29 | 4.27 | 5.31 | 4.82 |
| $Cr_2O_3$ | 0.00 | 0.00 | 0.01 | 0.01 | 0.01 | 0.01 | 0.01 | 0.01 | 0.01 |
| FeO | 12.69 | 13.47 | 15.31 | 14.84 | 15.69 | 11.09 | 13.60 | 10.47 | 12.27 |
| MnO | 0.07 | 0.24 | 0.60 | 0.64 | 0.40 | 0.01 | 0.18 | 0.01 | 0.63 |
| NiO | 0.00 | 0.00 | 0.01 | 0.04 | 0.01 | 0.07 | 0.01 | 0.01 | 0.05 |
| MgO | 12.17 | 11.88 | 10.67 | 9.96 | 10.39 | 12.94 | 11.29 | 12.77 | 11.42 |
| CaO | 12.13 | 11.71 | 11.49 | 11.60 | 11.49 | 12.16 | 11.65 | 12.29 | 11.90 |
| $Na_2O$ | 2.56 | 2.57 | 2.94 | 3.34 | 2.98 | 2.97 | 2.95 | 2.99 | 2.87 |
| $K_2O$ | 1.47 | 1.61 | 1.77 | 1.45 | 1.81 | 1.41 | 1.77 | 1.30 | 1.50 |
| TOTAL | 99.32 | 99.57 | 97.62 | 98.35 | 97.68 | 97.63 | 97.31 | 97.12 | 97.70 |
| | | | | | | | | | |
| $Fe_2O_3'$ | 0.21 | 0.00 | 0.42 | 0.00 | 0.14 | 0.00 | 0.00 | 0.00 | 0.00 |
| $FeO'$ | 12.50 | 13.47 | 14.94 | 14.84 | 15.57 | 11.09 | 13.60 | 10.47 | 12.27 |
| Sum | 99.34 | 99.57 | 97.66 | 98.35 | 97.69 | 97.63 | 97.31 | 97.12 | 97.70 |
| | | | | | | | | | |
| Si | 5.761 | 5.957 | 5.951 | 5.798 | 5.963 | 5.740 | 6.020 | 5.748 | 5.899 |
| $Al^{IV}$ | 2.239 | 2.043 | 2.049 | 2.202 | 2.037 | 2.260 | 1.980 | 2.252 | 2.101 |
| $Al^{VI}$ | 0.123 | 0.066 | 0.045 | 0.221 | 0.125 | 0.115 | 0.189 | 0.205 | 0.248 |
| Ti | 0.623 | 0.626 | 0.488 | 0.551 | 0.447 | 0.597 | 0.489 | 0.602 | 0.548 |
| Cr | 0.000 | 0.000 | 0.001 | 0.001 | 0.001 | 0.001 | 0.001 | 0.001 | 0.001 |
| $Fe^{2+}$ | 1.543 | 1.663 | 1.909 | 1.887 | 1.990 | 1.392 | 1.733 | 1.320 | 1.551 |
| $Fe^{3+}$ | 0.024 | 0.000 | 0.048 | 0.000 | 0.016 | 0.000 | 0.000 | 0.000 | 0.000 |
| Mn | 0.009 | 0.030 | 0.078 | 0.082 | 0.052 | 0.001 | 0.023 | 0.001 | 0.081 |
| Mg | 2.678 | 2.615 | 2.431 | 2.258 | 2.368 | 2.895 | 2.565 | 2.870 | 2.573 |
| Ca | 1.918 | 1.852 | 1.881 | 1.890 | 1.882 | 1.955 | 1.902 | 1.985 | 1.926 |
| $Na_X$ | 0.082 | 0.148 | 0.119 | 0.110 | 0.118 | 0.045 | 0.098 | 0.015 | 0.074 |
| $Na_A$ | 0.651 | 0.588 | 0.752 | 0.875 | 0.765 | 0.819 | 0.773 | 0.859 | 0.767 |
| K | 0.277 | 0.303 | 0.345 | 0.281 | 0.353 | 0.270 | 0.344 | 0.250 | 0.289 |
| Cattot | 15.928 | 15.891 | 16.097 | 16.156 | 16.119 | 16.088 | 16.117 | 16.109 | 16.056 |
| Oxygen | 23.000 | 23.009 | 23.000 | 23.083 | 23.000 | 23.046 | 23.103 | 23.126 | 23.113 |

$Al^{IV} = 8.00 - Si$
$Al^{VI} = Al_{total} - Al^{IV}$

$Na_X = 2.00 - Ca$
$Na_A = Na_{total} - Na_X$

$Fe_2O_3'$: Corrected $Fe_2O_3$
$FeO'$: Corrected FeO
Sum = (TOTAL + $Fe_2O_3'$ + $FeO'$) - FeO

Micas

| **Rock no.** | **88-924** | **88-924** | **88-924** |
|---|---|---|---|
| **RockType** | **Trachyte** | **Trachyte** | **Trachyte** |
| $SiO_2$ | 35.82 | 36.90 | 36.20 |
| $Al_2O_3$ | 14.79 | 14.89 | 14.62 |
| $TiO_2$ | 8.41 | 7.89 | 7.88 |
| FeO | 14.75 | 13.40 | 12.92 |
| MnO | 0.13 | 0.19 | 0.16 |
| MgO | 14.49 | 14.72 | 14.36 |
| CaO | 0.00 | 0.07 | 0.03 |
| $Na_2O$ | 0.69 | 0.95 | 0.82 |
| $K_2O$ | 8.42 | 8.59 | 8.70 |
| TOTAL | 97.50 | 97.60 | 95.69 |
| | | | |
| Si | 5.422 | 5.540 | 5.546 |
| $Al^{IV}$ | 2.578 | 2.460 | 2.454 |
| $Al^{VI}$ | 0.060 | 0.174 | 0.186 |
| Ti | 0.957 | 0.891 | 0.908 |
| $Fe^{2+}$ | 1.867 | 1.683 | 1.656 |
| Mn | 0.017 | 0.024 | 0.021 |
| Mg | 3.270 | 3.295 | 3.280 |
| Ca | 0.000 | 0.011 | 0.005 |
| Na | 0.203 | 0.277 | 0.244 |
| K | 1.626 | 1.645 | 1.700 |
| Mg# | 63.6 | 66.2 | 66.5 |

$Al^{IV} = 8.00 - Si$
$Al^{VI} = Al_{total} - Al^{IV}$

*Unidentified Zr mineral(s)*: In the matrix of the phonolites from F$^{me.}$ de Puy May and Trioulérou, submicroscopic grains with high contents of Ca, Ti, Zr and Si were detected by Energy Dispersive Spectrometry. It has not been possible to undertake complete chemical analyses, totals sum up only to 62 to 94 wt. %. F and the REE

Fig. 16. The $TiO_2$-$FeO$-$Fe_2O_3$ diagram with plots of Fe-Ti oxides.

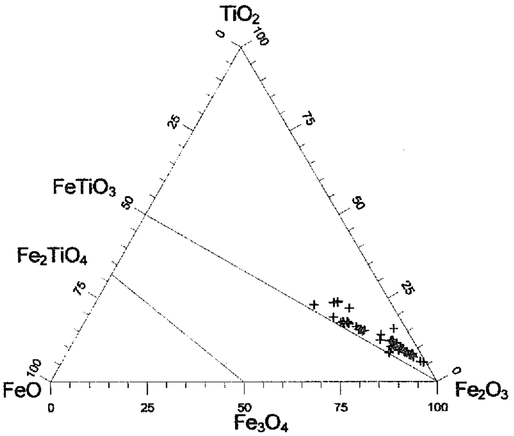

Table 4. Representative chemical analyses of Fe-Ti oxides from volcanic rocks, Col de Guéry area.

Fe-Ti oxides

| Rock no. | 88-948 | 88-948 | 88-924 | 88-924 | 88-941 | 88-941 | 88-941 | 88-940 | 88-951 | 88-951 | 88-953 | 88-953 | 97-107 | 97-107 |
|---|---|---|---|---|---|---|---|---|---|---|---|---|---|---|
| RockType | Hawaiite | Hawaiite | Trachyte | Trachyte | Trachyte | Trachyte | Trachyte | Teph.-pho | Phonolite | Phonolite | Phonolite | Phonolite | Enclave | Enclave |
| $SiO_2$ | 0.07 | 0.21 | 2.23 | 5.86 | 1.69 | 0.03 | 0.07 | 0.96 | 0.22 | 0.26 | 0.71 | 0.98 | 0.18 | 0.30 |
| $TiO_2$ | 22.12 | 23.12 | 15.99 | 14.01 | 16.62 | 17.12 | 14.84 | 18.55 | 8.67 | 7.98 | 11.74 | 9.01 | 10.55 | 9.97 |
| $Al_2O_3$ | 3.33 | 2.64 | 0.74 | 1.91 | 0.51 | 1.29 | 0.36 | 0.66 | 0.20 | 0.26 | 0.71 | 0.54 | 1.18 | 0.59 |
| $Cr_2O_3$ | 0.16 | 0.00 | 0.00 | 0.72 | 0.05 | 0.00 | 0.16 | 0.48 | 0.19 | 0.01 | 0.01 | 0.19 | 0.24 | 0.17 |
| FeO | 63.04 | 67.07 | 68.83 | 68.29 | 69.12 | 73.39 | 73.60 | 69.71 | 79.14 | 80.12 | 75.79 | 73.94 | 79.09 | 76.65 |
| MnO | 0.85 | 1.34 | 0.98 | 2.37 | 1.82 | 2.18 | 2.01 | 1.58 | 4.62 | 4.62 | 4.54 | 3.88 | 1.74 | 1.63 |
| MgO | 4.41 | 3.67 | 0.38 | 0.15 | 0.66 | 0.42 | 0.98 | 0.22 | 0.19 | 0.30 | 0.47 | 0.19 | 1.38 | 0.90 |
| CaO | 0.07 | 0.08 | 0.45 | 0.90 | 0.17 | 0.09 | 0.04 | 0.44 | 0.01 | 0.08 | 0.36 | 0.15 | 0.25 | 0.21 |
| $Na_2O$ | 0.00 | 0.00 | 0.00 | 0.00 | 0.00 | 0.00 | 0.00 | 0.00 | 0.01 | 0.01 | 0.01 | 0.07 | 0.01 | 0.01 |
| $K_2O$ | 0.00 | 0.00 | 0.00 | 0.00 | 0.00 | 0.00 | 0.00 | 0.00 | 0.10 | 0.19 | 0.01 | 0.18 | 0.08 | 0.07 |
| NiO | 0.00 | 0.00 | 0.00 | 0.00 | 0.00 | 0.00 | 0.00 | 0.00 | 0.01 | 0.09 | 0.01 | 0.07 | 0.01 | 0.01 |
| SUM | 94.05 | 98.12 | 89.60 | 94.21 | 90.65 | 94.58 | 92.06 | 92.60 | 93.37 | 93.93 | 94.37 | 89.22 | 97.71 | 90.52 |
| $Fe_2O_3^1$ | 57.65 | 60.21 | 62.37 | 64.86 | 63.56 | 67.74 | 71.17 | 61.15 | 84.87 | 86.95 | 78.55 | 77.98 | 82.05 | 78.85 |
| $FeO^1$ | 11.17 | 12.89 | 12.71 | 9.93 | 11.92 | 12.44 | 9.56 | 14.69 | 2.77 | 1.88 | 5.11 | 3.77 | 5.25 | 5.70 |
| TOTAL | 99.82 | 104.15 | 95.85 | 100.71 | 97.02 | 101.36 | 99.19 | 98.72 | 101.87 | 102.64 | 102.24 | 97.03 | 102.93 | 98.42 |
| Ti | 0.412 | 0.418 | 0.335 | 0.290 | 0.340 | 0.329 | 0.292 | 0.372 | 0.169 | 0.154 | 0.227 | 0.186 | 0.200 | 0.199 |
| Al | 0.097 | 0.075 | 0.024 | 0.062 | 0.016 | 0.039 | 0.011 | 0.021 | 0.006 | 0.008 | 0.022 | 0.017 | 0.035 | 0.019 |
| Cr | 0.003 | 0.000 | 0.000 | 0.016 | 0.001 | 0.000 | 0.003 | 0.010 | 0.004 | 0.000 | 0.000 | 0.004 | 0.005 | 0.004 |
| $Fe^{2+}$ | 0.231 | 0.259 | 0.296 | 0.228 | 0.271 | 0.266 | 0.209 | 0.327 | 0.060 | 0.040 | 0.110 | 0.086 | 0.111 | 0.127 |
| $Fe^{3+}$ | 1.075 | 1.089 | 1.306 | 1.343 | 1.302 | 1.303 | 1.402 | 1.226 | 1.653 | 1.683 | 1.523 | 1.607 | 1.559 | 1.579 |
| Mn | 0.018 | 0.027 | 0.023 | 0.055 | 0.042 | 0.047 | 0.045 | 0.036 | 0.101 | 0.101 | 0.099 | 0.090 | 0.037 | 0.037 |
| Mi | 0.000 | 0.000 | 0.000 | 0.000 | 0.000 | 0.000 | 0.000 | 0.000 | 0.000 | 0.002 | 0.000 | 0.002 | 0.000 | 0.000 |
| Mg | 0.163 | 0.132 | 0.016 | 0.006 | 0.027 | 0.016 | 0.038 | 0.009 | 0.007 | 0.012 | 0.018 | 0.008 | 0.052 | 0.036 |
| Cattot | 2.000 | 2.000 | 2.000 | 2.000 | 2.000 | 2.000 | 2.000 | 2.000 | 2.000 | 2.000 | 2.000 | 2.000 | 2.000 | 2.000 |
| Oxygen | 3.000 | 3.000 | 3.000 | 3.000 | 3.000 | 3.000 | 3.000 | 3.000 | 3.000 | 3.000 | 3.000 | 3.000 | 3.000 | 3.000 |

have, for instance, not been analyzed. One analysis shows a composition which is close to that of hainite described from phonolites in northern Bohemia (Blumrich, 1893; Johan & Cech, 1989 and Ulrych *et al.*, 1992). The other analyses could not be matched to known minerals.

## Geochemistry

### Major and trace elements

Chemical analyses of rocks from the Col de Guéry area are presented in Tables 5a, b and in Harker variation diagrams (Fig. 17a, b), in chondrite-normalized trace element variation diagrams (Fig. 18) and in REE diagrams (Fig. 19). Tables 6a, b list chemical analyses of enclaves from the area published by Brousse (1961c) and Decobecq (1987) together with two new analyses.

The Puy Cordé and Trioulérou phonolites have more than 10 % normative *ne* and are according to the IUGS classification (Le Maitre, 1989) true phonolites. The phonolite from F$^{me}$ de Puy May, which on the geological map (Brousse *et al.*, 1989) is marked as an agpaitic phonolite, has, however, in the new chemical analysis (Table 5a) only 7.81 % normative *ne*, which indicates a transition into trachytes in conformity with its position in the TAS diagram (Fig. 2) on the boundary between the trachyte and phonolite fields. The trachytes have in our analyses 0.99 % *qz* to 8.65 % *ne*. Normative *ac* is found in the Trioulérou and Puy Cordé phonolites, which are weakly peralkaline with agpaitic indices of 1.01-1.05. The other rocks have indices lower than 1.0 (Table 5a).

Trachybasalts and trachyandesites have up to 3.18 % normative *qz*. The silica-saturated and the silica-undersaturated series described in the literature on the Mont-Dore region (e.g. Brousse, 1961a) are thus both represented in the material studied by us.

The trachyandesites, trachytes and phonolites are rich in Na and K. The K contents are so high in the trachyandesites that they should be classified as latite and shoshonite according to the IUGS system (Le Maitre, 1989). Trachytes and phonolites, with the exception of the Trioulérou phonolite and one sample of Puy Cordé phonolite, are all potassic with $Na_2O - 2.0 < K_2O$ (Le Maitre, 1989).

The major elements of the silica-saturated and silica-undersaturated volcanic rocks are plotted in Fig. 17a and show a general increase in the contents of $Al_2O_3$, $Na_2O$ and $K_2O$, whereas MgO, $FeO_{tot.}$, CaO, $TiO_2$ and $P_2O_5$ decrease with increasing $SiO_2$. MgO and $FeO_{tot.}$ decrease in a way indicating the importance of olivine fractionation in the initial stage. $Al_2O_3$ shows a smooth trend from 42 to 55 % $SiO_2$ and a clustering of data points with $SiO_2$ contents higher than 55 %. It should be noted that at about 60 % $SiO_2$ there is a sharp increase in $Na_2O$ and an extreme de-

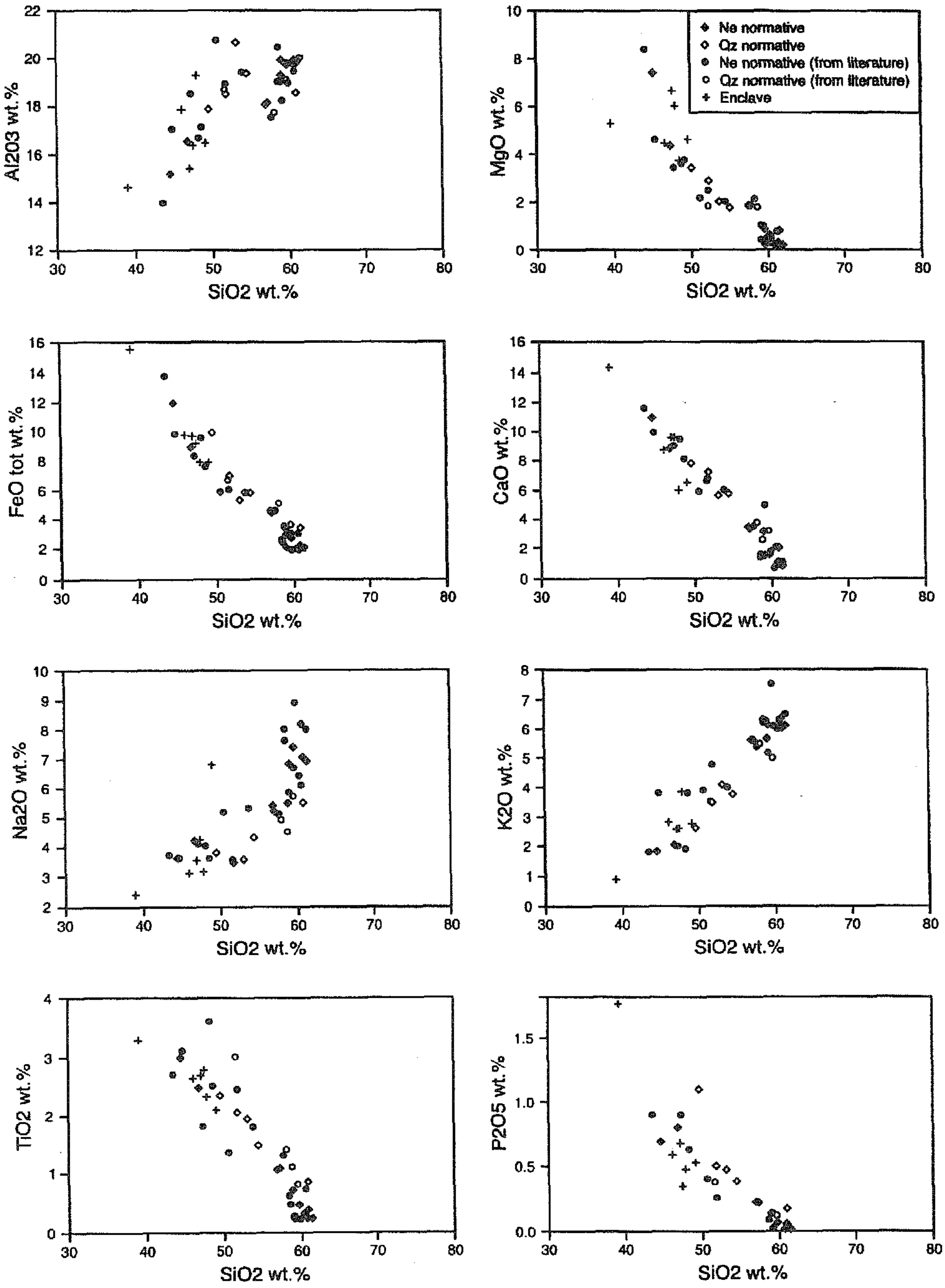

Fig. 17a. Harker variation diagrams of major elements.

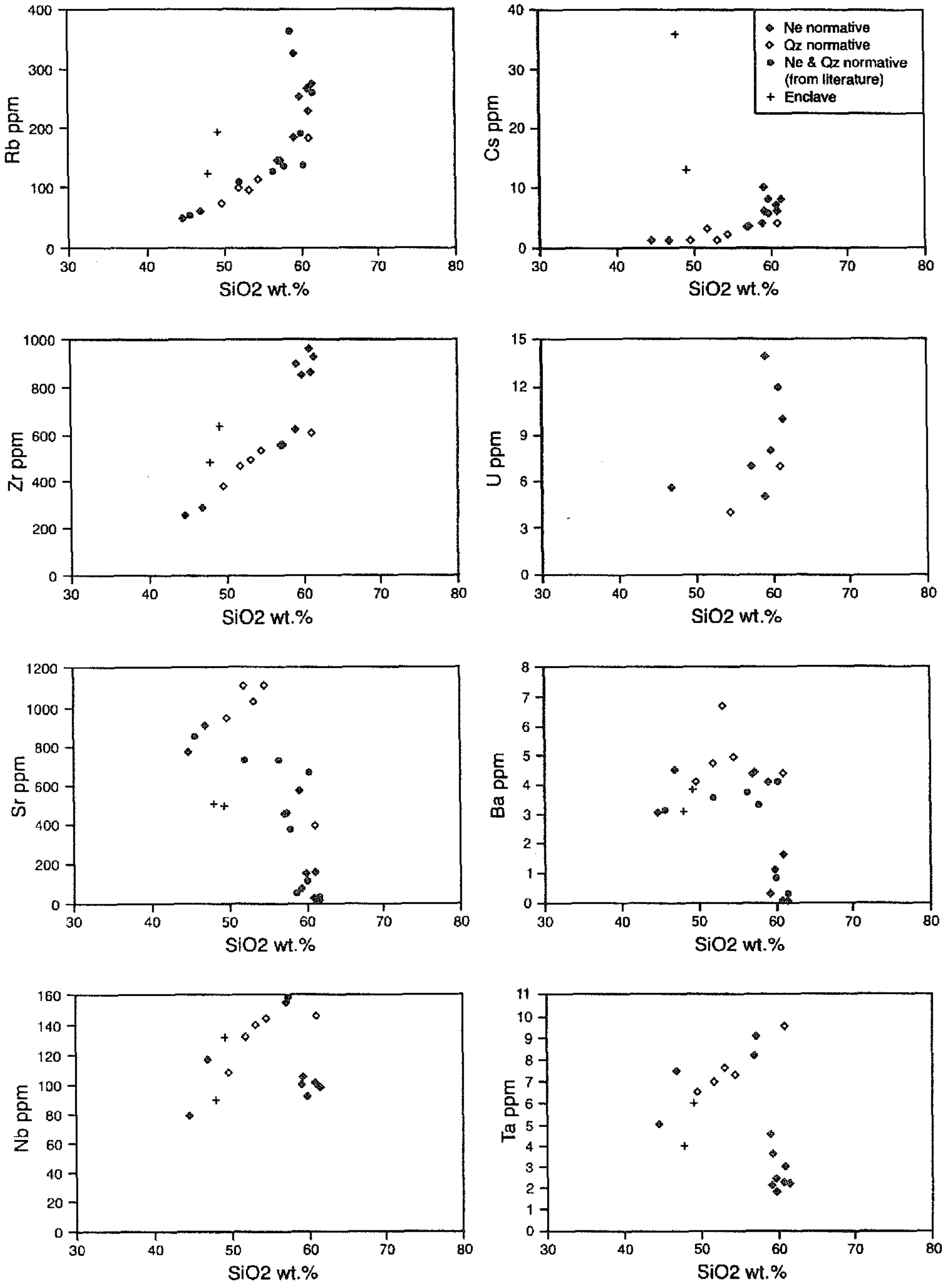

Fig. 17b. Harker variation diagrams of minor and trace elements.

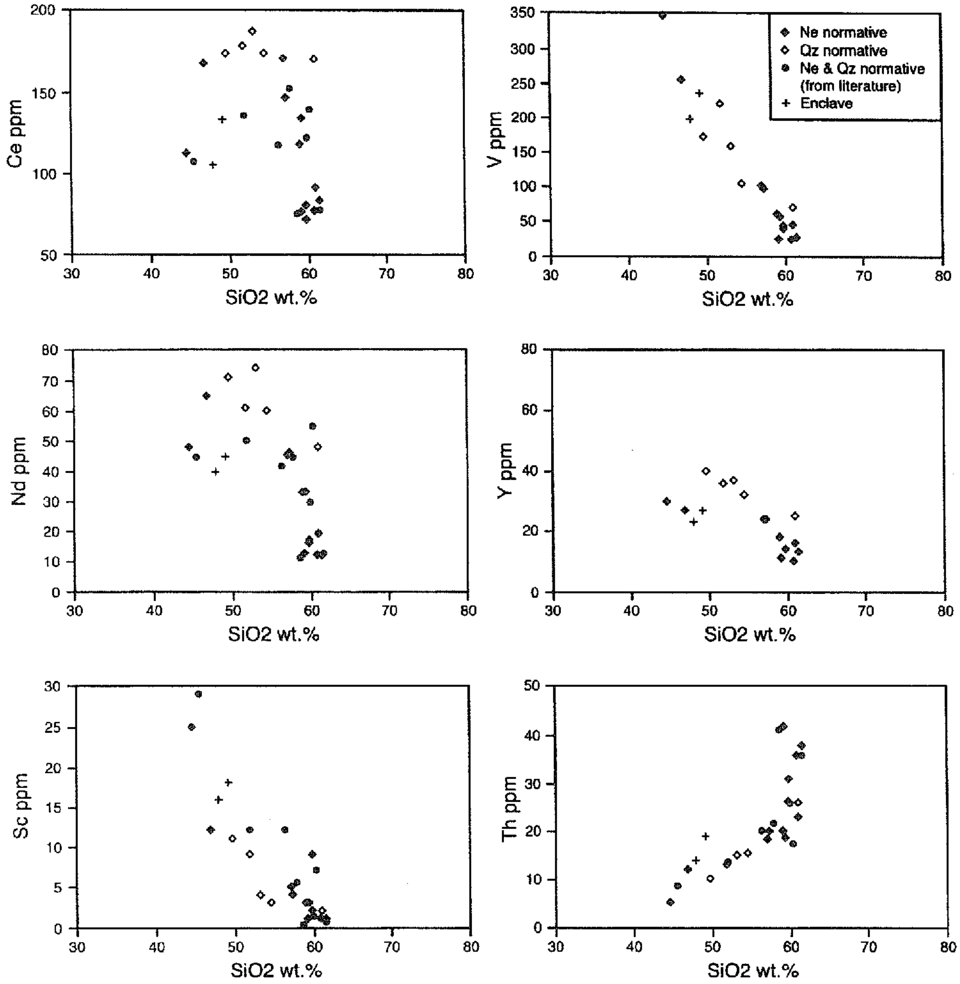

pletion in $P_2O_5$ and $TiO_2$, a feature also noted by Glangeaud & Létolle (1962). The data points of the silica-saturated and silica-undersaturated rocks fall along the same curves with minor exceptions ($FeO_{tot.}$, $Na_2O$, $K_2O$ and $P_2O_5$).

With the exception of Ce, Nd and Y, trace elements do not show any separation of the silica-saturated and silica-undersaturated rocks (Fig. 17b). Rb, Cs, Zr, U and Th behave as incompatible elements showing a moderate slope below 50-55 % $SiO_2$ and a very steep increase at about 60 % $SiO_2$ in phonolites and trachytes (Fig. 17b, Table 5b). This is accompanied by a steep decrease of Ni, Sc and V to extremely low values, showing the importance of fractionation of olivine, clinopy-

Table 5a. Whole rock chemical analyses, CIPW norms and D.I., and A.I of volcanic rocks from the Col de Guéry area.

| | Locality D | Rock 2 | Locality D | Locality 2 | Puy de l'Ouire | Malvialle | Col de Guéry | Locality B | Sanadoire | Sanadoire | Mouteyron | Tuilière | Trioulérou | Trioulérou | Puy Cordé | Puy Cordé | F$^{me.}$ Puy May | Bozat |
|---|---|---|---|---|---|---|---|---|---|---|---|---|---|---|---|---|---|---|
| Rock no. | 88-920 | 88-926 | 88-908 | 88-930 | 88-931 | 97-104 | 88-942 | 88-941 | 88-901 | HS88901B | 88-903 | 88-955 | 88-953 | 97-106 | 88-954 | 97108-2 | 88-951 | 97-110 |
| Age (Ma) | - | - | - | - | - | - | - | - | 1.83± 0.10 | | 1.92± 0.10 | 2.10± 0.10 | 2.01± 0.06 | | 2.03± 0.11 | | - | 0.73± 0.04 |
| | Basanite | Hawaiite | K-Trachyandesite | K-Trachyandesite | K-Trachyandesite | K-Trachyandesite | Trachyte | Trachyte | Trachyte | Trachyte | Trachyte | Trachyte | Phonolite | Phonolite | Phonolite | Phonolite | Phonolite | Phonolite |
| $SiO_2$ | 44.63 | 46.91 | 49.67 | 51.88 | 53.22 | 54.56 | 57.09 | 61.04 | 59.08 | 59.35 | 59.22 | 61.51 | 60.84 | 60.83 | 59.83 | 59.83 | 61.01 | 60.84 |
| $TiO_2$ | 2.99 | 2.48 | 2.34 | 2.05 | 1.94 | 1.48 | 1.06 | 0.85 | 0.70 | 0.69 | 0.22 | 0.22 | 0.23 | 0.25 | 0.45 | 0.43 | 0.37 | 0.50 |
| $Al_2O_3$ | 15.15 | 16.52 | 17.86 | 18.47 | 20.67 | 19.36 | 18.05 | 18.55 | 19.29 | 19.38 | 19.92 | 19.97 | 19.87 | 20.00 | 19.77 | 19.84 | 19.82 | 19.05 |
| $Fe_2O_3$ | 3.53 | 3.77 | 5.83 | 5.15 | 3.85 | 4.51 | 2.25 | 2.44 | 2.14 | 1.67 | 1.58 | 1.48 | 1.09 | 1.05 | 1.66 | 1.44 | 1.78 | 1.60 |
| Feo | 8.39 | 5.16 | 4.08 | 1.80 | 1.46 | 1.33 | 2.28 | 0.96 | 1.21 | 1.35 | 0.52 | 0.58 | 0.85 | 0.82 | 1.04 | 0.98 | 0.42 | 1.11 |
| MnO | 0.19 | 0.19 | 0.22 | 0.14 | 0.13 | 0.16 | 0.14 | 0.11 | 0.13 | 0.14 | 0.16 | 0.13 | 0.13 | 0.14 | 0.13 | 0.14 | 0.13 | 0.19 |
| MgO | 7.43 | 4.37 | 3.43 | 2.88 | 2.02 | 1.75 | 1.88 | 0.80 | 0.87 | 0.76 | 0.20 | 0.18 | 0.17 | 0.15 | 0.57 | 0.49 | 0.24 | 0.43 |
| CaO | 10.97 | 8.87 | 7.85 | 7.24 | 5.64 | 5.78 | 3.46 | 2.06 | 3.17 | 2.74 | 1.51 | 0.87 | 0.93 | 1.01 | 1.55 | 1.55 | 1.08 | 1.39 |
| $Na_2O$ | 3.62 | 4.20 | 3.79 | 3.45 | 3.56 | 4.31 | 5.38 | 5.49 | 5.48 | 6.34 | 6.82 | 6.92 | 8.18 | 8.64 | 7.39 | 8.21 | 7.04 | 7.76 |
| $K_2O$ | 1.84 | 2.05 | 2.61 | 3.49 | 4.09 | 3.76 | 5.61 | 6.07 | 5.66 | 5.71 | 6.14 | 6.13 | 6.08 | 6.25 | 6.07 | 6.09 | 6.36 | 5.80 |
| $P_2O_5$ | 0.69 | 0.80 | 1.10 | 0.50 | 0.47 | 0.38 | 0.22 | 0.17 | 0.13 | 0.13 | 0.02 | 0.01 | 0.01 | 0.03 | 0.06 | 0.06 | 0.05 | 0.08 |
| LOI | 0.37 | 4.05 | 0.75 | 2.10 | 2.28 | 1.82 | 2.05 | 0.73 | 1.47 | 1.19 | 3.05 | 1.18 | 0.41 | 0.89 | 0.73 | 0.63 | 1.12 | 0.27 |
| Total | 99.80 | 99.37 | 99.53 | 99.15 | 99.33 | 99.20 | 99.47 | 99.27 | 99.33 | 99.45 | 99.36 | 99.18 | 98.79 | 100.06 | 99.25 | 99.69 | 99.42 | 99.02 |

CIPW

| | | | | | | | | | | | | | | | | | | |
|---|---|---|---|---|---|---|---|---|---|---|---|---|---|---|---|---|---|---|
| *Qz* | 0.00 | 0.00 | 0.48 | 1.85 | 3.18 | 2.05 | 0.00 | 0.99 | 0.00 | 0.00 | 0.00 | 0.00 | 0.00 | 0.00 | 0.00 | 0.00 | 0.00 | 0.00 |
| *C* | 0.00 | 0.00 | 0.00 | 0.00 | 1.30 | 0.00 | 0.00 | 0.00 | 0.00 | 0.00 | 0.00 | 0.40 | 0.00 | 0.00 | 0.00 | 0.00 | 0.00 | 0.00 |
| *Or* | 10.94 | 12.71 | 15.62 | 21.25 | 24.91 | 22.82 | 34.04 | 36.41 | 34.18 | 34.35 | 37.68 | 36.97 | 36.53 | 37.25 | 36.42 | 36.34 | 38.24 | 34.71 |
| *Ab* | 10.83 | 28.21 | 32.46 | 30.08 | 31.04 | 37.45 | 39.36 | 47.14 | 44.81 | 43.61 | 43.94 | 50.45 | 44.23 | 38.87 | 42.54 | 39.14 | 46.19 | 47.42 |
| *An* | 19.77 | 21.17 | 24.31 | 25.36 | 25.67 | 22.98 | 8.76 | 8.17 | 11.57 | 7.70 | 5.83 | 4.34 | 0.00 | 0.00 | 2.90 | 0.00 | 3.77 | 0.02 |
| *Ne* | 10.82 | 4.91 | 0.00 | 0.00 | 0.00 | 0.00 | 3.99 | 0.00 | 1.39 | 5.95 | 8.65 | 5.04 | 13.68 | 16.14 | 11.33 | 16.07 | 7.81 | 10.33 |
| *Ac* | 0.00 | 0.00 | 0.00 | 0.00 | 0.00 | 0.00 | 0.00 | 0.00 | 0.00 | 0.00 | 0.00 | 0.00 | 0.76 | 3.06 | 0.00 | 1.17 | 0.00 | 0.00 |
| *Di* | 24.53 | 15.54 | 6.10 | 6.45 | 0.00 | 3.05 | 5.85 | 0.84 | 2.83 | 4.15 | 1.12 | 0.00 | 2.33 | 3.38 | 3.18 | 3.59 | 1.05 | 2.80 |
| *Wo* | 0.00 | 0.00 | 0.00 | 0.00 | 0.00 | 0.00 | 0.00 | 0.00 | 0.00 | 0.00 | 0.16 | 0.00 | 0.77 | 0.39 | 0.18 | 1.22 | 0.00 | 1.21 |
| *Hy* | 0.00 | 0.00 | 5.82 | 4.40 | 5.18 | 3.06 | 0.00 | 1.63 | 0.00 | 0.00 | 0.00 | 0.00 | 0.00 | 0.00 | 0.00 | 0.00 | 0.00 | 0.00 |
| *Ol* | 10.64 | 4.84 | 0.00 | 0.00 | 0.00 | 0.00 | 2.07 | 0.00 | 0.63 | 0.14 | 0.00 | 0.32 | 0.00 | 0.00 | 0.00 | 0.00 | 0.08 | 0.00 |
| *Mt* | 5.15 | 5.73 | 7.17 | 0.33 | 0.00 | 0.53 | 3.35 | 1.00 | 2.34 | 2.46 | 1.62 | 1.69 | 1.23 | 0.00 | 2.44 | 1.52 | 0.72 | 2.35 |
| *Hm* | 0.00 | 0.00 | 0.95 | 5.08 | 3.97 | 4.26 | 0.00 | 1.78 | 0.57 | 0.00 | 0.52 | 0.34 | 0.00 | 0.00 | 0.00 | 0.00 | 1.32 | 0.00 |
| *Il* | 5.71 | 4.94 | 4.50 | 4.01 | 3.46 | 2.88 | 2.07 | 1.64 | 1.36 | 1.33 | 0.43 | 0.43 | 0.44 | 0.48 | 0.87 | 0.82 | 0.71 | 0.96 |
| *Ru* | 0.00 | 0.00 | 0.00 | 0.00 | 0.18 | 0.00 | 0.00 | 0.00 | 0.00 | 0.00 | 0.00 | 0.00 | 0.00 | 0.00 | 0.00 | 0.00 | 0.00 | 0.00 |
| *Ap* | 1.64 | 1.99 | 2.64 | 1.22 | 1.15 | 0.92 | 0.53 | 0.41 | 0.31 | 0.31 | 0.05 | 0.02 | 0.02 | 0.07 | 0.14 | 0.14 | 0.12 | 0.19 |
| D.I. | 32.59 | 45.83 | 48.56 | 53.18 | 59.13 | 62.32 | 77.39 | 84.54 | 80.38 | 83.91 | 90.27 | 92.46 | 94.44 | 92.26 | 90.29 | 91.55 | 92.24 | 92.46 |
| A.I. | 0.52 | 0.55 | 0.51 | 0.51 | 0.50 | 0.58 | 0.83 | 0.84 | 0.78 | 0.86 | 0.90 | 0.90 | 1.01 | 1.05 | 0.95 | 1.01 | 0.93 | 1.00 |

Table 5b. Trace element composition and selected trace element ratios of the rocks of Table 5a.

| | Locality D | Rock 2 | Locality D | Locality 2 | Puy de l'Ouire | Malvialle | Col de Guéry | Locality B | Sanadoire | Sanadoire | Mouteyron | Tuilière | Triouľérou | Triouľérou | Puy Cordé | Puy Cordé | F$^{me.}$ Puy May | Bozat |
|---|---|---|---|---|---|---|---|---|---|---|---|---|---|---|---|---|---|---|
| Rock no. | 88-920 | 88-926 | 88-908 | 88-930 | 88-931 | 97-104 | 88-942 | 88-941 | 88-901 | HS88901B | 88-903 | 88-955 | 88-953 | 97-106 | 88-954 | 97108-2 | 88-951 | 97-110 |
| Age (Ma) | - | - | - | - | - | - | - | - | 1.83± 0.10 | | 1.92± 0.10 | 2.10± 0.10 | 2.01± 0.06 | | 2.03± 0.11 | | - | 0.73± 0.04 |
| | Basanite | Hawaiite | K-Trachyandesite | K-Trachyandesite | K-Trachyandesite | K-Trachyandesite | Trachyte | Trachyte | Trachyte | Trachyte | Trachyte | Trachyte | Phonolite | Phonolite | Phonolite | Phonolite | Phonolite | Phonolite |
| Sc | 25 | 12 | 11 | 9 | 4 | 3 | 4 | 2 | 3 | 3 | 0.5 | 1 | 0.4 | 0.4 | 2 | 3 | 1 | 0.9 |
| V | 348 | 256 | 172 | 221 | 158 | 104 | 98 | 70 | 60 | 57 | 25 | 27 | 24 | 25 | 43 | 39 | 45 | 24 |
| Cr | 144 | 68 | 11 | 7 | 7 | 2 | 51 | 7 | 13 | 9 | 5 | <1 | 0,4 | 0,7 | 6 | 5 | 0.7 | 1 |
| Ni | 69 | 31 | 6 | 13 | 9 | 4 | 24 | 5 | 7 | 6 | 4 | 5 | 3 | 3 | 7 | 6 | 3 | 4 |
| Cu | 67 | 30 | 9 | 25 | 21 | 14 | 11 | 5 | 8 | 10 | <2 | <2 | 5 | 4 | 5 | 10 | 6 | 8 |
| Zn | 113 | 84 | 106 | 105 | 109 | 87 | 80 | 69 | 76 | 71 | 84 | 76 | 76 | 71 | 71 | 69 | 61 | 72 |
| Rb | 47 | 59 | 72 | 98 | 94 | 112 | 145 | 182 | 184 | 199 | 326 | 275 | 266 | 275 | 253 | 253 | 228 | 209 |
| Sr | 773 | 908 | 947 | 1110 | 1030 | 1110 | 457 | 390 | 575 | 500 | 70 | 13 | 21 | 31 | 151 | 129 | 157 | 82 |
| Y | 30 | 27 | 40 | 36 | 37 | 32 | 24 | 25 | 18 | 21 | 11 | 13 | 10 | 10 | 14 | 12 | 16 | 20 |
| Zr | 256 | 287 | 379 | 468 | 493 | 534 | 560 | 609 | 624 | 681 | 899 | 929 | 965 | 952 | 851 | 869 | 863 | 794 |
| Nb | 79 | 117 | 108 | 132 | 140 | 144 | 158 | 146 | 100 | 102 | 105 | 98 | 101 | 96 | 92 | 88 | 100 | 144 |
| Cs | 1 | 1 | 1 | 3 | 1 | 2 | 3 | 4 | 4 | 6 | 10 | 8 | 7 | 7 | 8 | 6 | 6 | 5 |
| Ba | 606 | 902 | 816 | 944 | 1340 | 989 | 886 | 877 | 821 | 743 | 56 | 6 | 6 | 20 | 223 | 191 | 264 | 191 |
| La | 54 | 92 | 82 | 91 | 120 | 104 | 94 | 108 | 77 | 77 | 76 | 77 | 72 | 65 | 68 | 62 | 71 | 90 |
| Ce | 112 | 168 | 174 | 179 | 188 | 174 | 147 | 171 | 118 | 134 | 76 | 83 | 77 | 90 | 80 | 71 | 91 | 126 |
| Nd | 48 | 65 | 71 | 61 | 74 | 60 | 46 | 48 | 33 | 33 | 13 | 12 | 12 | 13 | 17 | 16 | 19 | 29 |
| Sm | 9.3 | 10.1 | 12.0 | 10.4 | 11.6 | 8.3 | 5.5 | 5.7 | 3.7 | 4.1 | 0.5 | 0.6 | 0.7 | 1.5 | 1.5 | 1.3 | 1.7 | 2.8 |
| Eu | 2.8 | 3.1 | 3.4 | 2.8 | 3.0 | 2.5 | 1.6 | 1.6 | 1.2 | 1.0 | 0.3 | 0.2 | 0.2 | 0.2 | 0.5 | 0.4 | 0.5 | 0.7 |
| Tb | 1.2 | 1.4 | 1.6 | 1.3 | 1.5 | 1.1 | 0.8 | 0.8 | 0.5 | 0.5 | 0.2 | 0.1 | 0.2 | 0.2 | 0.2 | 0.2 | 0.3 | 0.4 |
| Yb | 2.7 | 2.9 | 4.0 | 3.0 | 3.4 | 2.8 | 2.3 | 2.3 | 1.8 | 2.2 | 1.9 | 1.6 | 1.2 | 1.1 | 1.2 | 1.7 | 1.7 | 2.2 |
| Lu | 0.3 | 0.5 | 0.5 | 0.5 | 0.5 | 0.4 | 0.3 | 0.2 | 0.3 | 0.3 | 0.3 | 0.3 | 0.2 | 0.3 | 0.2 | 0.3 | 0.3 | 0.4 |
| Hf | 6.4 | 7.3 | 9.4 | 9.8 | 9.7 | 9.5 | 9.7 | 11.4 | 10.5 | 11.2 | 15.4 | 15.7 | 15.0 | 14.7 | 13.1 | 13.4 | 15.0 | 13.9 |
| Ta | 5.0 | 7.5 | 6.5 | 7.0 | 7.6 | 7.3 | 9.1 | 9.5 | 4.5 | 3.6 | 2.1 | 2.2 | 2.3 | 1.7 | 2.4 | 1.8 | 3.0 | 5.1 |
| Th | 5.2 | 12.1 | 10.1 | 12.8 | 14.6 | 15.5 | 20.0 | 26.4 | 20.3 | 18.6 | 42.4 | 37.9 | 36.2 | 26.0 | 31.1 | 26.1 | 23.0 | 28.5 |
| U | n.d. | 5.6 | n.d. | n.d. | n.d. | 4.0 | n.d. | 7.0 | 5.0 | n.d. | 14.1 | 9.7 | 12.1 | n.d. | 7.5 | n.d. | n.d. | 7.8 |
| Y/Nb | 0.380 | 0.231 | 0.370 | 0.273 | 0.264 | 0.222 | 0.152 | 0.171 | 0.180 | 0.206 | 0.105 | 0.133 | 0.099 | 0.104 | 0.152 | 0.136 | 0.160 | 0.139 |
| Yb/Ta | 0.542 | 0.387 | 0.620 | 0.429 | 0.443 | 0.384 | 0.253 | 0.242 | 0.400 | 0.611 | 0.905 | 0.727 | 0.522 | 0.647 | 0.500 | 0.944 | 0.567 | 0.431 |
| Sc/Nb | 0.316 | 0.103 | 0.102 | 0.068 | 0.029 | 0.021 | 0.025 | 0.014 | 0.030 | 0.029 | 0.005 | 0.010 | 0.004 | 0.004 | 0.022 | 0.034 | 0.006 | 0.006 |
| Ba/La | 11.243 | 9.836 | 9.903 | 10.408 | 11.167 | 9.510 | 9.476 | 8.120 | 10.621 | 9.649 | 0.737 | 0.078 | 0.083 | 0.309 | 3.279 | 3.081 | 3.718 | 2.127 |
| Zr/Nb | 3.241 | 2.453 | 3.509 | 3.545 | 3.521 | 3.708 | 3.544 | 4.171 | 6.240 | 6.676 | 8.562 | 9.480 | 9.554 | 9.917 | 9.250 | 9.875 | 8.630 | 5.514 |
| Ce/NB | 1.418 | 1.436 | 1.611 | 1.356 | 1.343 | 1.208 | 0.930 | 1.171 | 1.180 | 1.314 | 0.724 | 0.842 | 0.760 | 0.935 | 0.872 | 0.807 | 0.910 | 0.875 |
| Nb/Ta | 40.252 | 39.315 | 40.362 | 47.658 | 51.088 | 56.211 | 57.732 | 53.421 | 59.429 | 60.804 | 58.377 | 59.172 | 64.333 | 64.762 | 64.962 | 64.851 | 57.533 | 57.122 |
| La/Yb | 19.889 | 31.621 | 20.447 | 30.233 | 35.608 | 37.143 | 40.652 | 46.957 | 42.944 | 35.000 | 40.000 | 48.250 | 59.917 | 58.909 | 56.667 | 36.471 | 41.765 | 40.818 |

n.d. - not determined

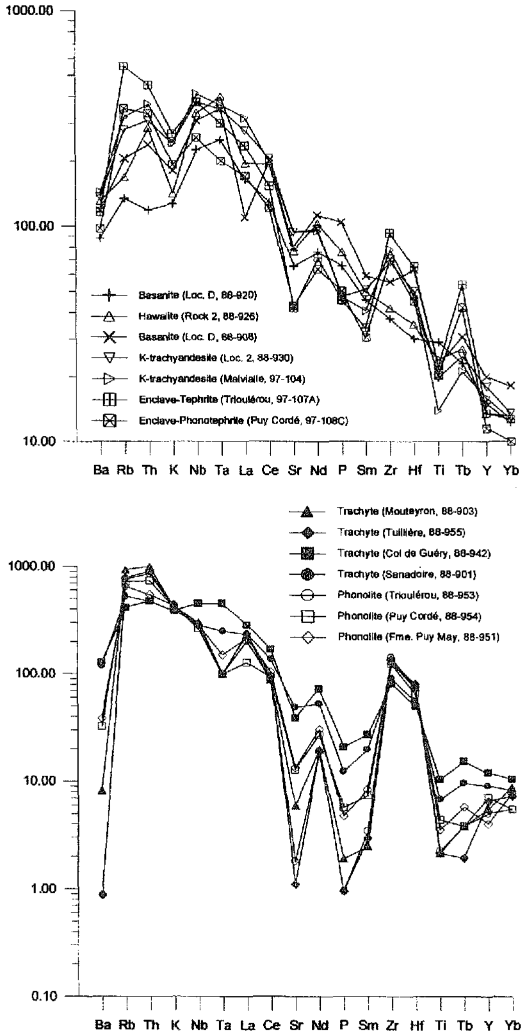

Fig. 18. Chondrite-normalized trace element variation diagrams (normalized according to Thompson *et al.*, 1984).

roxene and Fe-Ti oxides. In Fig 17b, Sr, Ba, Nb, Ta, La, Ce, Nd and Y behave as incompatible elements at low $SiO_2$ and show the highest values at 50-55 % $SiO_2$. At higher $SiO_2$ contents they behave as compatible elements reaching the lowest values in the phonolites and the Mouteyron and Tuilière trachytes. It is interesting to note that the Ce/Nb, Y/Nb, Nb/Ta and Zr/Nb ratios (Table 5b) are relatively constant from basanite to some trachytes, but that the most evolved trachytes and phonolites have lower Ce/Nb and Y/Nb ratios and higher Nb/Ta and Zr/Nb ratios than these rocks. This means that there has been a fractionation of Nb relative to Ce, Y, Ta and Zr during magma evolution.

Phonolites and the Mouteyron and Tuilière trachytes are geochemically related. They were formed around 2.0 Ma ago and will hereafter be termed the '2.0 Ma rocks'. The Puy Cordé and F$^{me}$ de Puy May phonolites differ from the other 2.0 Ma rocks by less evolved chemical compositions. They have higher contents of Ti, Fe, Mg, P, Sc, V, Sr, Ba, and lower contents of Rb, Zr, Th and U, and also exhibit different Ba/La, Rb/Sr and Sc/Nb ratios (Table 5b).

Fig. 18 shows that trachybasalts, when compared with basanite, are enriched in all elements with the exception of Ti, La and Y. Trachyandesites, when compared with trachybasalts, are enriched in all elements with the exception of Nd, Sm, Ti, P, (Yb), (Y), (Hf) and Tb. Some trachytes, including that from Sanadoire, when compared with the trachyandesites, are enriched in Rb, Th, K, Zr and Hf, impoverished in the REE, Sr, P, Ti, and have similar contents of Ba, Nb, Ta and Y. The 2.0 Ma rocks, when compared with the Sanadoire group of trachytes, are enriched in Rb, Th, Zr and Hf, and impoverished in Nb, Ta, REE and Y. These rocks show marked troughs for Ba, Ta, Sr, P, Ti and Tb and peaks for Rb, La, Nd, Zr, Hf and Th.

Basanite, trachybasalt and the Sanadoire group of trachytes show practically identical chondrite-normalized REE patterns (Fig. 19) which are characterized by enrichment in the LREE. There is a very weak positive Nd anomaly. The 2.0 Ma rocks have lower overall REE contents than the other examined rocks from the area (Table 5b, Fig. 19) and show a pronounced depletion in MREE (middle REE). The Trioulérou phonolite shows a weak negative Eu anomaly and the Mouteyron trachyte a very weak positive Eu anomaly.

For comparative reasons the Bozat phonolite located at Bois de la Reine about 10 km to the south of the Col de Guéry area was also examined. It is dated to 0.73 ± 0.04 Ma and belongs to the Upper Volcanic Series (Cantagrel & Baubron, 1983). Its chemical composition resembles that of the Puy Cordé phonolite (Tables 5a, b) with similar contents of $TiO_2$, $Fe_2O_3$, FeO, MgO, CaO, $Na_2O$, $K_2O$, $P_2O_5$, Ba, Hf, Th and U, but differs from that phonolite and the other 2.0 Ma rocks by higher contents of Nb, the REE and Ta, and lower contents of Rb, Zr and Cs. The Sr content is lower than in the Puy Cordé phonolite, but higher than in most other 2.0 Ma rocks. The element ratios (Table 5b) are also different from those of the 2.0 Ma rocks.

The enclaves from the trachytes and phonolites are generally small and often strongly altered. We have only found two enclaves large and fresh enough to be suitable for chemical analyses. These two analyses are presented in Tables 6a, b together with four analyses quoted from the literature. Four of the analysed enclaves plot in the tephrite field of the TAS diagram, two of them close to the trachybasalt field (Fig. 2). The enclave from Sanadoire plots in the foidite field and one of the Puy Cordé enclaves in the phonotephrite field. The chemical analyses of the

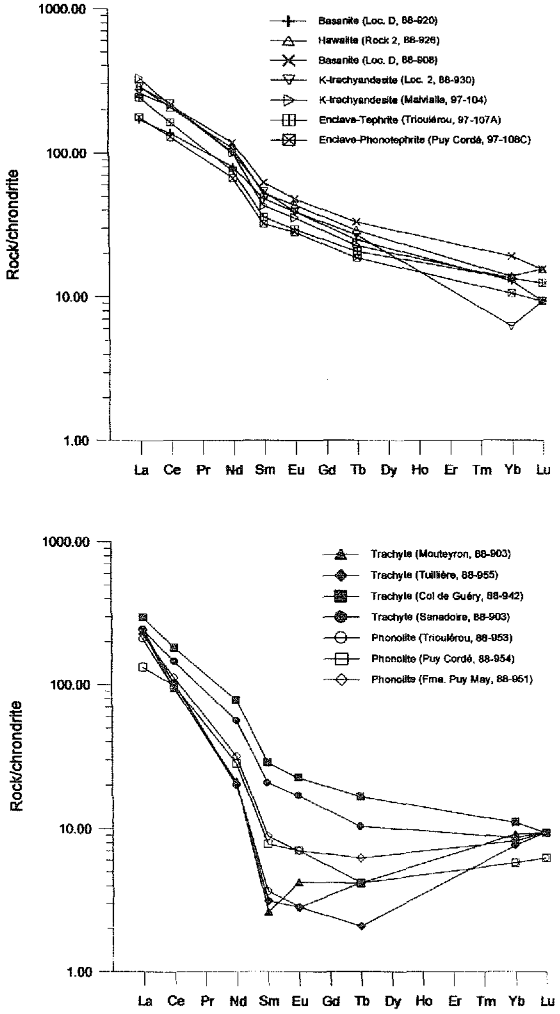

Fig. 19. Chondrite-normalized REE diagrams (normalized according to Sun, 1980).

tephritic enclaves (Tables 6a, b) are very similar to those of the trachybasalts (Tables 5a, b).

There is no information about the modal compositions of three of the enclaves of which analyses are quoted in Tables 6a, b: Sanadoire, Mout from Mouteyron and one of the Puy Cordé (no. 52) enclaves. Based on the chemical analysis, the Sanadoire enclave is a cumulate dominated by kaersutitic amphibole and is very probably represented by our sample 88-901g (Figs. 4, 5) which is a coarse-grained rock composed of large prismatic grains of brown amphibole, clusters of prismatic

Table 6a. Whole rock analyses, CIPW norms and D.I., and A.I. of enclaves, Col de Guéry area.
Table 6b. Trace element analyses and selected trace element ratios of the enclaves of Table 6a.

| a) | **Sanadoire** | **Mouteyron** | **Mouteyron** | **Puy Cordé** | **Puy Cordé** | **Trioulérou** |
|---|---|---|---|---|---|---|
| **Rock no.** | **L 5** | **MD 64** | **Mout** | **52** | **97108C** | **97107A** |
| "TAS name" | Foidite | Tephrite | Tephrite | Tephrite | Phonotephrite | Tephrite |
| $SiO_2$ | 39.15 | 46.05 | 47.08 | 47.54 | 49.16 | 47.94 |
| $TiO_2$ | 3.30 | 2.65 | 2.70 | 2.80 | 2.10 | 2.32 |
| $Al_2O_3$ | 14.60 | 17.88 | 15.42 | 16.35 | 16.43 | 19.28 |
| $Fe_2O_3$ | 9.15 | 4.40 | 4.70 | 4.61 | 3.78 | 5.16 |
| FeO | 6.45 | 5.39 | 5.00 | 4.62 | 4.14 | 2.74 |
| MnO | 0.70 | 0.20 | 0.06 | – | 0.17 | 0.16 |
| MgO | 5.30 | 4.47 | 6.68 | 6.08 | 4.64 | 3.73 |
| CaO | 14.40 | 8.77 | 9.62 | 9.64 | 6.57 | 6.06 |
| $Na_2O$ | 2.40 | 3.13 | 3.56 | 4.25 | 6.80 | 3.17 |
| $K_2O$ | 0.90 | 2.82 | 2.60 | 2.62 | 2.78 | 3.86 |
| $P_2O_5$ | 1.75 | 0.59 | 0.68 | 0.34 | 0.53 | 0.48 |
| LOI | 2.55 | 3.43 | 1.73 | 1.42 | 2.46 | 4.56 |
| TOTAL | 100.65 | 99.78 | 99.83 | 100.27 | 99.56 | 99.46 |
| CIPW | | | | | | |
| *Qz* | 0.00 | 0.00 | 0.00 | 0.00 | 0.00 | 0.00 |
| *C* | 0.00 | 0.00 | 0.00 | 0.00 | 0.00 | 0.02 |
| *Or* | 5.32 | 17.31 | 15.66 | 15.49 | 16.92 | 24.04 |
| *Ab* | 10.42 | 22.07 | 20.07 | 17.59 | 25.79 | 28.26 |
| *An* | 26.41 | 27.43 | 18.77 | 17.80 | 6.29 | 28.38 |
| *Ne* | 5.35 | 2.95 | 5.76 | 9.95 | 18.13 | 0.00 |
| *Ac* | 0.00 | 0.00 | 0.00 | 0.00 | 0.00 | 0.00 |
| *Di* | 26.18 | 10.67 | 19.84 | 21.65 | 18.68 | 0.00 |
| *Wo* | 0.00 | 0.00 | 0.00 | 0.00 | 0.00 | 0.00 |
| *Hy* | 0.00 | 0.00 | 0.00 | 0.00 | 0.00 | 1.10 |
| *Ol* | 0.83 | 6.31 | 6.08 | 3.61 | 3.18 | 6.09 |
| *Mt* | 13.26 | 6.62 | 7.00 | 6.68 | 5.64 | 2.77 |
| *Hm* | 0.00 | 0.00 | 0.00 | 0.00 | 0.00 | 3.53 |
| *Il* | 6.26 | 5.23 | 5.22 | 5.32 | 4.11 | 4.64 |
| *Ru* | 0.00 | 0.00 | 0.00 | 0.00 | 0.00 | 0.00 |
| *Ap* | 4.14 | 1.45 | 1.64 | 0.81 | 1.29 | 1.20 |
| D.I. | 21.09 | 42.33 | 41.49 | 43.03 | 60.84 | 52.30 |
| A.I. | 0.34 | 0.46 | 0.56 | 0.60 | 0.86 | 0.49 |
| | Brousse 1961 | Decobecq 1987 | Decobecq 1987 | Brousse 1961 | New analysis | New analysis |

| b) | **Trioulérou** | **Puy Cordé** |
|---|---|---|
| **Rock no.** | **97107A** | **97108C** |
| "TAS name" | Tephrite | Phonotephrite |
| Sc | 18.1 | 15.9 |
| V | 232 | 189 |
| Cr | 20 | 76 |
| Co | 25 | 30 |
| Ni | 15 | 46 |
| Cu | 28 | 27 |
| Zn | 255 | 96 |
| Rb | 193 | 123 |
| Sr | 495 | 508 |
| Y | 27 | 23 |
| Zr | 636 | 486 |
| Nb | 132 | 90 |
| Cs | 13 | 36 |
| Ba | 804 | 673 |
| La | 77 | 56 |
| Ce | 133 | 105 |
| Nd | 45 | 40 |
| Sm | 6.9 | 6.2 |
| Eu | 2.1 | 2.0 |
| Tb | 1.0 | 0.9 |
| Yb | 2.8 | 2.2 |
| Lu | 0.4 | 0.3 |
| Hf | 13 | 9 |
| Ta | 6 | 4 |
| Th | 19 | 14 |
| Y/Nb | 0.205 | 0.256 |
| Yb/Ta | 0.509 | 0.537 |
| Sc/Nb | 0.137 | 0.177 |
| Ba/La | 10.442 | 12.018 |
| Zr/Nb | 4.818 | 5.400 |
| Ce/Nb | 1.008 | 1.167 |
| Nb/Ta | 24.000 | 21.951 |

grains of green clinopyroxene, biotite, titanite, Fe-Ti oxides, apatite and plagioclase. The Mouteyron enclave (MD64) described by Decobecq (1987) is a porphyritic rock with phenocrysts of amphibole and clinopyroxene in a matrix of amphibole, pyroxene, plagioclase, alkali feldspar, Fe-Ti oxides and apatite. The Puy Cordé enclave (sample 97-108a), of which a new chemical analysis is presented in

Tables 6a, b, has macrocrysts of plagioclase, alkali feldspar, brown amphibole, green clinopyroxene, sodalite, hauyne, biotite, Fe-Ti oxides, titanite and subordinate olivine (which occurs as clusters of corroded grains). The matrix is made up of acicular brown amphibole and green clinopyroxene, Fe-Ti oxides and apatite with interstitial feldspar, sodalite and nepheline. Sample 97-108c differs, however, from the other tephrites in that it plots in the phonotephrite field and is characterized by lower CaO, $Fe_2O_3$ and FeO (reflected in lower normative *an*, *ol*, *mt* and *il*) and higher $SiO_2$ and $Na_2O$ (reflected in higher *ne* and *ab*) than these rocks. $K_2O$ and *or* are similar to the values of the three tephritic analyses. The difference can be best explained by the relatively large amount of analcime and albite filling the vesicles of the analyzed sample. Vesicles make up 20-30 % of the thin section. This interpretation is supported by the extremely high content of Cs in this rock (Table 6b).

The Trioulérou enclave (sample 97-107c) differs from the other tephritic rocks of Tables 6a, b by lacking normative *ne* and *di* and containing normative *c*, *hy* and *hm*. This rock is dominated by macrocrysts of brown amphibole with subordinate green clinopyroxene, brownish Ti-Al-rich clinopyroxene, scarce grains of strongly altered olivine, and scattered crystals of hauyne/nosean and Fe-Ti oxides. There are also macrocrysts of plagioclase, alkali feldspar, sodalite and biotite. The matrix consists of acicular brown amphibole and green clinopyroxene, Fe-Ti oxides and apatite with interstitial isotropic material, most probably sodalite. Similar rocks have been found as enclaves in the Mouteyron trachyte.

The two enclaves analyzed for trace elements (Table 6b) show higher contents of Ti, P, Sc, V, Cr, Ni, Cu, (Nb), Cs, Ba, Sr, Ta and the REE (with the exception of La) and lower contents of Rb, Zr, Hf and Th than their host rocks.

## Isotopic data

Sr, Nd and Pb isotopic data of volcanic rocks from the Col de Guéry area are listed in Table 7. Fig. 20 shows the variation of initial $^{143}Nd/^{144}Nd$ vs. $^{87}Sr/^{86}Sr$ for these rocks. K/Ar ages of Cantagrel & Baubron (1983) were used for calculating initial values. A correction age of 2.0 Ma was used for those samples for which K-Ar ages were not available. This translates to an uncertainty of the $^{87}Sr/^{86}Sr$ initial ratios of maximum ± 0.00010, whereas the effect on the Nd-initial ratios is negligible. Nd depleted mantle ages ($T_{DM}$) range consistently between 0.28 and 0.46 Ga, and there is no correlation of apparent model ages with main elemental composition of rock type. The data define a broad but coherent array away from the field of present-day MORB (DM) towards Bulk Earth (BE) values. Our data compare with other data from Massif Central volcanics, e.g. Briot *et al.* (1991); Wilson *et al.* (1995), and generally exhibit a rather pronounced and enhanced scatter. As illustrated in Fig. 20, the basanitic endmember with low initial Sr isotope ratios and high initial Nd isotope compositions can be described as a mixture of DM and HIMU mantle com-

Table 7. Sr-, Nd- and Pb isotope data of selected rocks of the Col de Guéry area.

| Sample | Location | Rock type | $^{206}Pb/^{204}Pb$ | ±2σ (abs.) | $^{207}Pb/^{204}Pb$ | ±2σ (abs.) | $^{208}Pb/^{204}Pb$ | ±2σ (abs.) |
|---|---|---|---|---|---|---|---|---|
| 88901 | Sanadoire | | 19.420 | 0.012 | 15.627 | 0.011 | 39.342 | 0.033 |
| 88903 | Mouteyron | | 19.411 | 0.018 | 15.630 | 0.017 | 39.332 | 0.048 |
| 88920 | Loc. D | | 19.679 | 0.021 | 15.611 | 0.018 | 39.470 | 0.048 |
| 88931 | Puy del l'Ouire | | 19.381 | 0.011 | 15.616 | 0.011 | 39.243 | 0.032 |
| 88942 | Col de Guéry | | 19.247 | 0.012 | 15.624 | 0.011 | 39.194 | 0.032 |
| 88951 | Fme Puy May | | 19.485 | 0.014 | 15.630 | 0.013 | 39.323 | 0.037 |
| 88953 | Trioulerou | | 19.444 | 0.012 | 15.630 | 0.011 | 39.357 | 0.035 |
| 88954 | Puy Corde | | 19.444 | 0.020 | 15.624 | 0.018 | 39.350 | 0.049 |
| 88955 | Tuiliere | | 19.419 | 0.015 | 15.638 | 0.013 | 39.379 | 0.037 |
| 97106 | Trioulerou | | 19.447 | 0.017 | 15.629 | 0.015 | 39.360 | 0.043 |
| 97108.2 | Puy Corde | | 19.437 | 0.014 | 15.616 | 0.013 | 39.325 | 0.037 |
| 97110 | Bozat | | 19.333 | 0.014 | 15.626 | 0.013 | 39.296 | 0.039 |
| 88901B2 | Sanadoire | | 19.422 | 0.015 | 15.629 | 0.014 | 39.349 | 0.039 |
| 97107A | Trioulerou | enclave | 19.396 | 0.013 | 15.623 | 0.012 | 39.298 | 0.035 |
| 97108C | Puy Corde | enclave | 19.437 | 0.016 | 15.616 | 0.014 | 39.309 | 0.041 |

| Sample | Location | Rock type | Rb (ppm) | Sr (ppm) | $^{87}Rb/^{86}Sr$ | ±1σ (abs.) | $^{87}Sr/^{86}Sr$ | ±2SE (abs.) | Age (Ma) | $^{87}Sr/^{86}Sr$ (age corr.) |
|---|---|---|---|---|---|---|---|---|---|---|
| 88901 | Sanadoire | | 184 | 575 | 0.93 | 0.009 | 0.703837 | 0.000013 | 1.83 | 0.703813 |
| 88903 | Mouteyron | | 326 | 70 | 13.48 | 0.135 | 0.704551 | 0.000013 | 1.92 | 0.704184 |
| 88920 | Loc. D | | 47 | 773 | 0.18 | 0.002 | 0.703562 | 0.000011 | 2 | 0.703557 |
| 88931 | Puy del l'Ouire | | 94 | 1030 | 0.26 | 0.003 | 0.703761 | 0.000011 | 2.2 | 0.703753 |
| 88942 | Col de Guéry | | 145 | 457 | 0.92 | 0.009 | 0.703916 | 0.000011 | 2 | 0.703890 |
| 88951 | Fme Puy May | | 228 | 157 | 11.58 | 0.116 | 0.704261 | 0.000015 | 2.01 | 0.703931 |
| 88953 | Trioulerou | | 266 | 21 | 36.66 | 0.367 | 0.705542 | 0.000025 | 2 | 0.704501 |
| 88954 | Puy Corde | | 253 | 151 | 4.85 | 0.049 | 0.703856 | 0.000013 | 2.03 | 0.703716 |
| 88955 | Tuiliere | | 275 | 13 | 61.22 | 0.612 | 0.705738 | 0.000014 | 2.1 | 0.703912 |
| 97106 | Trioulerou | | 275 | 31 | 25.67 | 0.257 | 0.704451 | 0.000017 | 2.01 | 0.703718 |
| 97108.2 | Puy Corde | | 253 | 129 | 5.68 | 0.057 | 0.703891 | 0.000023 | 2.03 | 0.703727 |
| 97110 | Bozat | | 209 | 82 | 7.38 | 0.074 | 0.704322 | 0.000020 | 0.7 | 0.704249 |
| 88901B2 | Sanadoire | | 199 | 500 | 1.15 | 0.012 | 0.703852 | 0.000013 | 1.83 | 0.703822 |
| 97107A | Trioulerou | enclave | 193 | 495 | 1.13 | 0.011 | 0.704043 | 0.000014 | 2 | 0.704011 |
| 97108C | Puy Corde | enclave | 123 | 508 | 0.70 | 0.007 | 0.703526 | 0.000011 | 2 | 0.703506 |

| Sample | Location | Rock type | Sm (ppm) | Nd (ppm) | $^{147}Sm/^{144}Nd$ | $^{143}Nd/^{144}Nd$ | ±2σ (abs.) | $T_{DM}$ | $T_{CHUR}$ | εNd(T=0) |
|---|---|---|---|---|---|---|---|---|---|---|
| 88901 | Sanadoire | | 3.70 | 33.0 | 0.072 | 0.512746 | 8 | 0.44 | -0.13 | 2.1 |
| 88903 | Mouteyron | | 0.50 | 13.0 | 0.024 | 0.512754 | 7 | 0.32 | -0.10 | 2.3 |
| 88920 | Loc. D | | 9.30 | 48.0 | 0.115 | 0.512852 | 5 | 0.46 | -0.40 | 4.2 |
| 88931 | Puy del l'Ouire | | 11.60 | 74.0 | 0.097 | 0.512830 | 7 | 0.42 | -0.29 | 3.7 |
| 88942 | Col de Guéry | | 5.50 | 46.0 | 0.072 | 0.512831 | 6 | 0.35 | -0.24 | 3.8 |
| 88951 | Fme Puy May | | 1.70 | 19.0 | 0.054 | 0.512832 | 7 | 0.30 | -0.21 | 3.8 |
| 88953 | Trioulerou | | 0.70 | 12.0 | 0.036 | 0.512810 | 6 | 0.29 | -0.16 | 3.4 |
| 88954 | Puy Corde | | 1.50 | 17.0 | 0.054 | 0.512836 | 7 | 0.30 | -0.21 | 3.9 |
| 88955 | Tuiliere | | 0.60 | 12.0 | 0.030 | 0.512759 | 5 | 0.33 | -0.11 | 2.4 |
| 97106 | Trioulerou | | 1.47 | 13.4 | 0.066 | 0.512821 | 6 | 0.34 | -0.21 | 3.6 |
| 97108.2 | Puy Corde | | 1.29 | 16.2 | 0.048 | 0.512848 | 6 | 0.28 | -0.22 | 4.1 |
| 97110 | Bozat | | 2.80 | 29.0 | 0.060 | 0.512764 | 7 | 0.38 | -0.14 | 2.5 |
| 88901B2 | Sanadoire | | 4.05 | 32.9 | 0.072 | 0.512738 | 11 | 0.45 | -0.12 | 2.0 |
| 97107A | Trioulerou | enclave | 6.90 | 45.0 | 0.091 | 0.512815 | 8 | 0.42 | -0.26 | 3.5 |
| 97108C | Puy Corde | enclave | 6.20 | 40.0 | 0.097 | 0.512870 | 7 | 0.37 | -0.35 | 4.5 |

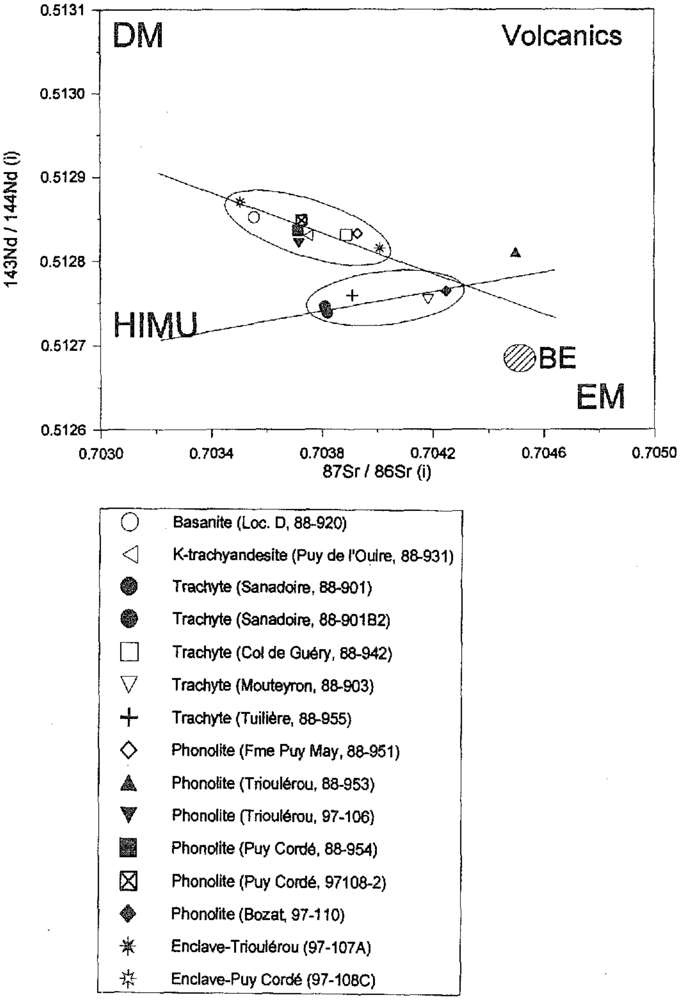

Fig. 20. $^{87}$Sr/$^{86}$Sr – $^{143}$Nd/$^{144}$Nd initial ratio diagram.

ponents, whereas the end member with radiogenic Sr initial values and low initial Nd isotope values has characteristics similar to that of an enriched mantle component (EM). On closer inspection, based on initial Nd isotope ratios, two groups of data may be distinguished. The first group comprises basanite, trachyandesites, one trachyte, the Puy Cordé and Trioulérou phonolites and the F$^{me.}$ de Puy May phonolite which have $^{143}$Nd/$^{144}$Nd initial ratios in the range of 0.512810-0.512852. The second group includes the Sanadoire, Mouteyron and Tuilière trachytes which have lower $^{143}$Nd/$^{144}$Nd initial ratios in the range of 0.512738-0.512764. The Bozat phonolite falls in this group.

The first group of volcanics, with the exception of one Trioulérou sample and the F$^{me.}$ de Puy May sample, have $^{87}Sr/^{86}Sr$ initial ratios in the range of 0.703557-0.703890. The second group of volcanics is characterized by slightly elevated initial $^{87}Sr/^{86}Sr$ ratios in the range of 0.703813-0.704501. The F$^{me.}$ de Puy May and Bozat phonolites have similar Sr isotope ratios. Sample 99-953, the Trioulérou phonolite, has the most radiogenic initial $^{87}Sr/^{86}Sr$ ratio and plots outside two mixing arrays (Fig. 20). This phonolite has a low Sr content (Table 5b) which renders it sensitive to late-magmatic hydrothermal and post-magmatic groundwater alteration. However, sample 88-955, the Tulière trachyte, is equally poor in Sr and does not show a high $^{87}Sr/^{86}Sr$ initial ratio which could be explained by post-fractional introduction of crustal Sr to the system. The flat mixing arrray is mainly outlined by the trachytes from Sanadoire (88-901) and Tuilière (88-955) and the samples from Mouteyron (88-903) and Bozat (97-110). The other samples, mainly those defining the above-mentioned first group with the exception of sample 88-953 from Trioulérou, plot along a steeper trend line which intersects the flat array in the vicinity of the Mouteron and Bozat data points.

The Puy Cordé (97-108c) and Trioulérou (97-107a) enclaves show $^{87}Sr/^{86}Sr$ and

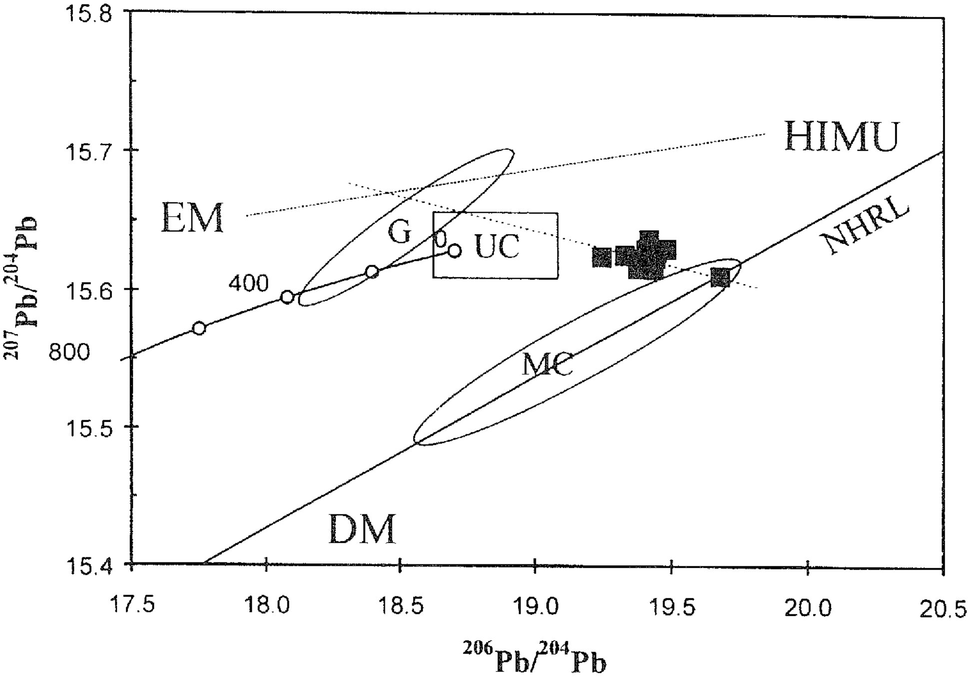

Fig. 21. $^{206}Pb/^{204}Pb$ – $^{207}Pb/^{206}Pb$ diagram.

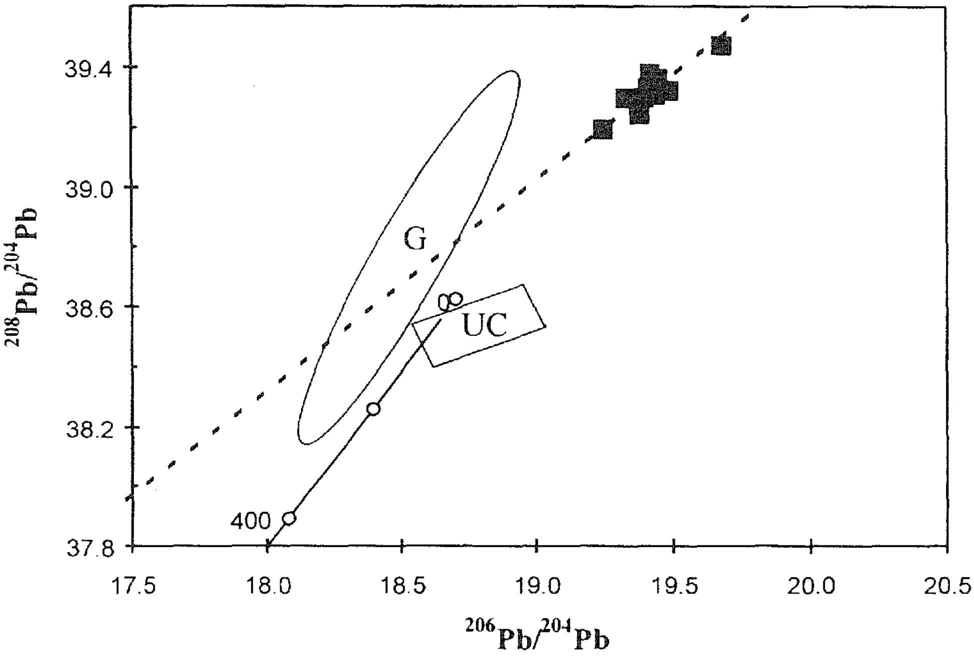

Fig. 22. $^{206}$Pb/$^{204}$Pb – $^{208}$Pb/$^{206}$Pb diagram.

$^{143}$Nd/$^{144}$Nd initial ratios that are in good agreement with the data for the two host phonolites. Data of these two phonolites and enclaves indicate a more primitive origin for Puy Cordé than Trioulérou.

Pb isotopic data are listed in Table 7 and plotted in uranogenic ($^{206}$Pb/$^{204}$Pb vs. $^{207}$Pb/$^{204}$Pb) and uranogenic-thorogenic $^{206}$Pb/$^{204}$Pb vs. $^{208}$Pb/$^{204}$Pb) diagrams (Figs. 21, 22). Data (with one exception) cluster away from the Northern Hemisphere Reference Line (NHRL, Hart, 1984) towards the composition of todays average crustal Pb (endpoint of the Stacey & Kramers (1975) average crustal growth curve). Compared to published data on Tertiary volcanic rocks of the Massif Central (field MC, Wilson & Downes, 1990), our data are compositionally more homogeneous, but show indications of an enhanced influence from upper crustal (UC) components or a long term enriched mantle (EM) source as represented by lower crustal mafic xenoliths in volcanic rocks from the Massif Central (field G, Downes *et al.*, 1991). The trend is compatible with the Sr-Nd data and compatible with a two component mixing between end members that can be best explained by a mixture between HIMU and DM reservoirs on the one, and EM on the other hand. Data in the uranogenic-thorogenic diagram (Fig. 22) are better correlated and a reference line passes through the field characteristic of meta-igneous rocks (field G).

The above-mentioned isotopic data are perfectly compatible with the trends depicted by the Tertiary continental volcanic rocks from Cantal to the south of the Mont-Dore region (Downes, 1984).

The sub-trends that can be defined in Sr vs. Nd isotopic space (Fig. 20) are not discernable in the combination with Pb isotopes of the respective volcanic rocks. The most radiogenic and least radiogenic Pb samples (88-920 and 88-942, respectively) fall on the steeper of the arrays in the Sr vs. Nd isotopic diagram (Fig. 20). Futhermore, the tendencies of samples 88-901 and 88-955 to show an increased HIMU component in Sr and Nd isotopic space (the flat trend which is oblique to the mantle array, Fig. 20) is not reflected by increased radiogenic Pb as it is usually observed in HIMU-contaminated basalts.

## Discussion

Similar to phonolites from other provinces, the 2.0 Ma trachytes and phonolites of the Col de Guéry area are enriched in Rb, Th and Zr, but they differ from most trachytes and phonolites in low contents of Nb, Ta, Ba and REE (especially MREE), weak Eu anomalies and relatively high Zr/Nb ratios. They have lower contents of most of the last-named elements than the accompanying trachyandesitic rocks. These are the main features we shall attempt to explain in this part of the paper.

In most volcanic provinces, trachytes and phonolites display high or relatively high levels of Nb, Ta, Ba and REE and marked negative Eu anomalies. They are considered to represent the most evolved products of fractional crystallization of alkali basaltic and basanitic magmas. This will be illustrated by means of a few examples.

A very clear example of the derivation of phonolitic melts from alkali basaltic melts is seen in the Bouzentès alkali basaltic lava flow in Cantal to the south of Mont-Dore (Caroff *et al.*, 1997). This flow contains in its upper part spherules of glassy phonolite which are interpreted as vesicles occupied by residual melt and vapour which from the lower part of the flow have moved upward and have been trapped at the base of the upper solidified crust of the flow. The basaltic magma had a high content of $H_2O$. In this case there appears to have been a direct evolutionary trend from basalt over hawaiite to phonolite. This is reflected in increasing contents of incompatible elements, from basalt to phonolite: Rb 16→116 ppm, Ba 350→980 ppm, Y 20→81 ppm, Zr 160→980 ppm, Nb 45→347 ppm, La 26→128 ppm, Ce 53→251 ppm, Nd 28→117 ppm, Eu 1.9→2.8 ppm, Dy 4→8 ppm, Er 2→8 ppm and Yb 1.5→6.8 ppm. The Zr/Nb ratio decreasses from 3.56 in the basalt over 3.4 in the hawaiitic part of the flow to 2.8 in the phonolite.

The phonolites from Cantal studied by Wilson *et al.* (1995) have higher contents of Nb and LREE than the 2.0 Ma rocks studied by us. Type A and type B phonolites are distinguished. The type A phonolites have very low contents of Ba (7-58 ppm) and Sr (4-42 ppm), but these rocks have relatively elevated contents of Nb (132-438 ppm). The type B phonolites are very similar to the Bozat phonolite, but with lower contents of V and higher contents of Rb, Sr, Ba, Nb and Zr. The type A phonolites show negative Eu anomalies, whereas type B phonolites, the least evolved type, show no Eu anomaly. The Cantal phonolites display a less pronounced depletion in MREE than the rocks from Mont-Dore according to Briot *et al.* (1991) and our data.

The phonolites of northern Bohemia are considered to have been formed by low-pressure fractionation of more than one parental magma (Vaneckova *et al.* (1993) and to have an origin different from the 'ordinary' sequence from trachyandesite to trachyte (Pazdernik, 1997). According to Pazdernik (1994), the Nb contents of these phonolites vary from 22 to 375 ppm, their Zr/Nb ratios from 2.7 to 28.1. Some of the phonolites have very low contents of Ba and Sr, but this is, contrary to the conditions in the Col de Guéry area, not coupled with low contents of Nb. Ulrych & Pivec (1997) distinguished three types of phonolites from northern Bohemia, which occur in a bimodal association with basanite. Their PH1 phonolites are high in Ba (1301 ppm) and Sr (1600 ppm) and have 98-222 ppm Nb, average Zr/Nb ratio = 6.2, average Nb/Ta = 37.8; the PH2 phonolites are low in Ba (25 ppm) and Sr (32.5 ppm) and have 134-349 ppm Nb, average Zr/Nb = 4.7, average Nb/Ta = 58.9. Some anomalous phonolites have low Ba and Sr (50 and 12 ppm), 1012 ppm Nb, Zr/Nb = 2.6 and Nb/Ta = 24.6. Phonolites PH1 and PH2 display no Eu anomalies in chondrite-normalized REE diagrams, whereas the diagram of the anomalous phonolite shows a marked negative Eu anomaly (Ulrych & Pivec, 1997). The phonolites have $^{87}Sr/^{86}Sr$ initial ratios of 0.70398-0.70534, and $^{143}Nd/^{144}Nd$ initial ratios of 0.51278-0.51280 (Ulrych & Pivec, 1997, Ulrych *et al.*, 1998) and are considered to have been derived from basanitic or olivine-poor nephelinitic melts by low pressure fractionation in combination with some crustal contamination.

The Laacher See (East Eifel, Germany) phonolitic tuffs are compositionally zoned which by Wörner & Schmincke (1984a, b) is explained by successive tapping of a zoned magma chamber, the lowermost tuff horizons representing the top of the magma chamber, the uppermost horizons the deep part of the chamber. The highly evolved phonolites formed in the top of the magma chamber are enriched in volatiles and Rb, Zr, Hf, Nb, La, Yb, Lu, Th and U and are depleted in Sr, Ba, Sc and Eu. A semicompatible behaviour is shown by Ta, Y, Nd and Sm which show minimum contents in the middle part of the magma chamber. The Zr/Nb ratio varies from 2.60 in the lower part to 6.30 in the upper part of the magma chamber, and the Nb/Ta ratio from 12 to 52. The rocks originated in the lower part of the magma chamber have >1000 ppm Ba and 7.0 % $K_2O$, those from the middle part have 49-597 ppm Ba and 6.40-7.00 % $K_2O$, and the rocks originating in the top have 20-47 ppm Ba and 5.50 % $K_2O$. The $^{87}Sr/^{86}Sr$ initial ratio varies from 0.70467 to 0.70480. The most primitive phonolite magma is proposed to have been formed from a basanitic magma by fractionation of 30 % clinopyroxene, 24 % amphibole, 4 % phlogopite, 3.8 % magnetite, 2.5-3.0 % olivine and 2 % apatite.

Peralkaline phonolites from the Fortaleza district, Brazil (Maciotta *et al.*, 1990) are interpreted as products of fractional crystallization of tephritic melts, but compositional differences indicate that the rocks are not strictly comagmatic. They have 146-362 ppm Nb, 6-438 ppm Sr and 24-566 ppm Ba and show depletion in the MREE and a pronounced negative Eu anomaly.

The phonolites of the East-African Rift have rather constant Zr/Nb ratios (3-4) and high Nb (generally higher than 200 ppm), indicating a derivation by crystal fractionation from a common magma source (MacDonald *et al.*, 1994, 1995). The Klinghardt Mountain phonolites, Namibia (Marsh, 1987), which mineralogically are very similar to the 2.0 Ma phonolites, show increasing Nb with differentiation and a negative correlation between Nb and Ti, contrary to the depletion in Nb and

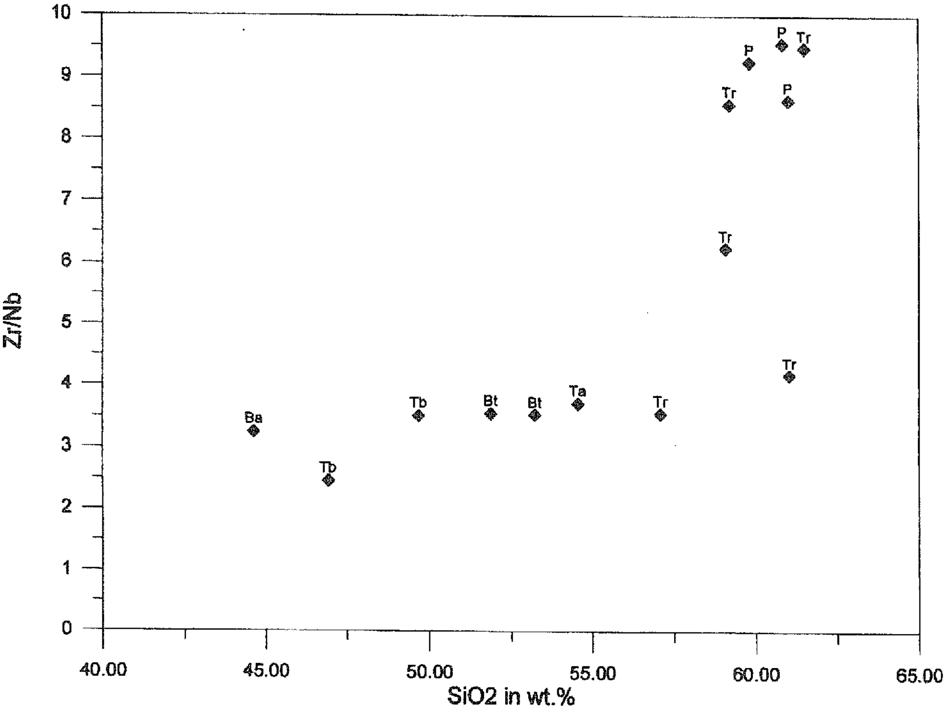

Fig. 23. $SiO_2$ – Zr/Nb diagram.

the positive correlation between Nb and Ti in the phonolites considered here. The Klinghardt Mountain phonolites have 151-781 ppm Nb, Zr/Nb = 3.5-6.0 and Ba and Sr decreasing with increasing Nb.

These examples indicate that the simultaneous depletion in Nb, Ta, REE, Sr and Ba in the 2.0 Ma trachytes and phonolites in the Col de Guéry area is rather unique.

### The mutual relationship of the volcanic rocks of the Col de Guéry area

In the Col de Guéry area, there are *ne*- and *qz*-normative rocks corresponding to the two magma series distinguished in Mont-Dore, the silica-saturated and -undersaturated series (e.g. Brousse & Lefèvre, 1990; Briot *et al.*, 1991). The major and trace elements of these suites (Figs. 17a, b) show a smooth evolution from basanite to trachyandesite and some trachytes and abrupt inflections and clustering of data between 55 and 60 wt.% $SiO_2$ at a differentiation index of about 90 in the field of trachytes and phonolites (Table 5a). The sequence from basanite over trachyandesite to some of the trachytes is exposed in a limited geographical area, but it is uncertain whether these rocks are contemporaneous. However, the linear trends in the Harker variation diagrams (Figs. 17a, b), the relatively constant Y/Nb, Zr/Nb and Ce/Nb ratios (Table 5b, Fig. 23) and the $^{87}Sr/^{86}Sr$ and $^{143}Nd/^{144}Nd$ initial ratios (Table 7) indicate that these rocks may be cogenetic and derived from a common basanitic magma source by crystal fractionation processes (cf. Weaver *et al.*, 1972; Wilson, 1989).

In Figs. 17a, b there is perhaps a vague separation of the plots of *qz* and *ne* normative rocks, which may be taken as support of the existence of two magma series. The volcanic rocks in question were, however, not formed at the same time according to the above-mentioned K/Ar dates. Furthermore, our isotopic data are not capable of distinguishing the two magmatic trends from each other. A more acceptable explanation is therefore that the shift from silica-undersaturated to silica-saturated rocks was a result of early fractionation of pargasite and kaersutite, a mechanism proposed by Maury *et al.* (1980b), Villemant *et al.* (1980), Downes (1987), and others. In this connection it is interesting to note that the analysed enclave from Sanadoire (sample L5, Table 6a, Fig. 17a) may be regarded as a segregation of amphibole and other minerals. According to our isotopic data (Table 7), upper crustal contamination has played a minor role in the transition from silica-undersaturated to -saturated compositions.

Alternatively, the more or less linear trends depicted by basanite to trachyandesite and some trachytes in Figs. 17a, b may also be explained as a result of mixing of basanitic and trachytic melts (Gourgaud, 1991) (see further below).

The Puy Cordé phonolite, one sample of Trioulérou phonolite and one trachyte may according to the $^{87}Sr/^{86}Sr$ and the $^{143}Nd/^{144}Nd$ initial ratios (Table 7, Fig.20) be cogenetic with the basanite-trachyandesite. Incompatible trace element data corroborate this for the trachyte, but not for the Puy Cordé and Trioulérou phonolites. The variability in initial Nd isotope ratios for the remaining trachytes and phonolites, in combination with the trace element data (Table 5b) and the fact that the 2.0 Ma rocks are *ne*-normative and the trachyandesitic rocks *qz*-normative, show that the 2.0 Ma rocks cannot have been derived from the exposed basanite-trachyandesite sequence by simple fractionation processes. Furthermore, the available K/Ar dates indicate, that the 2.0 Ma rocks differ in age from the accompanying volcanic rocks. The combined data support the view that the phonolites and some trachytes had an origin independent from that of the remaining exposed volcanic rocks in the area in conformity with views expressed in the literature (Cantagrel & Baubron, 1983; Briot *et al.*, 1991). In variation diagrams (Wilson *et al.*, 1995), the Cantal trachytes plot toward the end of the linear fractionation trends of the weakly alkaline series, whereas the most evolved rocks, rhyolites and phonolites, fall away from this trend, similar to the features of Figs. 17a, b for the volcanic rocks of the Col de Guéry area.

The 2.0 Ma rocks plot in a distinct cluster in Figs. 17a, b. Their Y/Nb and Zr/Nb ratios differ from those of the basanite-trachyandesites and the other trachytes of the area (Table 5b, Fig. 23). The Rb/Sr, Ba/La and Nb/Ta ratios of the Puy Cordé and F$^{me}$ de Puy May phonolites are, however, different from those of the other 2.0 Ma rocks which may indicate that the 2.0 Ma rocks do not form one comagmatic population. The new K/Ar ages for the Trioulérou and Puy Cordé phonolites of respectively 2.33 and 2.17 Ma (see p. 6) indicate a scatter in time of the emplacement of these two rocks.

The variation in trace element ratios may, however, also result from magma mixing coupled with fractionation. It should in this connection be born in mind that magma mixing coupled with crystal fractionation and fluid transport processes may cause variation in trace element ratios in series of igneous rocks (Rasmussen *et al.*, 1988; Neumann *et al.*, 1999) as it will also be demonstrated below.

In conclusion, the 2 Ma rocks were formed independently from the exposed volcanic rocks of the area. Their origin may be referred to magma chambers located deep in the continental lithosphere as has already been proposed in the case of the phonolites examined by Briot *et al.* (1991) and Wilson *et al.* (1995). In the following the role of processes such as fractional crystallization of alkali basaltic to basanitic parent melts, magma mixing and crustal contamination will be examined.

## The role of fractional crystallization

Brousse (1961b), Maury (1976), Villemant (1979), and others have emphasized the importance of crystal fractionation in the formation of the trachytes and phonolites of the Mont-Dore massif.

The behaviour of Mg, Fe$_{tot.}$, Ca, Ni, Sc and Sr of the trachytes and phonolites in

Figs. 17a, b can best be explained by fractionation of olivine, clinopyroxene and Ca-rich plagioclase in a basanitic/alkalibasaltic magma. The increasing contents of Al, Na and K are compatible with accumulation of alkali feldspar. The high contents of Na, Rb, Cs, Zr, U and Th in the 2.0 Ma rocks indicate accumulation of feldspathoids, zircon and the unidentified Zr-bearing minerals.

Fractionation of apatite can explain the low contents of P and the REE in the 2.0 Ma group of evolved rocks and fractionation of Fe-Ti oxides and other Ti-bearing minerals such as titanite, kaersutite and Ti-rich clinopyroxene may have led to the depletion of Ti in these volcanics. Amphibole fractionation may also be responsible for the low contents of the MREE in these rocks (cf. Wörner *et al.*, 1983, Briot *et al.*, 1991; Wilson *et al.*, 1995). Wilson & Downes (1991) have shown that amphibole fractionation was an important process at depth from the early stages of formation of the volcanic rocks from the Massif Central.

High contents of K are characteristic for the volcanic rocks of Mont-Dore (Brousse, 1961c, Briot *et al.*, 1991) and for the volcanic rocks of Massif Central in general (Downes, 1987). Most of the 2.0 Ma trachytes and phonolites of Mont-Dore are potassic but have low contents of Ba. This is also the case for the Mont Gerbier de Jonc phonolite and some of theVelay phonolites located about 100 km to the SE of Mont-Dore (Villemant & Treuil, 1983). This indicates that accumulation of K-rich feldspars is not the only explanation of the high K contents of volcanic rocks. Villemant & Treuil (1983) explained the enrichment in K in the magmatic liquid as a result of exchange of K between the magma and a fluid phase. Villemant (1988) proposed the same mechanism to be the cause of a surplus of K in the volcanic rocks of the Phlegrean Fields, Central Italy. It seems, however, to be rather fortuitous if separate volcanic bodies all have reacted with such fluids and have attained similar contents of $K_2O$.

Ba behaved as an incompatible element in the early stages of crystallization (Fig. 17b) which were characterized by fractionation of olivine, clinopyroxene and plagioclase, and as a compatible element in the later stages. Feldspar fractionation would be the straight-forward explanation of the low Ba contents in the 2.0 Ma rocks, but this is contradicted by the lack of pronounced Eu anomalies (see further below). Briot *et al.* (1991) have similarly not found any Eu anomalies for the Mont-Dore phonolites examined by them, but they report distinct negative Eu anomalies in the rhyolitic rocks of the area. The depletion in Ba in the 2.0 Ma rocks does not conform with the high content of K of these rocks, but may reflect fractionation of amphibole and titanite. Villemant *et al.* (1981) have for instance calculated Ba amphibole/liquid distribution coefficients of around 10 in volcanic rocks from Chaîne des Puys and Wörner *et al* (1983) have determined Ba crystal/liquid distribution coefficients for amphibole of 0.39-5.58 and for titanite 1.5-4.72. for the Laacher See phonolite. Phlogopite was found to have an even higher distribution coefficient, 10.1-11.2, but this mineral can be ruled out as a fractionated phase because of the very high K contents of the Col de Guéry rocks. The Puy Cordé and F$^{me}$ de Puy May phonolites have 191-264 ppm Ba, Ba/La = 3.081-3.718, the other 2.0 Ma rocks 6-56 ppm Ba, Ba/La ratios = 0.078-0.737; the Sanadoire trachyte 743-821 ppm Ba, Ba/La = 9.649-10.621; the Bozat phonolite 191 ppm Ba, Ba/La = 2.127; and the Cantal type A phonolites 7-58 ppm Ba, Ba/La = 0.07-0.56, the type B phonolites 163-949 ppm Ba, Ba/La = 1.66-10.60. Negative Eu anomalies and low Ba in the most evolved phonolites of Cantal are ascribed to fractionation of alkali feldspar (Wilson *et al.*, 1995), but again this is difficult to reconcile with the very high contents of K. A more likely mechanism is the above-mentioned depletion in Ba as a result of fractionation of amphibole and titanite.

The weak Eu anomalies and the low contents of Nb and Ta in the 2.0 Ma rocks can be explained by high oxygen fugacities in the magma which prevented formation of $Eu^{+2}$ and favoured the crystallization of hematite-ilmenite. Based on the similarly weak Eu anomalies in the volcanic rocks of Chaîne des Puys to the north of Mont-Dore, Villemant *et al.* (1980, 1981) calculated the very high oxygen fugacity values of $10^{-11}$ to $10^{-8}$. Maury *et al.* (1980a) found from Fe-Ti oxide geobarometry that the oxygen fugacity of the Mont-Dore magmas must have been well above the NNO buffer. This is in excellent agreement with our observation of Fe-Ti oxides in the trachytes and phonolites. These oxides belong to the hematite-ilmenite series having 60-80 mol. % hematite (Fig. 16). Also the presence of amphibole and biotite phenocrysts indicates a high oxygen fugacity (cf. Rutherford & Heming, 1978).

Nb and Ta behaved as incompatible elements in the early stages of crystallization and as compatible elements in the later stages (Fig. 17b). This is also depicted in the chondrite-normalized trace element diagrams of Fig.18 which show Nb and Ta peaks in the early more primitive rocks and troughs in the later evolved rocks. The depletion in Nb and Ta may be explained by the onset of ilmenite fractionation as it has been proposed by Stimac & Hickmott (1994). The covariation of V and Ti is in favour of a fractionation of Fe-Ti oxides and less importantly, titanite. The Fe-Ti oxides in the most primitive rocks are richer in the magnetite component than those of the more evolved rocks (Table 4). It is interesting to note that magnetite is the predominant Fe-Ti oxide in the alkaline rocks of Cantal, whereas hematite-ilmenite prevails in the 2.0 Ma rocks of Mont-Dore, an indication of different oxygen fugacities during crystallization and perhaps a partial explanation for the negative Eu anomalies in type A phonolites of Cantal and for different contents of Nb and Ta in the phonolites of these two volcanic provinces (cf. Wilson *et al.*, 1995).

Phonolites from Tenerife have 195-290 ppm Nb, 11.4-38.9 ppm Ta and Nb/Ta ratios varying from 14.9 in the more primitive rocks to 23.7 in the most evolved rock (Wolff 1984). It was suggested that the increase in Nb/Ta ratios with differentiation might be caused by preferential entry of Ta relative to Nb into titanite phenocrysts.

The speculative reason for this selective incorporation may have been that Nb was present as $Nb^{+3}$ ions, which might have suppressed the entry of Nb into titanite. The oxygen fugacity was estimated to have been just above the NNO buffer. In the Col de Guéry area, the Trioulérou phonolite and the Mouteyron and Tuilière trachytes have higher Nb/Ta ratios than the Puy Cordé phonolite and the other trachytes (Table 5b). The above-mentioned information about the oxygen fugacity does not, however, favour an explanation of the low Nb of the 2.0 Ma rocks of Mont-Dore by the model proposed by Wolff (1984). Wörner *et al.* (1983) report Ta crystal/liquid distribution coefficients of 0.85-1.25 for amphibole and 86.0-113.3 for titanite for the Laacher See phonolite. Nb, Rb, Zr, Th and U behave as incompatible elements in the Laacher See phonolite (Wörner & Schmincke 1984a). The Nb content varies from 95 ppm in the lower part of the zoned magma chamber to 435 ppm in the uppermost evolved part of the chamber. Ta on the contrary behaves as a semicompatible element; its contents decrease upward in the lower part of the chamber to a minimum value in the middle part and then increase toward the top of the chamber. Based on data for Ta (Wörner *et al.*, 1983) and data for Nb (Wörner & Scmincke, 1984a) a calculation of the Nb/Ta ratio results in Nb/Ta variations from 12-14 in the lower part over 20-30 in the middle part to 37-52 in the top of the magma chamber feeding the phonolite tuff of the Laacher See. This confirms the observation of Wolff (1984) that the Nb/Ta ratio varies with evolution of phonolitic magmas. The trace element data for the Col de Guéry volcanics (Table 5b) also show that Nb was separated from Y, Ce and Zr during the processes forming the trachytes and phonolites. Y/Nb and Ce/Nb ratios decrease, whereas the Zr/Nb ratio increases with magmatic evolution. The decreasing Y/Nb and Ce/Nb ratios can be explained by apatite fractionation, and the increasing Zr/Nb ratios may result from the perfect incompatible behaviour of Zr, whereas Nb is fractionated by titanite and ilmenite.

The differences in geochemistry and element ratio variations in the 2.0 Ma rocks of the Col de Guéry area might be related to tapping of melts at different levels in a zoned magma chamber similar to the mechanisms proposed for the Laacher See phonolite and phonolitic eruptive rocks at Tenerife (Wörner *et al.*, 1983; Wolff, 1985). In that case one would expect uniform Sr and Nd initial isotopic ratios, unless parts of the magma were contaminated by reactions with the country rocks (cf. Halliday *et al.*, 1984). It is in this connection interesting to note that the two examined samples of Trioulérou phonolite collected at respectively the north and south side of the plug show different Sr initial ratios, the sample from the north side indicating that contamination with radiogenic Sr has taken place.

## Information from the enclaves

The granular enclave from the Sanadoire trachyte (samples 88-901g and L5, Table 6a) is composed of amphibole, clinopyroxene, biotite, Fe-Ti oxides and apatite with some plagioclase and is, as discussed in the geochemistry section, very probably a cumulate formed by fractionation processes in the parent magma of this trachyte (cf. Lacroix, 1893, 1917; Decobecq, 1987).

Most of the enclaves studied in the present paper are, however, porphyritic and vesicular. They are wrapped by the trachytic texture of the host rocks, but the parallel arrangement of the feldspar laths is often disturbed adjacent to enclaves; fragments may be loosened from the enclaves and float in the enclosing rock. These features indicate that some enclaves were solid bodies when erupted with the trachytic and phonolitic melts. On the other hand, lenticular enclaves appear to have been drawn out and flattened during emplacement of the host rocks (Fig. 6). They have behaved as soft, not completely consolidated bodies at the time of eruption of the host rocks.

The tephritic enclaves from Puy Cordé and Trioulérou are composed of the same minerals as the host phonolites. They have accumulations of phenocrysts and xenocrysts of olivine, kaersutitic amphibole, Ti-poor green clinopyroxene and Ti-Al-bearing brown clinopyroxene, whereas the host rocks have widely scattered pheno- or xenocrysts of green and brown clinopyroxenes, amphibole, olivine and mica. The enclaves have a fine-grained to dense matrix, also with high contents of amphibole and pyroxene and interstitial feldspars and feldspathoids.

The textures and modal compositions of the tephritic enclaves and their low contents of MgO, Ni and Cr (Tables 6a, b) show that the enclaves do not represent samples of the parent magma of the 2.0 Ma trachytes and phonolites and that they cannot be xenoliths of earlier lavas picked up by the ascending melts. The slender prismatic amphibole phenocrysts, which may make up more than 50 % of the volume of the enclaves, are for instance almost always undeformed, and the groundmasses are texturally and mineralogically different from those of the surface volcanic rocks of the area. It is also evident that the matrix of the enclaves, mineralogically and texturally is markedly different from the trachytes and phonolites, which means that the segregation of minerals did not take place in the trachytic-phonolitic melts. The hollow prismatic grains of amphibole and the swallow-tails of many amphibole crystals (Fig. 12) are indications of rapid growth, which may be a result of supersaturation of the melt. This was followed by a rapid crystallization of the interstitial melts. The vesicular textures is an additional indication of rapid crystallization at a high level in the magmatic system.

Two mechanisms may be proposed to explain the origin of the tephritic enclaves:

1. Based on textural relations, the tephritic enclaves appear to have been formed by segregation of amphibole, green clinopyroxene, Fe-Ti oxides and plagioclase crystallizing from the melt together with admixtures of xenocrystic olivine, brown Ti-Al-rich pyroxene and perhaps titanite (cf. Decobecq, 1987). This may have taken place by means of the mechanism proposed by Irving & Price (1981), that phonolitic

magmas may form by fractionation of kaersutite, olivine, Fe-Ti spinel and apatite in basaltic magmas at mantle pressures (10-15 kbar) followed by fractionation of Al-rich clinopyroxene, mica and apatite. They envisage that magmas ascended unmodified through the crust and that dynamic flow crystallization in the conduits have plastered crystals on the walls. In the Col de Guéry area, the Ti-Al-rich clinopyroxene, anorthite-rich plagioclase and olivine found in enclaves in the Trioulérou phonolite were formed at depths in the early stages of crystallization, whereas the trachytes and phonolites and their enclaves were formed by low-pressure fractionation, which is in conformity with their mineralogy and vesicular nature.

The two new chemical analyses of enclaves from the Puy Cordé and Trioulérou phonolites (Tables 6a, b) show, when compared with the host phonolites, enrichment in Ti, P, Mg, Fe, Ca, V, Ni, Sc, Ba, Sr, (Nb) and REE, and impoverishment in Si, Na, K, Rb, Zr, Hf and Th, features complementary to the chemical composition of the host rocks. This supports the view that fractional crystallization can be responsible for the formation of the 2.0 Ma rocks. In Figs. 17a, b tephritic enclaves plot close to hawaiite-trachybasalts, while the Sanadoire enclave plots in a position indicating that this enclave represents an accumulation of amphibole, clinopyroxene, Fe-Ti-oxides and apatite. The Sr and Nd initial isotope ratios indicate that the Puy Cordé enclave represents a less modified melt than the Trioulérou enclave, which is in accordance with the petrographical information about these two enclaves.

2. Mineralogically and texturally the tephritic enclaves in the Puy Cordé and Trioulérou phonolites recall enclaves in trachyte from Westerwald, Germany (Schreiber *et al.*, 1999). It is demonstrated that these enclaves formed by disintegration of a latitic dyke which intruded into a trachytic magma chamber. The disintegrated latitic melt reacted with the trachytic magma and became chemically and mineralogically modified, the endproduct attaining a phonolitic composition. The Westerwald volcanic province in Germany resembles the Col de Guéry area in having an oversaturated series consisting of alkali basalt, trachybasalt, trachyandesite and trachyte and an undersaturated series comprising basanite and phonolite. The phonolite has 196.9 ppm Ba, 32.2 ppm Sr, 83.3 ppm Nb and Zr/Nb = 9.6.

According to this interpretation, the tephritic enclaves of the Col de Guéry area represent modified basic magma injected into the magma chambers in which the trachytes and phonolites were formed. The association of xenocrysts and phenocrysts in the enclaves indicates that also the basic magma had a complex evolution. This interpretation is in agreement with the distinct features of magma mixing observed in the Col de Guéry rocks (see further below). Further support for this interpretation is supplied by Neumann *et al.* (1999) who emphasized the importance of fractional crystallization combined with periodical filling of magma chambers, FCM processes, in explaining the origin of a suite of volcanic rocks including basanite and phonolite from Tenerife. They demonstrated that this may lead to a significant fractionation between incompatible trace elements and to changes in element ratios as for instance Ba/Th and Zr/Nb which differ from those of the parental melts. This may result in a decoupling of major and trace elements. The phonolite shows, as the Col de Guéry phonolites, pronounced negative Sr, Ba, Ti and P anomalies, but differs from these rocks in increasing Nb, Ta and REE with decreasing MgO contents. Nb is considered to be a strongly incompatible element in melts having olivine, clinopyroxene, plagioclase and apatite on the liquidus. The pattern of trace element distribution is explained as a result of mixing of mafic melts relatively depleted in lithophile elements and evolved melts enriched in lithophile elements.

## Magma mixing

Mixing of magmas has been proposed to be an important process in the evolution of the volcanic rocks of Mont-Dore (e.g. Gourgaud & Maury (1984); Downes (1987); Gourgaud (1991)). Another example of magma mixing is provided by phonolitic tuffs from Tenerife (Wolff, 1984, 1985) which have three phenocryst assemblages corresponding to alkali basaltic, trachyandesitic and phonolitic melts. This is considered to be the result of magma mixing caused by injection of basaltic melts into a stratified magma chamber consisting of a lower layer of trachyandesitic melt and a roof zone of phonolitic melt. The phonolites have 195-290 ppm Nb, 11.4-38.9 ppm Ta, there is a separation of Nb and Ta as shown by the highest Nb/Ta ratios in the most evolved rocks.

In the Col de Guéry area the petrographical data for the 2.0 Ma trachytes and phonolites and their enclaves including disequilibrium features such as embayment of grains and reaction zones indicate complex processes of formation. The macrocrysts of alkali feldspar, plagioclase and clinopyroxene show resorption phenomena, overgrowths and discontinuous zonation, which may be taken as evidence for a xenocrystic origin of the cores of these grains. Thus, the partly resorbed cores of basic plagioclase in zoned grains af feldspars, the corroded and broken grains of brown Al-rich clinopyroxene and the olivine may represent remnants from a more basic magma, which coexisted with the phonolitic magma. The olivine shows strong resorption, reaction rims and clustering which, together with the forsterite-rich composition, support a xenocrystic origin. The amphibole macrocrysts of the trachytes and phonolites show zonation and destabilization rims. The rims are generally missing in the aggregations of amphibole in the enclaves in these rocks. This indicates that the amphibole phenocrysts originated at deeper levels where the crystallization of the amphiboles of the enclaves took place. All these features suggest that the rocks are mixtures of crystals brought up from depth and minerals formed by *in situ* crystallization of the magma.

Also the trace element data indicate a mixed origin of the rocks of the enclaves (Table 6b). The contents of Sc, V, Cr, Ni, Cu, Ba and Y are similar to those of the basanite-hawaiite stage; Rb, Sr, Zr, Sm and Th recall the trachyte stage; REE, Nb, Hf, and Ta both the basanite and the trachyte stages. The enclaves have higher contents of Cs than the other rocks of the area. Most of the element ratios of the enclaves (Table 6b) are similar to those of the basanite to trachyandesite sequence, but the enclaves have slightly higher Zr/Nb and Nb/Ta ratios than these rocks.

A quantitative discussion of the fractionation and mixing processes is considered not to be feasible because of the lack of knowledge of the composition of the magmatic end members involved. The basic rocks analysed by us are too low in MgO and Ni (Tables 5a, b) to be considered primary mantle-derived magmas.

## Isotopic data

In the $^{87}$Sr/$^{86}$Sr – $^{143}$Nd/$^{144}$Nd diagram (Fig. 20), the Col de Guéry rocks display a trend away from the DM field towards lower Nd and higher Sr initial ratios similar to the features described by Downes (1984) and Wilson & Downes (1991) for volcanic rocks from the Massif Central and Central Europe. In the same diagram, Wilson & Downes (1991, Fig. 5A) demonstrate a general trend towards the Bulk Earth composition but the rocks from Massif Central deviate and show the same shallow trend as displayed by the Col de Guéry rocks (Fig. 20). Wilson & Downes (1991) point out that the most primitive rocks examined by them may be interpreted as results of mixing of melts from a depleted mantle (DM) and a HIMU mantle source. The same applies to the most primitive Col de Guéry rocks ( Fig. 20): basanite (88-920) and the Puy Cordé enclave (97-108C). The trend from basanite via trachyandesite (88-931) to the Col de Guéry trachyte (88-942) and the Trioulérou enclave (97-107A) may be explained by crustal contamination of the melts or perhaps rather by mixing with melts derived from an enriched mantle source (EM). The trend toward the $^{\mathrm{Fme.}}$ de Puy May (88-951) and Bozat (97-110) phonolites may similarly have involved melts from an enriched mantle source (EM).

The Nd and Sr initial isotope ratios of the Puy Cordé phonolite and one sample of the Trioulérou phonolite (Table 7) are close to the value determined for the basanite and indicate a formation from mantle-derived melts. One of the phonolites examined by Downes (1984), that from Puy Griou, Cantal, has the same isotopic composition as the coexisting basanites. This phonolite, similar to the Trioulérou and Puy Cordé phonolites, contains blebs of basic melts, an indication of a hybrid origin. It resembles also the Col de Guéry phonolites in having lower contents of Nb and REE than most of the other phonolites analysed by Wilson *et al.* (1995). As pointed out above, differences in trace element ratios make it most unlikely that the phonolites are comagmatic with the basanite-trachyandesite-trachyte sequence exposed in the Col de Guéry area. Mixing processes between trachytic/phonolitic and basic melts in deep magma chambers appear to give a more satisfactory explanation of the origin of these rocks.

The high initial Sr isotope ratio of one Trioulérou sample (88-953) is evidence of crustal contamination or hydrothermal alteration of the northern part of the plug, whereas the low initial ratio of sample (97-106) indicates that the rocks of the southern part of the plug are practically uncontaminated and unaltered.

The Bozat phonolite and the Mouteron (88-903) trachyte have rather low Nd initial isotope ratios and rather high Sr initial isotope ratios and indicate a trend toward the isotope ratios of the Sanadoire trachyte (88-901 and 88-901B2) via the Tuilière trachyte (88-955) (Fig. 20). In the Sanadoire trachyte, the Nd and Sr isotope initial ratios vary from respectively 0.512738 to 0.512746 and from 0.703813 to 0.703840, that is a combination of rather low Nd and Sr isotope initial ratios. This marks a trend towards the HIMU mantle type and could be a result of a new wave of mixing with melts of HIMU composition. This trachyte carries enclaves of tephrite, granite and sediments, which are partially disintegrated into the host rock. The low Sr isotope ratios show, however, that contamination with crustal material has been insignificant, the rather low Nd isotope ratios that disintegration of tephritic enclaves cannot be the reason for the combination of Nd and Sr isotopic initial ratios.

The lead isotope ratios (Figs. 21, 22) which show trends away from the mixing line between DM and HIMU compositions towards EM compositions are in conformity with this interpretation of the origin of the Col de Guéry rocks. When plotted in a $^{206}Pb/^{204}Pb$ vs. $^{143}Nd/^{144}Nd$ diagram (Fig. 24), our data cluster within the triangle defined by HIMU, DM and EM components and do not fall along a defined trend. Consequently, they can be interpreted to have resulted from a mixture of all three components.

This interpretation of the origin and evolution of the trachytic and phonolitic melts which consolidated to form the 2.0 Ma rocks is in fair agreement with earlier published views on the origin of trachytes and phonolites from Massif Central.

Chauvel & Jahn (1984) proposed that the magmas forming the Mont-Dore phonolites were derived from a depleted, slightly heterogeneous, metasomatized mantle source corresponding to the source of ocean island basalts. Briot *et al.* (1991) similarly found that the Mont-Dore volcanic rocks in a $^{143}Nd/^{144}Nd$ – $^{87}Sr/^{86}Sr$ diagramme plot in the field of oceanic and continental volcanic rocks. The basanites and phonolites have practically the same initial $^{43}Nd/^{144}Nd$ ratio indicating a formation from uncontaminated mantle-derived magmas, whereas the silica-undersaturated rocks have slightly higher $^{87}Sr/^{86}Sr$ ratios than the basanites. The $\delta^{18}O$-values indicate that this may be due to secondary hydrothermal alteration. All other plots, especially those of the intermediate rocks, show evidence of crustal contamination. The high contents of K have according to this interpretation been derived from the mantle source of the melts. Briot *et al.* (1991) concluded that the

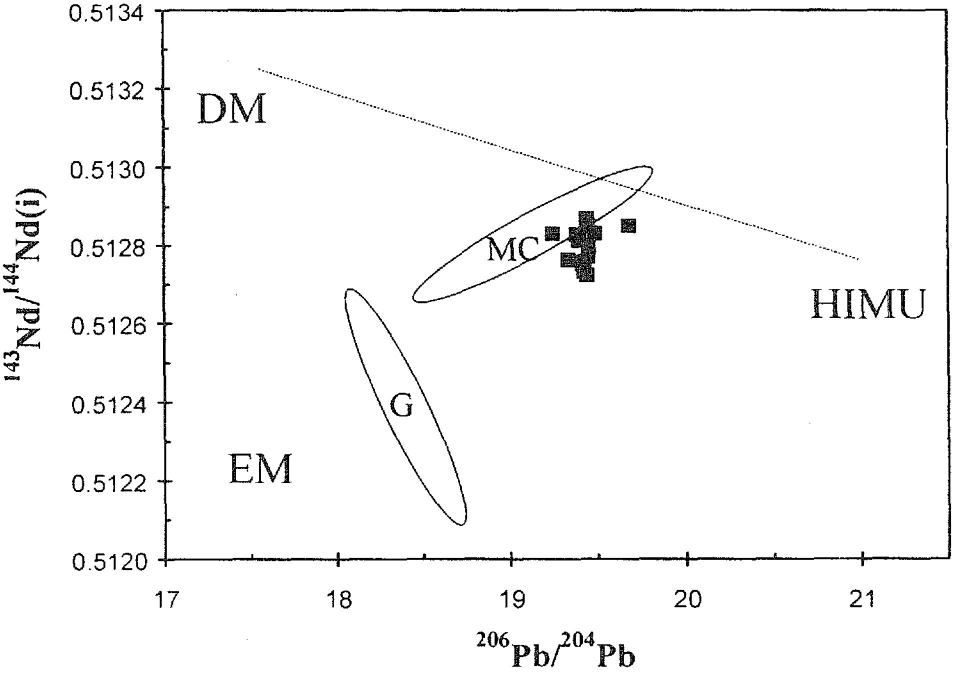

Fig. 24. $^{206}$Pb/$^{204}$Pb – $^{143}$Nd/$^{144}$Nd diagram.

silica-undersaturated series was formed by crystal fractionation processes at great depth or in ancient inactive reservoirs of the saturated series after exhaustion of contamination with crustal material. It should, however, be pointed out that the rocks examined by Briot *et al.* (1991) do not have the same age according to their Table II.

Cantagrel & Baubron (1983), have similarly proposed that the Mont-Dore tephrites and phonolites have their origin in deep magma reservoirs which were independent from the reservoirs feeding the trachyandesitic volcanics.

Wilson *et al.* (1995) arrived at the conclusion that the parental magmas of the Cantal phonolites were formed by partial melting of a relatively homogeneous mantle-source and that the apparent Sr-Nd-Pb isotopic heterogeneity of the source may reflect mixing of asthenosphere-derived melts with isotopically-enriched lithosphere-derived partial melts. Wilson & Downes (1991) pointed out that the asthenospheric component has affinities with the source of the St. Helena (HIMU) OIB type and may in part be recycled 500-400 Ma old oceanic lithosphere, or it could represent a zone of enriched mantle at the base of the subcontinental lithosphere which was partially melted during extension processes.

The $T_{DM}$ values in Table 7 indicate that the rocks of the lithosphere in which the melts forming the 2.0 Ma rocks were generated have an age of 460-280 Ma which is in excellent agreement with the above-mentioned data of Wilson and Downes (1991)

### The combination of low initial Sr and Nd isotope ratios

The Sanadoire trachyte and to a lesser degree the Mouteryron and Tuilière trachytes show a combination of low initial Sr and Nd isotope ratios which in a preceding paragraph was interpreted as a result of mixing of melts forming the other 2.0 Ma rocks with melts derived in an HIMU type mantle source. Other explanations of this combination of isotope ratios are, however, also possible.

Considering the high K contents of the volcanic rocks of Massif Central reference should be made to Pervov *et al.* (1997) who pointed out that potassic igneous rocks often have low Sr and Nd initial isotope ratios. The early magmatic phase of the Sakun pluton, the Aldan Shield, Southeastern Siberia, for instance has Sr initial isotope ratios of 0.70398-0.70445 and Nd initial isotope ratios of 0.511924-0.512096. This is considered to be a result of a long interval of time between enrichment of the magma source in the lithospheric mantle and the generation of the magma.

A number of studies have demonstrated a decoupling of chemical and isotopic systems and that interdiffusion between co-existing basic and more evolved melts can result in a diffusional decoupling of Sr isotope ratios from Sr concentration. Sr isotopes are homogenized by self-diffusion, whereas Sr ions migrate along chemical gradients, the isotopic homogenization covering a wider area than the elemental homogenization. Isotopic equilibrium is attained before chemical equilibrium and homogenization, Sr isotopes react more rapidly than Nd isotopes. This means that Nd remains more or less unmodified and is a more reliable indicator of the source of the melts than Sr isotopes (cf. Baker, 1989; Davidson *et al.*, 1990; Blichert-Toft *et al.*, 1992; Glodny, 1993 and Lesher, 1994). In the examination of the relations between co-existing tholeiitic basaltic melt and anatectic rhyolitic melts, Blichert-Toft *et al.* (1992) found that the distribution of Sr and Nd isotope initial ratios and the concentrations of major and trace elements is controlled by interdiffusion between the basic and acid melts during magma mingling and roofward segregation of the rhyolitic melt. Si, Rb, Na, K, Ba, Nd and Sm migrate from the acid melt toward the basic melt; Ti, Fe, Mg, Mn, Ca, Sr, Sc and Zr from the basic toward the acid melt, that is there is a separation of Rb and Sr. The element distribution is partially controlled by crystallization of apatite and zircon which behave as sinks for Zr, REE and Y. Schreiber *et al.* (1999) have produced additional information about the importance of interdiffusion between co-existing latitic and trachytic melts. Diffusional exchange of elements between the melts has resulted in an enrichment in Na, Rb, Th and Zr and an impoverishment in Ti, Ca, Fe, Mg, Sr, Ba, P and MREE in the modified latitic melt compared to the host trachyte and the original latite.

Mineralogically and texturally the relations described by Schreiber *et al.* (1999) recall the enclaves in the Col de Guéry trachytes and phonolites. It may therefore be proposed that the combination of low Nd and Sr isotope initial ratios in some of the volcanic rocks of the Col de Guéry area may be a result of a decoupling of the isotopic and chemical systems and a separation of Rb and Sr because of interdiffusion between host magmas and partly consolidated enclaves. It is in this connection of interest to note that there may be bleached zones in phonolite in contact with enclaves (Fig. 6).

The rather low Nd initial isotope ratios in the Sanadoire trachyte, which in accordance with the above-mentioned information about the behaviour of Nd and Sr isotopes, most probably are less modified than the Sr isotope initial ratios, indicate some crustal contamination of the melt which formed the Sanadoire trachyte, or as mentioned above a mixing with HIMU type melts. The rather low Sr initial isotope ratios may then be explained by homogenization of the Sr isotopes by means of interdiffusion between the trachytic melt and the tephritic enclaves.

## Crustal contamination

The extent of crustal contamination of the volcanic rocks of the Massif Central is debated. In most magmatic suites the differentiated rocks show more evidence of crustal contamination than the less evolved rocks (Grove *et al.*, 1982; Downes, 1984). This is in agreement with the position of the most evolved phonolite, that from Trioulérou, in the $^{87}Sr/^{86}Sr$ – $^{143}Nd/^{144}Nd$ diagram (Fig. 20).

The chondrite-normalized trace element diagrams for the 2.0 Ma trachytes and phonolites (Fig. 18) show a characteristically spiked pattern and especially a marked Ta trough. Distinct troughs for Nb in diagrammes for the Cantal trachytes and phonolites are proposed to be a result of crustal contamination of the magmas coupled with fractionation of titanite (Wilson *et al.*, 1995). This explanation is less likely in the case of the Col de Guéry phonolites, since there are no Nb troughs in the chondrite-normalized trace element diagrams (Fig. 18). Instead, the diagrams of basanite – trachyandesite show peaks for Nb and Ta as an indication of an early separation of Nb and Ta in the exposed rocks. A similar process may have taken place in the magma chambers from which the 2.0 Ma rocks have been derived. The Ta troughs in the diagrams of the 2.0 Ma rocks are consistent with the elevated Nb/Ta ratios in these rocks (Table 5b) and shows, as has been discussed in an earlier section, that Nb and Ta have been separated during mixing and fractionation processes.

Crustal contamination can explain the transition from *ne* normative to *qz* normative compositions seen in the Mont-Dore volcanic area as it has been proposed by Brousse (1961c), see also Brotzu *et al.* (1997). The isotopic data of Table 7 indicate that most trachytes and phonolites of the Col de Guéry area have higher Sr, and lower Nd initial isotope ratios than the basanites, which may be taken as evidence of some crustal contamination of their melts. According to Briot *et al.* (1991) crustal contamination, assimilation and fractional crystallization, AFC processes, played a role in the formation of the trachyandesitic rocks. It may, however, be questioned, if AFC processes would result in the more or less constant Y/Nb, Yb/Ta, Zr/Nb element ratios in the basanite – trachyandesite series. Our isotopic data (Table 7) indicate a limited crustal influence on the isotopic signatures of these rocks. As mentioned above, Briot *et al.* (*op.cit.*) and Wilson *et al.* (1995) point out that according to the Nd-isotope data no crustal contamination was involved in the formation of the phonolitic rocks of Mont-Dore and Cantal. Our Sr-Nd-isotope data show that the Puy Cordé phonolite and parts of the Trioulérou phonolite may have been formed from uncontaminated mantle-derived melts, whereas the remaining 2.0 Ma trachytes and phonolites have more likely been formed from contaminated melts or by mixing of the magma with melts derived from an enriched mantle. Only the plot of one sample of Trioulérou phonolite in Fig. 20 marks a trend parallel to the $^{87}Sr/^{86}Sr$ axis similar to trends described by Downes (1984) from Cantal. The unmodified Nd initial isotope ratio of this phonolite makes hydrothermal alteration a more likely explanation of the Sr isotope ratios than a process of assimilation of a crustal component during fractionation of the melts. As also observed by Briot *et al.* (1991), this rock has a very low Sr contents which makes it vulnerable to alteration by groundwater and hydrothermal solutions.

K, Rb and Th are easily mobilized by partial melting of the continental crust. Such processes could explain the enrichment in these elements in the 2.0 Ma trachytes and phonolites considered here, but cannot explain the simultaneous depletion in REE, Ba, Sr, Ta and Nb. It is therefore concluded that, with the exception of one sample of the Trioulérou phonolite, crustal contamination has played an insignificant role in the formation of the 2.0 Ma trachytes and phonolites.

## Conclusions

The volcanic rocks of the Col de Guéry area comprise basanite, hawaiite, trachyandesite, trachyte and phonolite and consist of silica-saturated as well as silica-undersaturated rocks. The suite from basanite via hawaiite to trachyandesite and some of the trachytes may according to the geochemical and Nd-Sr isotope data have been formed from a basanitic magma by crystal fractionation processes involving olivine, clinopyroxene, amphibole, Fe-Ti oxides, titanite, apatite and plagioclase.

Fractionation of amphibole rather than crustal contamination is considered to be the cause of the transition from silica-undersaturated to silica-oversaturated rocks.

The trachytes and phonolites of the Col de Guéry area, which were emplaced 1.83 to 2.0 Ma ago, the 2.0 Ma rocks of the present paper, are mineralogically as well as geochemically related. They have, for instance, the same types of clinopyroxenes and amphiboles, diopside-hedenbergite and pargasite-kaersutite. They are enriched in Na, K, Cs, Th, Zr and Y and depleted in Mg, Fe, Ca, Nb, Ta, Ba, Sr, Ti, P and the REE, especially the MREE from Nd to Tb. The element ratios (Table 5b and Fig. 23) are markedly different from those of the other rocks of the area and there is a depletion in the REE when compared with the basanite-trachyandesite-trachyte sequence. Furthermore, the 2.0 Ma trachytes and phonolites form separate clusters in all the geochemical diagrams. It is consequently concluded that they cannot be comagmatic with the exposed basanite-trachyandesite series of the area. From Fig. 18 it is also clear that there is a break between the 2.0 Ma rocks and the basanite-trachyandesite-trachyte series. It is therefore proposed that the trachytes and phonolites have been formed from independent pulses of melts originating in deep reservoirs. The geochemical data indicate that these melts have been formed by extreme fractionation processes in basanitic/tephritic magmas. The $^{143}$Nd/$^{144}$Nd initial ratios show that the Puy Cordé and Trioulérou phonolites may have been formed from an uncontaminated mantle-derived magma, whereas the more elevated $^{87}$Sr/$^{86}$Sr and the lower $^{143}$Nd/$^{144}$Nd initial ratios of the Tuilière and Mouteyron trachytes suggest a formation from mixing of melts derived from different mantle sources. This also applies to the Sanadoire trachyte which combines low Sr and low Nd isotope initial ratios indicating the involvement of melts originated in a HIMU type mantle source.

The literature on the volcanic rocks of Massif Central distinguishes two main series of rocks, a silica-undersaturated and a silica-saturated series. According to our data, the exposed suite from basanite to some of the trachytes, as it is pointed out in a preceding paragraph, most probably represents one series. A second series could comprise the 2.0 Ma trachytes and phonolites and the unexposed basanitic/tephritic rocks which formed by consolidation of the parental magmas of the 2.0 Ma rocks.

The differences in contents of Nb, Ba, etc. and Zr/Nb, Nb/Ta and Ba/La ratios between the phonolites in the Col de Guéry area, Bozat and Cantal is most probably a result of different fractionation patterns of independent melts, not least differences in oxygen fugacities during crystallization of the melts. A high oxygen fugacity explains the practical absence of Eu anomalies in the Mont-Dore phonolites and their related trachytes.

Contamination of the trachytic and phonolitic melts during their ascent may be the cause of the depletion in Nb and Ta, but crustal contamination alone cannot explain the trace element geochemistry of the rocks. Instead, the depletion in Nb and Ta is proposed to be a result of fractionation of ilmenite, titanite and perhaps amphibole. This has resulted in a fractionation of Nb relative to Ta, REE and Zr.

The combination of high contents of $K_2O$ and low contents of Ba may be explained by early separation of Ba by fractionation of amphibole and titanite and late enrichment in K by fluid transfer processes. The viscous nature of the melts may have hampered the fractionation processes at the trachyte-phonolite stage of evolution, thus explaining the presence of enclaves and partly resorbed and overgrown pheno-/xenocrysts of forsteritic olivine, bytownitic plagioclase, Ti-Al-rich clinopyroxene and titanite.

The tephritic enclaves in the trachytes and phonolites are most probably modified blebs of basic magma injected into the magma chambers in which these rocks were formed. The heterogeneous distribution of trace elements and the variation in Nd and Sr initial isotope ratios can be explained by interdiffusion between the coexisting melts which has resulted in a decoupling of isotopes from element concentrations and has prevented the attainment of equilibrium.

These last-named features indicate that mixing processes combined with crystal fractionation played an important role in the formation of the trachyte and phonolites and can explain the observed variation in trace element concentrations and ratios and the Sr, Nd and Pb isotope data. The exact nature of these processes cannot, however, be outlined since the chemical compositions of the end member magmas involved are unknown.

## Acknowledgements

Ulla Bernth's study visit to the Laboratoire de Pétrographie–Volcanologie, Université de Paris-Sud, Orsay and a part of the field work was made possible by an ERASMUS grant from the European Union. The kind and efficient assistance of staff members of the Laboratory is gratefully acknowledged. The field work of Henning Sørensen and a part of the analytical work was covered by grants from the Danish Natural Science Research Council and the Carlsbergfoundation. John C. Bailey and Jørn Rønsbo, Geological Institute, University of Copenhagen, and Raymond Gwozdz, Tracechem A/S, Copenhagen offered valuable assistance in the analytical work. The major element whole rock analyses were supplied by the laboratories of the Geological Survey of Greenland (now the Geological Survey of Denmark and Greenland, GEUS). Britta Munch and Ole Bang Berthelsen, Geological Institute, University of Copenhagen, prepared some of the illustrations for publication.

# References

Azambre, B. & Girod, M. 1966: Phonolites agpaïtiques. Bulletin Société française de Minéralogie et Cristallographie **89**, 514-520.

Baker, D.R. 1989: Tracer versus element diffusion: Diffusional decoupling of Sr concentrations from Sr isotope compositions. Geochimica et Cosmochimica Acta **53**, 3015-3023.

Bernth, U. 1996: A petrological study of the Col de Guéry area, Mont-Dore, Massif Central, France. Unpublished cand.scient. dissertation, Institute of Geology, University of Copenhagen, 106 pp. + appendices.

Blichert-Toft, J., Lesher, C.E. & Rosing, M.T. 1992: Selectively contaminated magmas of the Tertiary East Greenland macrodike complex. Contributions to Mineralogy and Petrology **110,** 154-172.

Blumrich, J. 1893: Die Phonolite des Friedländer Bezirkes in Nordböhmen. Tschermaks Mineralogische, Petrographische Mitteilungen **13**, 465-595.

Briot, D., Cantagrel, J.M., Dupuy, C. & Harmon, R.S. 1991: Geochemical evolution in crustal magma reservoirs: trace-element and Sr-Nd-O isotopic variations in two continental intraplate series at Monts Dore, Massif Central, France. Chemical Geology **89**, 281-303.

Brotzu, P., Gomes, C.B., Melluso, L., Morbidelli, L., Morra, V. & Ruberti, E. 1997: Petrogenesis of coexisting $SiO_2$-undersaturated to $SiO_2$-oversaturated felsic igneous rocks: the alkaline complex of Itatiaia, southeastern Brazil. Lithos **40**, 133-156.

Brousse, R. 1961a: Minéralogie et pétrographie des roches volcaniques du massif du Mont-Dore (Auvergne). Bulletin Société française de Mineralogie et Cristallographie **84**, 131-186.

Brousse, R. 1961b: Minéralogie et pétrographie des roches volcaniques du massif du Mont-Dore (Auvergne). III: Les deux associations magmatiques. Bulletin Société française de Mineralogie et Cristallographie **84**, 245-259.

Brousse, R. 1961c: Analyses Chimiques des Roches Volcaniques Tertiaires et Quaternaire de la France. Bulletin Service Carte Géologique de la France **263**,(58), 140 pp.

Brousse, R. & Julien, R. 1987: Remplisage et limites de la fosse de la Haute-Dordogne : importance de la série inférieure du Mont-Dore. Rapport GPF 3, Thème 9, Doc. BRGM 145, 53-65.

Brousse, R. & Lefèvre, C. 1990: Le Volcanisme en France et en Europe Limitrophe. Guides Géologiques Régionaux. Masson, Paris, 263 pp.

Brousse, R., Varet, J. & Bizouard, H. 1969: Iron in the Minerals of the Sodalite Group. Contributions to Mineralogy and Petrology **22**, 169-184.

Brousse, R., Wimmenauer, W. & coll.: 1979: Le volcanisme alcalin lié aux distensions cénozoïques de l'Ouest Européen (Massif Central, Fossé Rhénan). 26. International Geological Congres Paris 1980. Livret-Guide d'Excursion **G 25,** 1-60.

Brousse, R., Rançon, J-P., Tempier P. & Veyret Y. 1989: Bourg-Lastic, Carte Géologique de la France à 1/50 000. Editions du BRGM – BP 6009 – 45060 Orléans Cedex 2 – France.

Cantagrel, J.M. & Baubron, J.C. 1983: Chronologie des éruptions dans le massif volcanique des Monts Dore. (Méthode potassium – argon). Implications volcanologiques. Géologie de la France, Bulletin du BRGM, n° **1/2**, 123-142.

Caroff, M., Ambrics, C., Maury, R. & Cotten, J. 1997: from alkali basalt to phonolite in hand-size samples: vapor-differentiation effects in the Bouzentès lava flow (Cantal, France). Journal of Volcanology and Geothermal Research **79**, 47-61.

Chauvel, C. & Jahn, B-M. 1984: Nd-Sr isotope and REE geochemistry of alkali basalts from the Massif Central, France. Geochimica et Cosmochimica Acta **48**, 93-110.

Davidson, J.P., Shanaka, L. de Silva, Holden, P. & Halliday, A.N. 1990: Small-scale disequilibrium in a magmatic inclusion and its more silicic host. Journal of Geophysical Research **95 B11**, 17661-17675.

Decobecq, D. 1987: Approche Pétrologique du Reservoir Magmatique du Massif du Mont-Dore par les Enclaves Associes. Thesis. Université de Paris-Sud, Orsay, 204 pp.

Downes, H. 1984: Sr and Nd isotope geochemistry of coexisting alkaline magma series, Cantal, Massif Central, France. Earth and Planetary Science Letters **69**, 321-334.

Downes, H. 1987: Tertiary and Quaternary volcanism in the Massif Central, France. In: Fitton, J.G. & Upton, B.G.J. (eds). Alkaline Igneous Rocks. Geological Society Special Publication **30**, 517-530.

Downes, H., Kempton, P.D., Briot, D., Harmon, R.S. & Leyreloup; A.F. 1991: Pb- and O-isotope systematics in granulite facies xenoliths, French Massif Central; implications for crustal processes. Earth Planeratry Science Letters **102**, 342-357.

Glangeaud, L. & Létolle, R. 1962: Evolution géochimique et géodynamique des magmas du massif volcanique du Mont-Dore et de l'Auvergne. Méthodes et conséquences générales. Bulletin Société française de Mineralogie et Cristallographie **85**, 296-308.

Glangeaud, L., Bobier, C., Dumesnil, P., Letolle, R., Lepvrier, P. & Vigneron, M. 1965: Géochronologie et évolution paléomagnétique, géochimique, pétrologique et tectonophysique du massif volcanique du Mont-Dore (France). Bulletin Société géologique de la France **7**, 1010-1025.

Glodny, J. 1993:Magmenmischung, Stofftransport und Sr-isotopenaustauch in der variszischen Gil-Marquez-Intrusion (SW-Spanien). Dipl. Thesis Mineralogical Institute, Münster, Germany (quoted from Schreiber *et al.*, 1999).

Gourgaud, A. 1991: Comagmatic enclaves in lavas from the Mont-Dore composite volcano, Massif Central, France. In: Didier, J. & Barbarin, B. (eds): Enclaves and Granite Petrology. Elsevier, Amsterdam, 221-233.

Gourgaud, A. & Maury, R.C. 1984: Magma-mixing in alkaline series: an example from Sancy volcano (Mont-Dore, Massif Central, France). Bulletin Volcanologique **47,** 827-847.

Grove, T.L., Gerlach, D.C. & Sando, T.W. 1982: Origin of calc-alkaline series lavas at Medicine Lake Volcano by fractionation, assimilation and mixing. Contributions to Mineralogy and Petrology **80**, 160-182.

Halliday, A.N., Fallick, A.E., Hutchinson, J & Hildreth, W. 1984: A Nd, Sr and O isotopic investigation into the causes of chemical and isotopic zonation in the Bishop Tuff, California. Earth and Planetary Science Letters 68, 379-391.

Hart, S.R. 1984: A large scale isotope anomaly in the Southern Hemisphere mantle. Nature **309**, 753-757.

Irving, A. J. & Price, R. C. 1981: Geochemistry and evolution of lherzolite-bearing phonolitic lavas from Nigeria, Australia, East Germany and New Zealand. Geochimica et Cosmochimica Acta **45,** 1309-1320.

Johan, Z. & Cech, F. 1989: Nouvelles données sur la haïnite, $Na_2Ca_5[(Ti,Zr,Mn,Fe,Nb,Ta)_{1,50\ 0.50}(Si_2O_7)_2$ et ses relations cristallochimiques avec la götzenite, $Na_2Ca_5Ti(Si_2O_7)_2F_4$. Compte Rendu de l'Académie des Sciences Paris **308**, Série II, 1237-1242.

Julien, R. 1988: Magmatologie des Trois Phases d'Edification du Massif du Mont-Dore. Donnees Volcanologiques sur le Site de Croizat. Thesis, Université de Paris-Sud, Orsay. 194 pp + Annexes

Lacroix, A. 1893: Les Enclaves des Roches Volcaniques. Mason, Paris, 710 pp.

Lacroix, A. 1917: Les laves à haüyne d'Auvergne et leurs enclaves homeogènes: importance théorique de ces dernières. Compte Rendu Hebdomadaire de l'Académie des Sciences. Paris. **164**, 581-588.

Leake, B.E. et al. 1997: Nomenclature of amphiboles: report of the Subcommission on Amphiboles of the InternationalMineralogical Association, Commission on New Minerals and Mineral Names. Canadian Mineralogist **35**, 219-246.

Le Maitre, R.W.(ed). 1989: A Classification of Igneous Rocks and Glossary of Terms. Blackwell Scientific Publications. 193 pp.

Lesher, C.E. 1994: Kinetics of Sr and Nd exchange in silicate liquids: theory, experiments, and applications to uphill diffusion, isotopic equilibration, and irreversible mixing of magmas. Journal of Geophysical Research **99, B5**, 9585-9604.

Macdonald, R., Navarro, J.M., Upton, B.G.J. & Davies, G.R. 1994: Strong compositional zonation in peralkaline magma: Menengai, Kenya Rift Valley. Journal Volcanological Research **60**, 301-325.

MacDonald, R., Davies, G.R., Upton, B.G.J., Dunkley, P.N., Smith, M. & Leat, P.T. 1995: Petrogenesis of Silali volcano, Gregory Rift, Kenya. Journal Geological Society London **152**, 703-720.

Maciotta, G., Almeida, A., Barbieri, M., Beccaluva, L., Gomes, C., Morbidelli, L., Ruberti, E., Siena, F. & Traversa, G. 1990: Petrology of the tephrite-phonolite suite and cognate xenoliths of the Fortaleza district (Ceará, Brazil). European Journal of Mineralogy **2**, 687-709.

Marsh, J.S. 1987: Evolution of a strongly differentiated suite of phonolites from the Klinghardt Mountains, Namibia. Lithos **20**, 41-58.

Maury, R.C. 1976: Contaminations (par l'encaissant les enclaves) et cristallization fractionnée de séries alcalines continentales (Massif Central français et océaniques (Pacifique Central): l'origine des laves acides. Thesis, Université de Paris-Sud, Orsay, 360 pp.

Maury, R.C., D'Arco, P. & Brousse, R. 1980a: Températures et fugacités d'oxygène des magmas intermédiaires et différenciés du Mont-Dore. Compte Rendu sommaire Société géologique de la France 1980, **6**, 242-245.

Maury, R.C., Brousse, R., Villemant, B., Joron, J.L. & Treuil, M. 1980b: Cristallization fractionée d'un magma basaltique alcalin: la série de la Chaîne des Puys (Massif Central, France). I. Minéralogie et Pétrologie. Bulletin Minéralogique **103**, 250-266.

Morel, J-M., Gourgaud, A. & Vincent, P.M. 1992: Un épisode hydromagmatique majeur dans l'histoire des Monts Dore (Massif central français): le massif d'Aiguiller. Bulletin Société géologique de la France **163**, 625-634.

Morimoto, N. 1988: Nomenclature of Pyroxenes. Bulletin Minéralogique **111**, 535-550

Neumann, E.-R., Wulff-Pedersen, E., Simonsen, S.L., Pearson, N.J., Marti, J. & Mitjavila, J. 1999: Evidence for fractional crystallization of periodically refilled magma chambers in Tenerife, Canary Islands. Journal of Petrology **40**, 1089-1123.

Pazdernik, P. 1994: Petrographische und geochemische Untersuchungen an trachytischen und phonolitischen Gesteinen der Böhmischen Mittelgebirges (Ceské stredohori). Erlanger Beiträge Petrographie Mineralogie **4**, 1-40.

Pazdernik, P. 1997: Phonolitic and trachytic rocks in the Ceske Stredohori Mts., North Bohemia: geochemistry and petrology. Journal of the Czech Geological Society **42**, 68.

Pervov, V.A., Kononova, V.A., Suddaby, P., Thirlwall, M.F., Vroon, P., Bogatikov, O.A., Upton, B.G.J. & Woolley, A.R. 1997: Potassic magmatism of the Aldan Shield, Southeastern Siberia: an indicator of the multistage evolution of the lithospheric mantle. Petrology **5**, 415-430.

Rasmussen, E., Neumann, E.-R., Andersen, T., Sundvoll, B., Fjerdingstad, V. & Stabel, A. 1988: Petrogenetic processes associated with intermediate and silicic magmatism in the Oslo rift, southeast Norway. Mineralogical Magazine **52**, 293-307.

Rutherford, N.F. & Heming, R.F. 1978: The volatile component of Quaternary ignimbrite magmas from the North Island, New Zealand. Contributions Mineralogy and Petrology **65**, 401-411.

Schreiber, U., Anders, D. & Koppen, J. 1999: Mixing and chemical interdiffusion of trachytic and latitic magma in a subvolcanic complex of the tertiary Westerwald (Germany). Lithos **46**, 695-714.

Sørensen, H., Bernth, U. & Brousse, R. 1999: Trachytes and phonolites from the Mont-Dore region, Auvergne, France. GeoLines **9**, 114-118.

Stacey, J.S. & Kramers, J.D. 1975: Approximation of terrestrial lead isotope evolution by a two stage model. Earth and Planetary Science Letters **26**, 207-221.

Stimac, J. & Hickmott, D. 1994: Trace-element partition coefficients for ilmenite, orthopyroxene and pyrrhotite in rhyolite determined by micro-PIXE analysis. Chemical Geology **117**, 313-330

Sun, S.-S 1980: Lead isotopic study of young volcanic rocks from mid-ocean ridges, ocean islands and island arcs. Philosophical Transactions of the Royal Society London **A297**, 409-445.

Thompson, R.N., Morrison, M.A., Hendry, G.L. & Parry, S.J. 1984: An assessment of the relative roles of crust and mantle in magma genesis: an elemental approach. Philosophical Transactions of the Royal Society London **A310**, 51-70.

Todt, W., Cliff, R.A., Hauser, A. & Hofmann, A.W. 1993: Re-calibration of NBS lead standards using a $^{202}$Pb + $^{205}$Pb double spike. Tema Abstr. **5** (Suppl. I, 1), 396.

Ulrych, J. & Pivec, E. 1997: Age-related contrasting alkaline volcanic series in North Bohemia. Chemie der Erde **57**, 311-336.

Ulrych, J., Cajz, V. & Adamovic, J. 1998: Magmatism and Rift Basin Evolution. Czech Geological Survey, Prague. 97 pp.

Ulrych, J., Pivec, E., Frychly, R. & Rutsek, J. 1992: Zirconium mineralization of young alkaline volcanic rocks from Northern Bohemia. Geologica Carpatithica **43**, 91-95.

Vaneckova, M., Holub, F.V., Soucek, J. & Bowes, D.R. 1993. Geochemistry and petrogenesis of the Tertiary alkaline volcanic suite of the Labe tectono-volcanic zone, Czech Republic Mineralogy and Petrology **48**, 17-34.

Villemant, B. 1979: Étude géochimique des éléments en traces dans les séries volcaniques du Massif Central. Thesis. P. and M. Curie Université, Paris, 348 pp.

Villemant, B. 1988: Trace element evolution in the Phlegrean Fields (Central Italy): fractional crystallization and selective enrichment. Contributions to Mineralogy and Petrology **98**, 169-183.

Villemant, B., Joron, J-L., Jaffrezic, H., Treuil, M., Maury, R. & Brousse, R. 1980: Cristallization fractionnée d'un magma basaltique alcalin: la série de la Chaîne des Puys (Massif Central, France). II. Géochimie. Bulletin Minéralogique **103**, 267-286.

Villemant, B., Jaffrezic, H., Joron, J.-L. & Treuil, M. 1981: Distribution coefficients of major and trace elements; fractional crystallization in the alkali basalt series of Chaîne des Puys (Massif Central, France). Geochimica Cosmochimica Acta. **45**, 1997-2016.

Villemant, B. & Treuil, M. 1983: Comportement des éléments traces et majeurs dans la serie alcaline du Velay; comparaison avec la Chaîne des Puys (Massif Central, France). Bulletin Minéralogique **106**, 465-486.

Weaver, S.D., Sceal, J.S.C. & Gibson, I.L. 1972: Trace-element data relevant to the origin of trachytic and pantelleritic lavas in the East African Rift System. Contributions Mineralogy and Petrology **36**, 181-194.

Wilson, M. 1989: Igneous Petrogenesis. Unwin Hyman, London. 466 pp.

Wilson, M. & Downes, H. 1991: Tertiary-Quaternary extension-related alkaline magmatism in western and central Europe. Journal of Petrology **32**, 811-849.

Wilson, M., Downes, H. & Cebria, J.-M. 1995: Contrasting fractionation trends in coexisting continental alkaline magma series; Cantal, Massif Central, France. Journal of Petrology **36**, 1729-1753.

Wolff, J.A. 1984: Variation in Nb/Ta during differentiation of phonolitic magma, Tenerife, Canary Islands. Geochimica et Cosmochimica Acta **48**, 1345-1348.

Wolff, J.A. 1985: Zonation, mixing and eruption of silica-undersaturated alkaline magma: a case study from Tenerife, Canary Islands. Geological Magazine **122**, 623-640.

Wörner, G., Beusen, J.M., Duchateau, N,. Gijbels, R. & Schmincke, H.U. 1983: Trace element abundances and mineral/melt distribution coefficeints in phonolites from Laacher See Volcano (Germany) Contributions to Mineralogy and Petrology **84**, 152-173.

Wörner, G. & Schmincke, H.-U. 1984a: Mineralogical and chemical zonation of the Laacher See tephra sequence (East Eifel, W.Germany). Journal of Petrology **25**, 805-835.

Wörner, G. & Schmincke, H.-U. 1984b: Petrogenesis of the zoned Laacher See tephra. Journal of Petrology **25**, 836-851.